UNIVERSITÀ DEGLI STUDI DI TRIESTE

UNIVERSITÀ DEGLI STUDI DI TRIESTE

XXXV CICLO DEL DOTTORATO DI RICERCA IN BIOMEDICINA MOLECOLARE

Identification and characterization of therapeutic molecules affecting expression levels of the tumor suppressor DAB2IP in cancer

Settore scientifico-disciplinare: **BIO/13**

DOTTORANDA
ROSSELLA DE FLORIAN FANIA

COORDINATORE
PROF. GERMANA MERONI

SUPERVISORE DI TESI
PROF. LICIO COLLAVIN

ANNO ACCADEMICO 2021/2022

TABLE OF CONTENTS

ABSTRACT

In tumors, the reciprocal communication between malignant cells and non-transformed stromal cells involves a variety of signaling proteins and modulators that cooperate to control proliferation, migration and apoptosis. Among them, the tumor suppressor DAB2IP, a Ras-GAP and signaling adaptor protein, modulates signal transduction in response to several extracellular stimuli, negatively regulating multiple oncogenic pathways. Accordingly, the loss of DAB2IP in tumor cells fosters metastasis and enhances chemo- and radio-resistance. DAB2IP is rarely mutated in cancer but is frequently downregulated or inactivated by multiple mechanisms. Solid experimental evidences indicate that DAB2IP reactivation can reduce cancer aggressiveness in tumors driven by multiple different oncogenic mutations. In this regard, we showed that the ectopic overexpression of DAB2IP is sufficient to significantly affect the behavior of prostate cancer cells, possibly slowing tumor dissemination. All these evidences indicate DAB2IP as a strong target for anti-cancer therapy. Nevertheless, therapeutic approaches to increase DAB2IP function in cancer are still not available. Based on these observations, we performed a high-throughput screening with more than 1200 FDA-approved drugs to search for molecules that increase DAB2IP protein levels. Since detection of endogenous DAB2IP is technically difficult due to relatively low expression levels and the limitations of available antibodies, we exploited CRISPR/Cas9 gene editing to generate two prostate cancer cell models expressing endogenous DAB2IP fused to HiBiT, a peptide tag that enabled luminescence-based detection of protein levels in a sensitive and quantitative manner. Using this approach, we identified a set of candidate drugs able to increase DAB2IP levels. We focused our attention on the three more effective drugs: one antibacterial, one antileukemic and one antiasthmatic. Although not conclusive, functional experiments indicate that DAB2IP-upregulating drugs can inhibit some cancer-associated phenotypes, and that some of these effects are at least in part dependent on DAB2IP. These findings, if further confirmed, may suggest a potential repurposing of these drugs for solid cancers' treatment, as support to current therapies.

INTRODUCTION

1.1 CANCER AND THE CHALLENGE OF THERAPEUTIC RESISTANCE

1.1.1 Cancer initiation and survival as processes of adaptation

Natural selection is the process identified by Charles Darwin by which nature selects traits or phenotypes to pass on offspring to better "fit" the organism to the environment (Darwin, 1859). Cancer development can be considered as a natural selection process, in which the environment inputs lead to an intricate cellular adaptive response. The spontaneous genetic mutations and the ones which occur after chemotherapy are examples of survival responses of cells to environmental conditions. Assuming cancer cells behavior not only as an effect of intrinsic cellular genetic changes but rather a consequence of cell adaptation to external pressures may help to better understand mechanisms underlying tumor development. Indeed, cancer is characterized by a deep dysregulation of the mechanisms involved in the control of cell fate, cell survival and genome maintenance (Vogelstein et al., 2013), in which the response of cancer cells to the environment, as local as distant, plays a crucial role in determining tumor fate. Therefore, it is not surprising that alterations also in stromal cells of the tumor niche in turn lead to deep changes in normal tissue development, fostering cancer initiation (Bremnes et al., 2011).

Notably, tumor-cell subpopulations within the tumor site reveal a spatial heterogeneity: each cell differs from another for its mutational signature, giving origin to distinct cell subclones. In addition, cancer cells are characterized by genetic changes during cancer evolution, revealing a temporal heterogeneity (Dagogo-Jack & Shaw, 2018) (Zhu et al., 2021). Indeed, subclones will compete with each other for survival under pressures driven by both intrinsic (i.e. physical and chemicals) and exogenous (i.e. therapies) factors, leading to tumor evolution (Vendramin et al., 2021). According to the theory of clonal evolution of cancer, just the clones that are able to adapt to the 'challenging' environmental conditions are able to persist giving origin to the tumor; mentioning Darwin: *"It is not the strongest of the species that survives, nor the most intelligent that survives. It is the one that is most adaptable to change"* (Darwin, 1859).

Understanding that cancer is a response of the cell to the surroundings and investigating how the environment inputs promote cellular adaptive modifications enable to anticipate the response of cancer to therapy as well as to develop more efficient therapeutic strategies. Multiple alterations occur in the tumor tissues during carcinogenesis that promote the creation of a tumor-promoting microenvironment. The adaptative response of cells to the surrounding results in genetic and epigenetic reprogramming that alter the processes involved in the regulation of normal tissue

homeostasis, including the immune response, the vascular permeability, the extracellular matrix remodeling, as well as the metabolic processes (Bremnes et al., 2011).

1.1.2 The balance between onco-genes and onco-suppressors

The evolution of a normal cell into a cancerogenic cell is the outcome of a complex process that involved genetic and epigenetic alterations. Genetic mutations usually occur in two broad classes of genes. The first class are the so-called oncogenes, genes that are abnormally "activated" after alterations of proto-oncogenes, genes that under normal conditions are usually involved in cell growth control. Mutations in oncogenes usually affect just one allele, which act in a "dominant" or positive (gain-of-function) manner. The proto-oncogenes are usually altered by deletional or insertional mutations (which result in the production of iper-activated pro-oncogenic proteins), or by amplifications or chromosomal translocations (that produce too high amount of a normal functioning protein or generation of a fusion protein with pro-oncogenic properties, respectively). Recent studies have identified numerous patients harboring multiple mutations within the same oncogenes. These multiple mutations synergistically activate the mutated oncogene indicating a positive epistatic interaction between different mutations. Secondary multiple mutations in the oncogenes usually result in major resistance to molecularly targeted therapies; sometimes secondary mutations occur in different subclones, suggesting a parallel evolution, which may contribute to relapse and treatment failure (Saito et al., 2021).

The second class is referred to the tumor suppressor genes (TSGs). These genes work to block the onset of oncogenic phenotypes; thus, once mutated or deregulated, they promote tumor advantage. In this case, both alleles must be or mutated, deleted, functionally suppressed or lost, because they act via recessive mechanisms to wild-type (loss-of-function). Most of them restrain cell proliferation or are involved in DNA repair. They are usually inactivated by gene mutations that produce unfunctional proteins, or by deletions that lead to the loss of protein expression (Anderson, 1989).

Whereas mutations are the main described events involved in carcinogenesis, also epigenetic alterations play a fundamental contribution in the cancer onset and progression. Epigenetic events are non-heritable and include modifications of DNA, RNA, and protein which influence the cell behavior, without altering gene sequence. For instance, hypomethylation of oncogenes' promoters or hypermethylation of tumor suppressor' ones are frequently observed events in cancer. Also histone modifications and RNA-interference are responsible of altered expression of these genes in cancer (Anderson, 1989).

Not only, recent research has found that the tumor suppressors are also downregulated by post-translational modifications, including phosphorylation, SUMOylation, acetylation. Rb, p53, PTEN

are examples of genes regulated by these kinds of mechanisms. The reversibility of post-translational modifications makes them potential targets of anti-cancer therapies as well as biomarkers of disease status (L. Chen et al., 2020).

Moreover, ubiquitin-mediated proteasomal degradation, abnormal cellular localization, and transcriptional regulation are also involved in the inactivation of TSGs (L. H. Wang et al., 2019).

Determining alterations in oncogenes and oncosuppressor genes in tumors is useful for diagnosis, prognosis, and designing therapeutic strategies. Nowadays, innovative cancer therapies are based to the delivery of drugs or RNAs that directly or indirectly inhibit oncogene overexpression or promote the re-expression of downregulated tumor suppressor genes. In this regard, approaches aim to interfere with oncogenes activity may counteract the pro-oncogenic effects due to their aberrant expression. The delivering of monoclonal antibodies that recognize and block the extracellular domain of over-expressed transmembrane receptors is an example (Wykosky et al., 2011). On the other hand, the discovery of molecules able to interfere with the mechanisms of tumor suppressor inhibition may be a promising strategy to counteract tumor development. It is well established that the loss of function of TSGs is associated with anti-cancer drug resistance. Nowadays viral vectors approaches are developed to re-express TSGs in order to re-sensitize tumor cells to therapies. Also, small molecules compounds were found to be able to restore the expression of down-regulated genes (Gao et al., 2021).

1.1.3 Chemoresistance: the challenge in prostate cancer

Prostate cancer (PC) is one of the most common cancer in men; with an age-related incidence it is indeed the second leading cause of cancer death in men in the United States (Daniyal et al., 2014) (Rawla, 2019). Current approaches used to eradicate prostate cancer include local treatments such as surgery and radiation therapy and systemic treatments such as chemotherapy, immune therapy and hormonal therapy. In the last years targeted therapy is increasingly used to treat advance cancers. Despite current approaches can be efficient for most cases, there are patients who do not completely recover from the disease. Indeed, has been known that some patients develop resistance to chemo- and radiotherapy, thus rendering the treatment inefficient or even detrimental. The reasons for such resistance are not understood at all. For this, deeply investigating the intrinsic causes of cancer resistance is fundamental to direct and improve future therapies.

A big challenge in the treatment of prostate cancer is played by Castrate-Resistant Prostate Cancer (CRPC). CRPC is defined by disease progression despite Androgen Depletion Therapy (ADT). ADT has been the standard treatment for initial intervention of advanced or metastatic prostate cancer. Usually, progression to castration-resistant prostate cancer occurs within 2-3 years of initiation of

ADT. Multiple mechanisms of resistance have been described to contribute to the progression to castration resistant disease. The main driver of this progression is the androgen receptor (AR) (Chandrasekar et al., 2015). Different mechanisms of AR alterations are reported. Among them: AR amplification and hypersensitivity, AR mutations, mutations in coactivators/corepressors, androgen-independent aberrant AR activation, alternative androgen production, and AR spliced variants that are constitutively active (Chandrasekar et al., 2015).

Docetaxel, an inhibitor of microtubule depolymerization, is the current first-line treatment for CRPC, but in recent years, newer agents have been developed that target some of these mechanisms of resistance, thereby providing additional survival advantages. Since alteration in AR pathways are the leading events in CRPC development, targeting the AR may be a promising strategy to fight advance-prostate cancer (Chandrasekar et al., 2015).

Nevertheless, novel therapeutic advances put the attention also on other mechanisms underlying the development of metastatic CRPC (mCRPC). For instance, defects in DNA damage repair are co-drivers of prostate cancer progression. Targeting enzymes involved in DNA repair such as PARP inhibitors has been indeed showed a higher sensitivity in mCRPC patients harbor defects in DNA repair genes (Westaby et al., 2021). At the same time, genomic alterations in the PI3K-AKT pathway are common in primary prostate cancer and enriched in mCRPC. Also, this pathway is showed to be aberrantly activated in patients resistant to androgen depletion therapy. Clinical trials have showed that the combination of traditional chemotherapeutics with AKT inhibitors are able to reduce cancer progression in mCRPC patients compared to the use of chemotherapeutics alone (Westaby et al., 2021) (Ku, Gleave, & Beltran, 2019).

Notably, a gene whose mutations have a broad impact on responsiveness to chemotherapy is TP53. Gain-of-function or loss-of function mutational events in p53 gene are showed to cause altered response of cancer cells to different chemotherapeutics (Brosh & Rotter, 2009) (Mantovani et al., 2019). Notably, it has been reported that the combined loss of p53 and RB1 increases resistance to antiandrogen therapy in mice models of prostate cancer. In this context, hormone resistance in not associated to AR-signaling dependent mechanisms but rather to the reprogramming of the activity of SOX2 and EZH2, two genes essential for maintaining cell self-renewal properties, as a result of the loss of p53 and RB1. This evidence highlights a novel approach to re-sensitize prostate tumors to antiandrogen therapies by preventing the SOX2 and EZH2 upregulation in tumors deficient for p53 and RB1 (Ku et al., 2018) (Mu et al., 2017).

Also, promising agents include agents targeting the prostate-specific membrane antigen PSMA, such as monoclonal antibodies and chimeric-antigen receptor-T cells (CAR-T) (Sayegh et al., 2022).

Interestingly, also non-coding RNAs have been showed to promote drug resistance of prostate cancer. Several miRNAs, lncRNAs and circRNAs have been found to participate in drug resistance by influencing Receptor tyrosine kinases (RTKs) pathways related genes, apoptosis and histone modification. Therefore, correcting the anomalous expression of noncoding RNA may be a promising strategy to overcome the chemoresistance of prostate cancer. Currently, there are several ongoing RNA therapy clinical trials using nucleic acids technology to manipulate the expression of noncoding RNAs (Ding et al., 2021).

1.1.4 Molecular mechanisms of cancer drug resistance

Understanding molecular mechanisms underlying drug resistance is important to find out novel therapeutic approaches for cancer therapy. The main mechanisms of chemoresistance include transporter pumps. The ATP-binding cassette transporters (ABC transporters) are a transport system superfamily responsible for the translocation of various substrates (e.g. ions, amino acids, peptides, lipids, sugars, and xenobiotic) across cellular membranes. The multi drug resistance (MDR) is frequently associated with overexpression of ABC transporters, that caused an excessive expulsion of drug from cells. To date novel therapeutic strategies based on the use of RNA interference are developed and applied to reverse ABC-transporter-mediated MDR in cancer cells (Zheng, 2017). Another mechanism involved in chemoresistance is that referred to the amplification or excessive activation of oncogenes. For instance, an overexpression of the epidermal growth factor receptor (EGFR) can activate multiple pathways involved in differentiation, proliferation, survival and chemoresistance, such as JAK/stat3, PI3K/AKT/mTOR and Src/FAK/ROS and SOS/Grb2/Ras pathways.

Also, is has been showed that mitochondrial dysfunctions lead to failure of apoptosis after drug treatment (Bukowski et al., 2020). Also an excessive DNA repair or autophagy after irradiation of drug treatment can reduce responsiveness to therapies (Zheng, 2017). Importantly, changing in the drug metabolism may increase drug resistance. Usually reactions such as oxidation, reduction and hydrolysis are fundamental in protecting normal cells against toxic agents. These reactions reduce the drug sensitivity of cancer cells via two manners: limiting the conversion of pro-drugs into activated drugs and increasing the metabolic tourn-over (Mansoori et al., 2017).

Moreover, drug resistance could be enhanced by modifications of the targets of the chemotherapeutic agents after genetic mutations or epigenetic alterations (Mansoori et al., 2017) (Bukowski et al., 2020).

Importantly, also mutations in the oncogenic signaling proteins involved in the PI3K/AKT, ERK, NF-kB pathways are responsible to chemo-resistance (Zheng, 2017).

Among the plethora of genes whose dysregulation impact drug sensitivity the tumor suppressor DAB2IP (Disabled-2 Interacting Protein) seems to play an important role. DAB2IP counteracts cancer progression by negatively modulating multiple of the above mentioned cytoplasmatic signaling pathways. In line with its onco-suppressive role the loss of its function correlates with more aggressive and less chemo-responsiveness tumors (Bellazzo et al., 2017). DAB2IP functions and regulation in cancer are described in depth in the next chapter.

1.2 DAB2IP: A RAS-GAP THAT INHIBITS KEY ONCOGENIC PATHWAYS

1.2.1 DAB2IP: a protein involved in various human diseases

The tumor suppressor Disabled-2 Interacting Protein (DAB2IP) is a cytoplasmic Ras GTPase-activating (GAP) and an adaptor protein involved in mediating signal transduction by multiple inflammatory cytokines and growth factors, negatively modulating key oncogenic pathways, including TNF signaling via NF-kB, WNT/β-catenin, PI3K/AKT, and Androgen Receptors (AR) (Bellazzo et al., 2017). DAB2IP is also known as ASK1-interacting protein (AIP1), for its role in inducing the release of ASK1 from the inhibitory binding of 14-3-3 in response to TNF-α, favoring consequent activation of the pro-apoptotic ASK1-JNK pathway (Zhang et al., 2003).

The loss of DAB2IP functions represents an advantage for cancer initiation and progression and accordingly, it is frequently downregulated in various human malignancies (**Figure 1**) (https://tnmplot.com/analysis/).

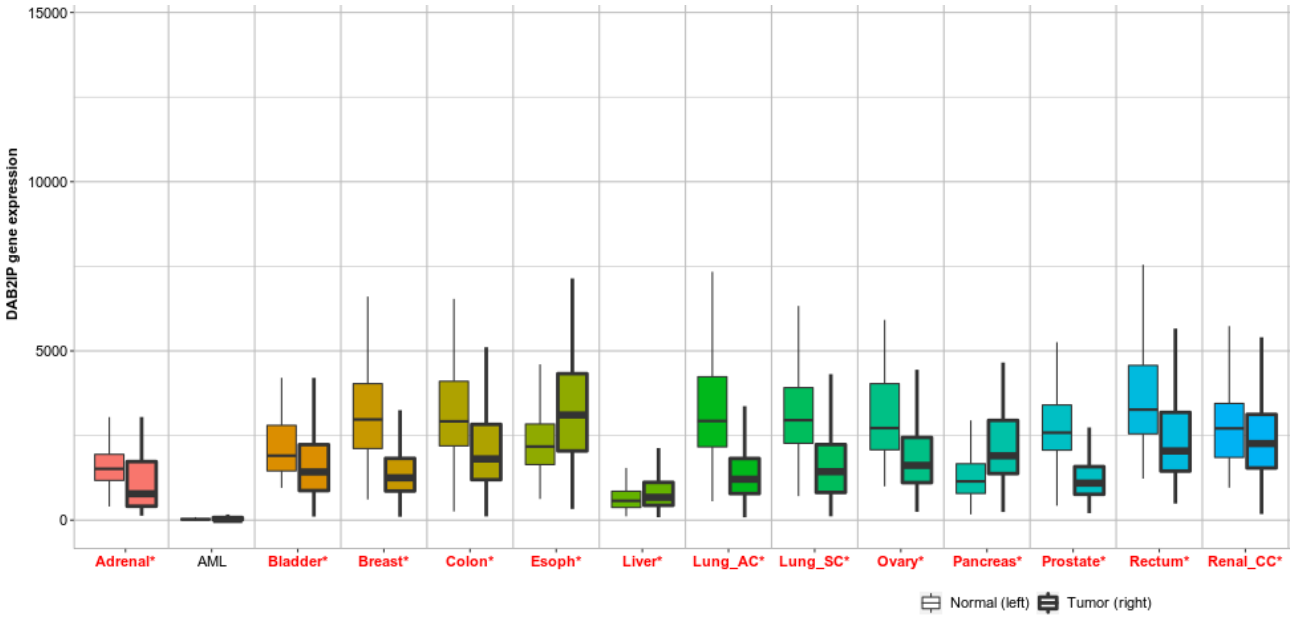

Figure 1 | Differential DAB2IP expression in normal versus tumor tissues. Significant differences by Mann-Whitney U test are marked with red* (TNMplot.com).

Not only, DAB2IP inhibition is involved in multiple other human diseases. For instance, some variants of DAB2IP are associated with risk of coronary heart disease. In particular, genome-wide association studies demonstrate the association of the polymorphism rs7025486 G>A within DAB2IP gene with abdominal aortic aneurysm, early onset myocardial infarction and peripheral arterial disease (Gretarsdottir et al., 2010). Accordingly, evidences show that DAB2IP deletion significantly induces an increase of number and size of aortic plaques in mouse models of atherosclerosis, concurrently with an augment of inflammation (Huang et al., 2013).

Furthermore, DAB2IP plays an important role in neural system development. Evidences reveal that DAB2IP is involved in the regulation of maturation of Purkinje cell dendrites, and synapse formation in the cerebellum (Shuhong Qiao et al., 2013). DAB2IP knockdown in neuronal progenitor cells in the embryonic mouse neocortex causes a reduction in neuronal migration (Lee et al., 2012) (Shuhong Qiao & Homayouni, 2015). Also, a very recent work describes DAB2IP as a potential predictor of type 2 diabetes: the loss of DAB2IP can cause insulin resistance by activating JNK, p38 MAPK, and ERK1/2 signaling (Song et al., 2022).

All these evidences reveal the deleterious effects of the loss of DAB2IP functions in multiple diseases, determining the importance to further investigate the mechanisms implicated in its downregulation, with the aim to develop possible therapies.

1.2.2 Structure of DAB2IP protein

The human DAB2IP gene is located on the long arm of the chromosome 9.

It gives rise to multiple transcripts, as suggested by the presence of 5 different transcription start sites (TSS) at the 5'-end of DAB2IP gene identified by CAGE (Lizio et al., 2019). Considering only the three major transcripts listed in the NCBI database, DAB2IP can be potentially translated from 3 different start codons (**Figure 2A**).

Additionally, the last exon undergoes alternative splicing, resulting in the production of two different C-terminal sequences. Therefore, considering different N- and C-terminal combinations, multiple DAB2IP protein isoforms can be generated (data from NCBI, Homo sapiens Annotation Release 150) (**Figure 2B**).

The hDAB2IP 2 (NM_138709.1) is the best characterized isoform, and it presents, respectively from its N-terminus to C-terminus (**Figure 2B**):

- a *Pleckstrin Homology (PH) domain*: a module involved in interaction with phosphatidylinositol lipids within biological membranes and also implicated in promoting protein-protein interactions (Musacchio et al., 1993);

- a *Protein kinase C conserved region 2 (C2)*: a Ca^{2+}- binding motif that mediates several cell functions. It is also involved in the binding to phospholipids, inositol polyphosphates and intracellular proteins (Nalefski & Falke, 1996);
- a *GTPase-Activating Protein domain (GAP)*: a module that promotes the GTPase activity, fostering hydrolysis from GTP to GDP of target proteins (Schaber et al., 1989);
- a *Period-like domain (PER)* and a *Proline-rich domain (PR)*: important for protein-protein interactions (Williamson, 1994);
- *Leucine zipper (LZ)*: a motif involved in the interaction with a specific DNA sequence, it is usually found within the DNA-binding domain of transcription factors (Landschulz et al., 1988);
- *Nuclear localization signal (NLS)*: a sequence required for nuclear protein import.

The presence of different isoforms complicates the study of human DAB2IP in physiology and pathology. Interestingly, a recent work described different functions and opposite mechanisms of regulation for two N-terminal variants of DAB2IP in vascular disease (Z. Li et al., 2020). They report that a shorter DAB2IP isoform, named AIP1B (ASK1-interacting protein-1), lacking the N-terminal PH domain, localizes to the mitochondria and enhances TNFα-induced ROS generation and neointima formation in vascular remodeling models, thus displaying an opposite effect compared to the full DAB2IP isoform (Z. Li et al., 2020).

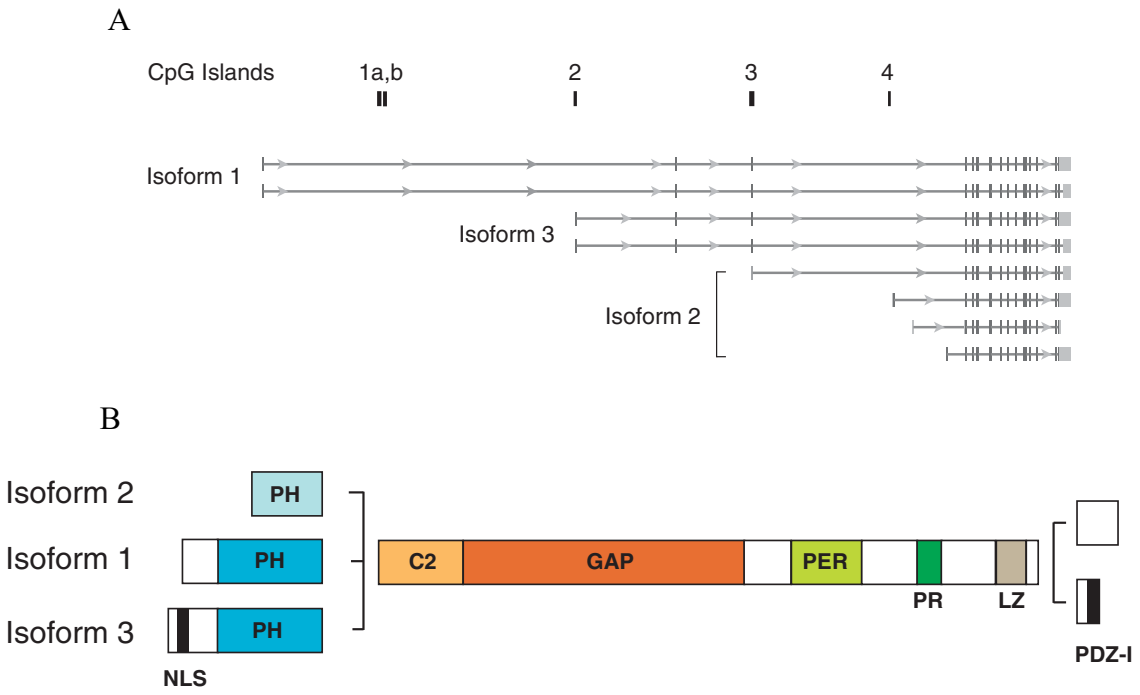

Figure 2 | Structure of the human DAB2IP gene and encoded proteins. **A)** Scheme of the main hDAB2IP transcripts and the relative position of CpG islands on the genome. The predicted protein isoforms encoded by the various transcripts are also indicated (data from NCBI, Homo sapiens Annotation Release 150). **B)** Structure of six predicted hDAB2IP isoforms, with possible combinations of alternative N- and C- termini. Two human DAB2IP transcripts are currently annotated in RefSeq: variant 1 (NM_032552.3) and variant 2 (NM_138709.1). Bioinformatic tools predict at least four different transcriptional start sites (TSS) of DAB2IP, encoding three possible N-termini of the protein; moreover, alternative splicing generates two possible C-terminal variants (Bellazzo et al., 2017).

1.2.3 DAB2IP: a tumor suppressor that counteracts multiple key oncogenic pathways

In accordance with his GTPase-activating activity, DAB2IP plays a crucial role in fostering the inactivation of the GTPase Ras, inducing hydrolysis from Ras-GTP to Ras-GDP (Rajalingam et al., 2007). Not only DAB2IP limits Ras-induced proliferative signals, preventing the activation of its canonical downstream pathway, but it also decreases the Ras-induced activation of phosphoinositide-3-kinase (PI3K), inhibiting the pro-oncogenic PI3K-AKT axis (Bellazzo et al., 2017) (**Figure 3A**). Additionally, through its PR and PER domains, DAB2IP respectively binds to PI3K and AKT, and prevents the interaction between PI3K and AKT, directly counteracting the PI3K-induced phosphorylation and activation of AKT (Xie et al., 2009) (**Figure 3B**).

In endothelial cells, DAB2IP also counteracts VEGF signaling, directly binding the phosphotyrosine residues within the activation loop of VEGFR2, via its C2 domain, and at the same time, counteracting downstream activation of PI3K/AKT (Zhang et al., 2008) (**Figure 3B**).

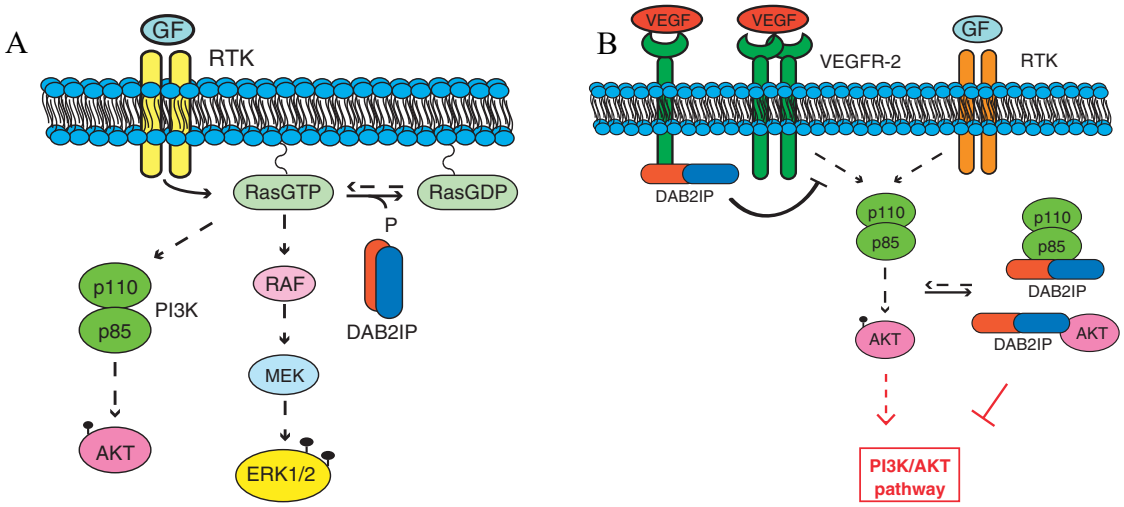

Figure 3 | Model of signaling pathways modulated by DAB2IP. A) DAB2IP effects on RAS-induced pathways. **B)** DAB2IP disrupts the interaction between PI3K and AKT (Bellazzo et al., 2017).

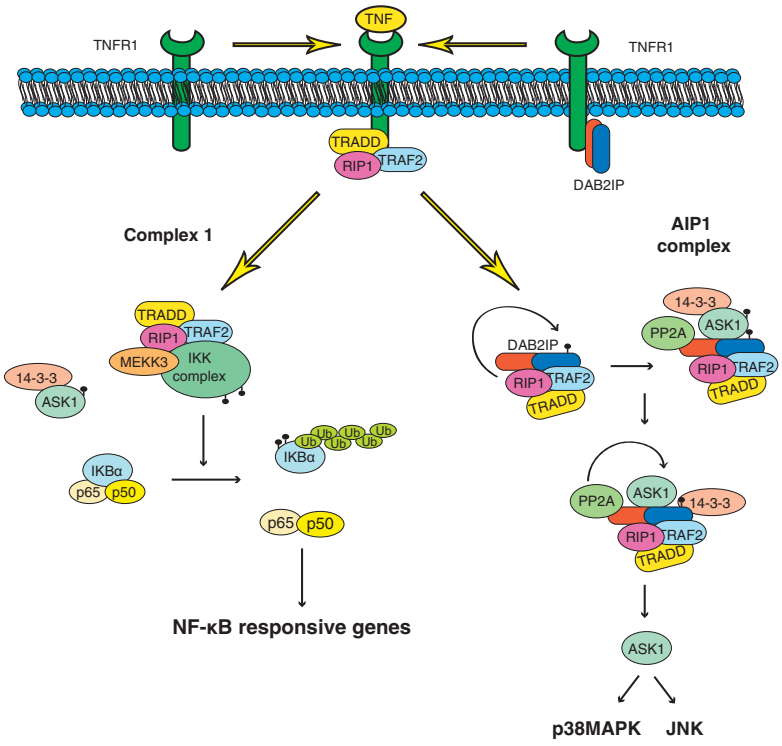

Figure 4 | DAB2IP in TNFα-mediated activation of ASK1/JNK pathway (Bellazzo et al., 2017).

Notably, DAB2IP can modulate cells response to the inflammatory cytokine TNFα, counteracting NF-κB-mediated transcription of pro-inflammatory and pro-invasive genes, while fostering apoptosis. In detail, DAB2IP can sequester the adaptor proteins TRADD and TRAF2, and the kinase RIP1, recruited to the intracellular domain of the activated TNF-receptor, driving the formation of the so-called AIP1-complex, counteracting NF-κB signaling and fostering the activation of the pro- apoptotic ASK1/JNK pathway in response to TNF (Zhang et al., 2004) (**Figure 4**).

Furthermore, DAB2IP coordinates apoptosis upon endoplasmic reticulum (ER) stress (Luo et al., 2008), via the activation of the ASK1/JNK pathway: it interacts with the ER-stress regulator IRE1α, supporting its dimerization in response to the accumulation of unfolded proteins, and promoting the consequent activation of ASK1 (Luo et al., 2008) (**Figure 5A**).

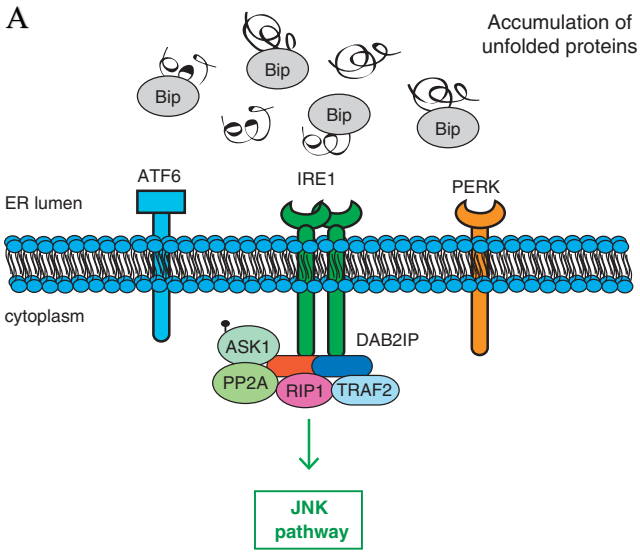

Additionally, DAB2IP can counteract JAK-STAT signaling, a pathway frequently upregulated in many types of cancer (Dutta & Li, 2013). After stimulation by inflammatory cytokines, JAK proteins dimerize and act as tyrosine-kinases, recruiting and phosphorylating the transcription factors STATs, that, once activated, modulate cell proliferation, migration and apoptosis (Dutta & Li, 2013). DAB2IP interacts with JAK2 through its N-terminal region and with the transcription activator STAT3 through its PR domain, inhibiting its activation and anti-apoptotic effects (Zhou et al., 2015a) (**Figure 5B**).

Various experiments show that DAB2IP prevents the over-activation of WNT pathway, supporting GSK3β stabilization (Xie et al., 2010). In particular, after stimulation of its receptor, the ligand WNT activates a signal transduction that culminate with GSK3β inhibition, and a consequent accumulation of β-catenin in the nucleus of cancer cells (Polakis, 2000). DAB2IP, binding GSK3β through its C2 domain, potentiates GSK3β activation, increasing its inhibitory binding with β-catenin, thus promoting proteasomal degradation of β-catenin (Xie et al., 2010) (**Figure 5C**).

Additionally, DAB2IP is a key regulator of prostate cancer progression. Studies reveal its role in counteracting the pro-oncogenic Androgen Receptor (AR) signaling in prostate cancer cells, preventing AR nuclear translocation. Through its PR domain, DAB2IP can disrupt the interaction of AR with the oncogene c-Src, inhibiting AR-mediated c-Src activation. In addition, DAB2IP can interact with several AR splice variants, resulting in a decrease of AR expression levels (Wu et al., 2014). (**Figure 5D**). Also, very recently was uncovered that DAB2IP regulates the synthesis of testosterone and participate to the growth of castration-

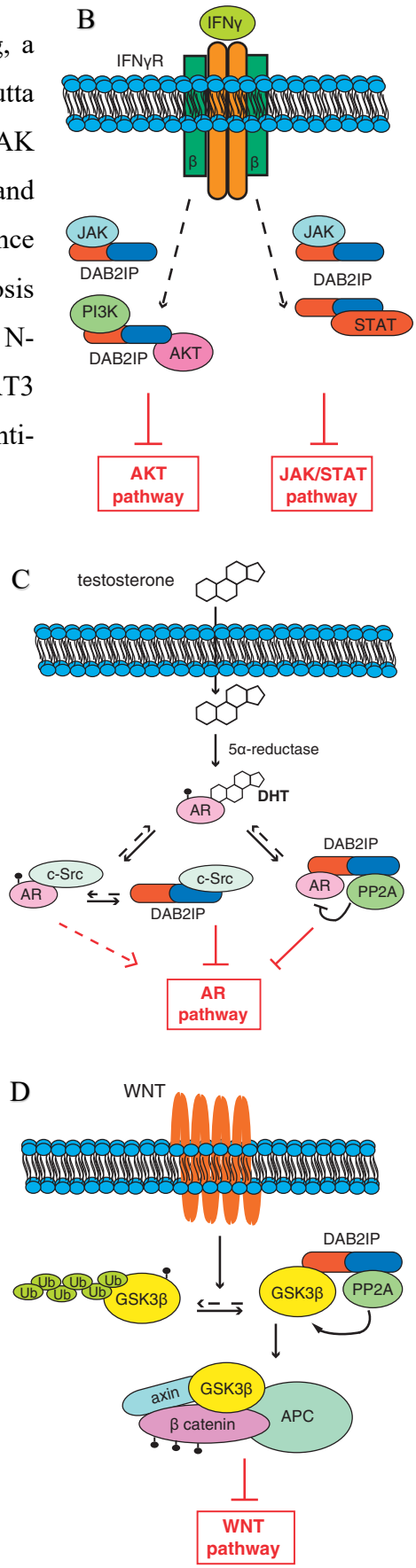

Figure 5 | Model of main signaling pathways regulated by DAB2IP

resistant prostate cancer (CRPC) through PI3K/AKT/mTOR/ETS1 signaling; these studies indicate DAB2IP as a potential therapeutic target for CRPC treatment (Gu et al., 2022).

Although the oncogenic pathways in which DAB2IP is implicated and the biological consequences of the loss of DAB2IP as tumor suppressor are widely studied, the subcellular localization and functional molecular partners remain almost unexplored. DAB2IP seem to be a ubiquitously present in the cell. It likely binds phosphatidylinositol lipids of the plasma membrane through its Pleckstrin Homology (PH) domain (Musacchio et al., 1993). Nevertheless, one study reported DAB2IP in the nucleus, where it suppresses the transcription of the stem cell factor receptor CD117, modulating cancer stem cells properties (Yun et al., 2015). Furthermore, DAB2IP is demonstrated to co-localize with the small GTPase protein ARF6 at the plasma membrane and endocytic vesicles, where it negatively regulates toll-like receptor 4 (TLR4) signaling (Wan et al., 2010).

1.2.4 Biological consequences of DAB2IP loss-of-function

DAB2IP plays a role in modulating cellular behavior in response to different extracellular stimuli, such as growth factors, hormones, inflammatory cytokines, among others. In detail, as an onco-suppressor it has an impact on diverse biological processes including proliferation (Wang et al., 2002), apoptosis (Xie et al., 2009), survival (Luo et al., 2008) (Zhang et al., 2007), epithelial-to-mesenchymal transition (Xie et al., 2010), cancer stemness (CSC) (Yun et al., 2015) and angiogenesis (Zhang et al., 2008) (**Figure 6**).
Accordingly, DAB2IP expression is frequently downregulated in human malignancies (Liu et al., 2015). The loss of DAB2IP function in cancer cells counteracts pro-apoptotic signaling, fosters cell proliferation and resistance to chemo- and radiotherapy, promoting tumor growth and survival.

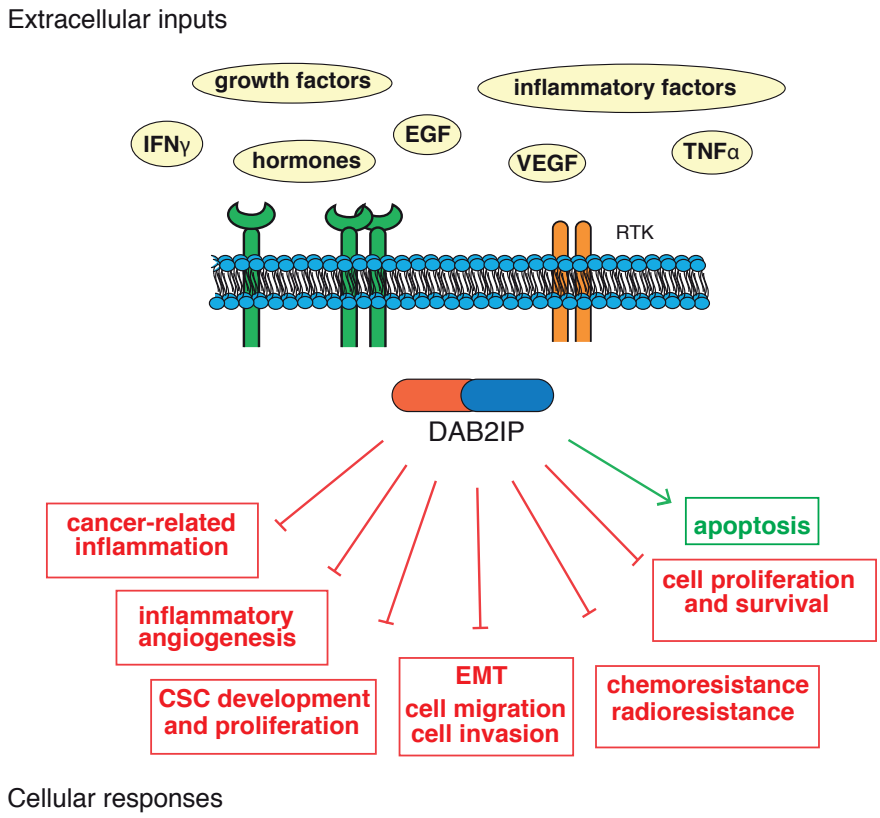

Figure 6 | DAB2IP influences the cellular response to extracellular stimuli
(Adapted from Bellazzo et al., 2017).

Impact of DAB2IP loss on cell proliferation, survival and resistance to apoptosis

The depletion of DAB2IP in prostate cancer cells sustains PI3K-induced AKT activation, and at the same time, suppresses ASK1 pathway, fostering survival and dissemination of prostate cancer cells in vivo (Xie et al., 2009). Also DAB2IP has been reported to maintain spindle assembly checkpoint and chromosomal stability through activating PLK1-Mps1 signal pathway thus, the loss of DAB2IP reduces the formation of mitotic checkpoint complex, resulting in aberrant proliferation (L. Yu et al., 2022). Additionally, DAB2IP loss in prostate cancer promotes a higher rate of DNA double-strand break (DSB) repair and resistance to apoptosis (Kong et al., 2010), concurrently to an augment of autophagy (L. Yu et al., 2015) after radiation exposure, supporting resistance to radiotherapy. Moreover, prostatic epithelial cells with DAB2IP knockdown show higher resistance to chemotherapeutic agents compared to control cells. Furthermore, cells depleted for DAB2IP express elevate levels of anti-apoptotic factors associated with chemoresistance (Wu et al., 2013). These evidences suggest the importance to measure the amount of DAB2IP in prostate cancer patients, before the treatment, in order to establish eventual alternative therapies (Wu et al., 2013). Recently, it has been uncovered that the loss of DAB2IP promotes progression of colorectal cancer by

facilitating the activation of the HSP90AA1/SRP9/ASK1/JNK signaling axis (Mengna Zhang et al., 2022)

Impact of DAB2IP loss on EMT induction, cell migration and metastasis formation

Important evidences indicate the role of DAB2IP inactivation in supporting epithelial-mesenchymal transition, in increasing cell migration and invasion, and in enhancing cancer cells dissemination in vivo (Figure 6) (Xie et al., 2010) (Min et al., 2010). The loss of DAB2IP correlates with an increase of mesenchymal markers as vimentin, twist, and fibronectin, and a concurrently reduction in membrane bound E-cadherin (Xie et al., 2010) (Min et al., 2010). Mechanistically, DAB2IP acts as an epithelial-mesenchymal transition inhibitor, negatively modulating WNT/β-catenin, PI3K/AKT and NF-κB axis (Xie et al., 2010) (Min et al., 2010) (Di Minin et al., 2014).

Not only, studies reveal that DAB2IP depletion in vascular endothelial cells (ECs) augments tumor growth and metastasis in mouse models of melanoma and breast cancer (W. Ji et al., 2015). The loss of DAB2IP in ECs induces an augment of VEGFR2 signaling, an increased secretion of molecules involved in supporting EMT and angiogenesis, promoting tumor neovascularization and the formation of a pre-metastatic microenvironment (W. Ji et al., 2015).

Again, DAB2IP downregulation enhances proliferation and metastasis of gastric cancer cells by activating ERK1/2 pathway (Sun et al., 2020).

Impact of DAB2IP loss on cell stemness

DAB2IP depletion can also foster cancer stem cells proliferation (Figure 6). Mechanistically, DAB2IP interacts, via its Leucine Zipper domain, with the transcriptional repressor GATA-1, inhibiting the expression of Stem Cell Factor Receptor CD117, a cytokine receptor tyrosine kinase that promotes cell proliferation and survival through the activation of multiple pro-oncogenic pathways, such as PI3K-AKT, Ras-MEK-MAPK and JAK-STAT (Liang et al., 2013) (E. J. Yun et al., 2015). Importantly, this is the first description of the DAB2IP nuclear transcriptional-modulating activity (E. J. Yun et al., 2015).

Furthermore, DAB2IP epigenetic downregulation mediated by EZH2 is responsible of cancer stem cells maintenance in ovarian cancer (Zong et al., 2020). It has also been showed that DAB2IP loss increase cancer stem cells renewal in colorectal cancer by promoting c-Myc expression (H. Li et al., 2021).

Impact of DAB2IP loss on cancer-related inflammation

Additionally, multiple evidences demonstrate that DAB2IP negatively modulates signal transduction by various cytokines (i.e. TNF, IFN-gamma, TRL4 and IL-1 beta), counteracting activation of NF-

κB and STAT3 pathways, thus acting as an anti-inflammatory protein, especially in vascular endothelial cells (Figure 6) (Bellazzo et al., 2017). For example, endothelial cells-specific DAB2IP knockdown mice show an increase of ROS production and vascular inflammation and remodeling, with consequent increase of atherosclerosis (Zhang et al., 2018).

DAB2IP activity as pro-inflammatory factors can also impinge the behavior of cancer cells in an inflamed tumor environment. For examples, DAB2IP inhibition mediated by the binding with mutated form of p53 protein, reprograms cancer cell response to TNF, triggering upregulation of NF-κB target genes encoding metalloproteinases, pro-inflammatory cytokines and chemokines involved in matrix-remodeling and immune cells recruitment (Di Minin et al., 2014). Also, DAB2IP expression inversely correlates with immune cell infiltration in renal cell carcinoma, resulting in a potential clinical biomarker for patient with this type of carcinoma (Cao, Zhang, & Wang, 2020).

Impact of DAB2IP loss on chemo- and radio-resistance

There is plenty of evidences indicating that metastatic cancer cells deficient in DAB2IP show major survival in response to chemotherapeutic drugs and ionizing radiation (IR) compared to control cells. The loss of DAB2IP favors the expression of the antiapoptotic factor Clusterin, a key contributor in resistance to anticancer drugs. Mechanistically, DAB2IP inhibits the expression of Clusterin by blocking the cross-talk between Wnt/b-catenin and IGF-I signaling thus preventing cell death after chemotherapeutic treatments. On the contrary, restoring DAB2IP reduces drug resistance as observed after knocking down of Clusterin (Wu et al., 2013). Additionally, the overexpression of DAB2IP reduces the survival of invasive bladder cancer cells after pirarubicin treatment through the regulation of STAT3/Twist1 pathway, signaling crucial for the pirarubicin chemoresistance (Wu et al., 2015).

Again, Zhou et al. demonstrated that DAB2IP loss in prostate cancer counteract chemo-response through the activation of STAT3 and the expression of survivin (Zhou et al., 2015). Moreover, in gastric cancer has been showed that the loss of DAB2IP contributes to cisplatin resistance potentially via regulation of AKT and ERK signaling pathway, whereas DAB2IP upregulation is sufficient to counteract cell proliferation and re-sensitize cells to the drug (Wang et al., 2021). Again, in colorectal cancer the loss of DAB2IP promotes cell growth and migration and unsensitizes the cells to the cisplatin, oxaliplatin, and doxorubicin by promoting the phosphorylation of AKT and ERK (G. Wu et al., 2021). Loss of DAB2IP is also responsible of temozolomide-resistance in glioblastoma multiforme by promoting the activation of Wnt/β-catenin signaling pathway (E.-J. Yun et al., 2020). Also, higher rate of DNA double-strand break (DSB) repair, more accurate G2-M cell cycle checkpoint control and major resistance to IR-induced apoptosis are observed in DAB2IP-deficient prostate cancer cells after radiation exposure (Kong et al., 2010). Interestingly, DAB2IP expression

decreases after fractionated irradiation and this diminishing is associated to major resistance to γ-rays and α-particles in prostate cancer cells (Yang et al., 2016). Also, downregulation of DAB2IP in renal cell carcinoma results in resistance to IR; the block of the formation of the complex between PARP-1 and E3 ligase caused by DAB2IP downregulation, results in an increase of PARP-1 levels that converges in radio-resistance (E.-J. Yun et al., 2019). Finally, very recently, it has been demonstrated that DAB2IP regulates esophageal squamous cell carcinoma radiosensitivity via enhancing IR-induced activation of the ASK1-JNK signaling pathway (Tong et al., 2022).

1.2.5 Mechanisms involved in DAB2IP downregulation

Multiple mechanisms of DAB2IP inactivation have been identified in cancer cells, suggesting that tumor cells take advantage from the inhibition of a single protein that negatively modulate various oncogenic signals. Intriguing, DAB2IP is usually not inactivated by genetic mutations but it is preferentially inhibited at transcriptional and post-transcriptional level via different mechanisms (Maertens & Cichowski, 2014) (Bellazzo et al., 2017) (**Figure 7**).

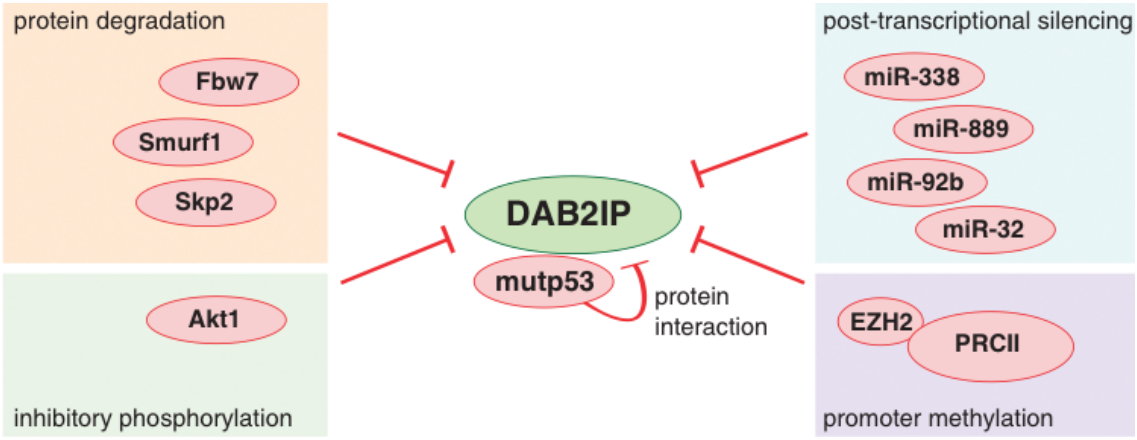

Figure 7 | Main mechanisms involved in DAB2IP regulation (Adapted from Bellazzo et al., 2017).

Promoter methylation

Multiple studies have revealed excessive methylation of the promoter of DAB2IP gene in many types of cancer (Wang et al., 2016) (Yano et al., 2005). The aberrant methylation on DAB2IP gene has been found to be associated with advanced disease stage of lung cancer (Yano et al., 2005). Authors suggest that levels of DAB2IP methylation could be monitored to get information about disease progression (Yano et al., 2005).

The main factor controlling the methylation of DAB2IP gene is the polycomb-repressive complex 2 (PCR-2)-Enhancer of Zeste homolog 2 (EZH2). EZH2 is an epigenetic writer that catalyzes the

trimethylation of H3K27, a modification that induces the consequent recruitment of histone deacetylase (HDAC1), and the decrease of histones acetylation, resulting in reduction of chromatin accessibility by transcription factors. Studies demonstrated that elevated EZH2 levels inversely correlates with hDAB2IP expression and are associated with augment of prostate cancer progression (Chen et al., 2005) (Smits et al., 2012) (Wang et al., 2015).

Proteasome-dependent protein degradation

Additionally, multiple ubiquitin-ligases have been identifying as DAB2IP post-translational regulators. A work revealed the capability of S-phase kinase-associated protein-2 (Skp2), an E3 ubiquitin ligase, to regulate DAB2IP proteasome-mediated degradation, after N-terminal ubiquitination (Tsai et al., 2014). Also another E3 ubiquitin ligase, Smurf1 (SMAD ubiquitylation regulatory factor-1), participates to DAB2IP ubiquitination and elimination (Xiaoning Li et al., 2016). Notably, authors have identified Smurf1 as a target of AKT1/2-mediated phosphorylation; thus, AKT plays an indirect role in enhancing DAB2IP degradation, by increasing Smurf1 stability (Xiaoning Li et al., 2016). On the contrary, the deletion of Smurf1 represses ovarian cancer invasion and EMT by inhibiting AKT/Skp2 signaling loop (Fan et al., 2019). Furthermore, DAB2IP can also be downregulated by the ubiquitin-ligase complex SCF/Fbw7, that was shown to bind the two sequences of the recognition motif of Fbw7, present on DAB2IP protein (Dai et al., 2014).

Protein-protein interaction

Importantly, DAB2IP function can be inhibited through aberrant protein-protein interactions (Bellazzo et al., 2017). DAB2IP can be bound and functionally inhibited by mutant forms of p53 protein in the cytoplasm of cancer cells. This inhibitory binding reprograms the way cancer cells respond to inflammatory cytokines, in particular TNF, and to hormones and grown factors, such as insulin, causing the inhibition of apoptosis, and sustaining tumor cells proliferation and invasiveness, by fostering TNF-dependent NF-κB pathway (Di Minin et al., 2014) and insulin-induced AKT1 activation (Valentino et al., 2017).

Intriguingly, a recent work unveils that DAB2IP improves the stability of wild-type p53 by inhibiting its degradation thorough the binding to ubiquitin ligase-related protein GRP75; all together these studies suggest the existence of a reciprocal regulation between DAB2IP and p53 (Feng et al., 2022). Additionally, DAB2IP is reported to be a target of AKT that weakens DAB2IP inhibitory binding to the protein Ras, through phosphorylation on Serine-847 within its proline-rich domain (Dai et al., 2014). This and other evidences previously described indicate that AKT can modulate DAB2IP

activation and its consequent functions by different ways, standing up a mechanism of reciprocal regulation between DAB2IP and AKT.

Post-transcriptional silencing

Finally, due to the long 3′ UTR sequence of its main transcript, DAB2IP is a strong candidate for microRNAs (miRNAs)-mediated regulation (Bellazzo et al., 2018). By binding the 3′ UTR region of their complementary mRNAs, miRNAs or can act as inhibitors of translation or can induce target transcripts degradation (Oliveto et al., 2017). Different miRNAs involved in DAB2IP downregulation have been identified. For instance, DAB2IP was reported to be downregulated by miR-338, an intronic microRNA that targets a family of modulators of neural differentiation (Barik, 2008). Further studies have shown that miR-32, by targeting DAB2IP, enhances tumor cell survival and decreases radiosensitivity in prostate cancer cells (Liao et al., 2015). Furthermore, miR-889, downregulating DAB2IP expression, promotes proliferation of esophageal squamous cell carcinomas (Xu et al., 2015) and colorectal cancer (Xiao, Li, & Bi, 2019). Also, miR-182 contributes to cell proliferation, invasion and tumor growth in colorectal cancer by inhibiting DAB2IP (Xiaoli Li et al., 2019). Again, microRNA-556-3p promotes the progression of esophageal cancer via targeting DAB2IP (H.-B. Lu, 2018). Also, miR-92b was showed to target DAB2IP and promotes epithelial-mesenchymal transition in bladder cancer (Huang et al., 2016) and growth of gastric cancer by activating DAB2IP-mediated PI3K/AKT signaling pathway (Ni et al., 2020).

Also, miR-149-3p has been identified as a negative post-transcriptional modulator of DAB2IP (Bellazzo et al., 2018). This miRNA, reducing DAB2IP levels and activating NF-κB signaling, enhances prostate and breast cancer cell motility and invasiveness, and promotes the expression of pro-inflammatory and pro-angiogenic factors (Bellazzo et al., 2018). Importantly, miR-149-3p is secreted by prostate cancer cells, and can induce DAB2IP downregulation in nearby vascular endothelial cells, promoting their consequent migration and proliferation (Bellazzo et al., 2018). This study described for the first time a mechanism of cell non-autonomous downregulation of DAB2IP in the tumor environment; such a mechanism may be quite general and involve additional miRNA and possibly other mediators, and has the potential to affect the behavior of stromal cells, thus remodeling the TME to favor dissemination and aggressiveness.

A circular RNA (circRNA) was shown to inhibit the progression of hepatocellular carcinoma by interacting and blocking the miR-328-5p, a negative regulator of DAB2IP (Z. Liu et al., 2019).

Very recently, it has been reported that the lncRNA DMDRMR, as a sponge of miR-378a-5p, increases EZH2 and SMURF1 expression, thus promoting both DAB2IP EZH2-mediated transcriptional repression and DAB2IP SMURF1-mediated degradation. Consequently to DAB2IP

depletion, VEGFA/VEGFR2 signaling pathway is activated, promoting angiogenesis in cell renal cell carcinoma (Y. Zhu et al., 2022).

Extracellular stimuli

Despite multiple molecular mechanisms of DAB2IP inhibition have been described, less information about extracellular stimuli involved in promoting DAB2IP inactivation are present in literature. Qiang Xiao and colleagues have demonstrated that extracellular glucose and insulin could be involved in the regulation of the tumor suppressor DAB2IP in vascular endothelial cells (Li et al., 2015). High amount of glucose in the culture medium of HUVECs, augment mRNA and protein levels of DAB2IP. Curiously, high insulin concentration in culture medium, reverses the effects of high glucose, at least on DAB2IP mRNA; however, authors have not explained the mechanism involved (Li et al., 2015).

Moreover, Zhang and colleagues recently reported that colon cancer cells grown in a soft fibrin matrix display lower DAB2IP expression levels. Specifically, DAB2IP protein levels are reduced in 3D cultures compared to 2D, whereas restoring matrix stiffness is sufficient to increase DAB2IP levels (Zhang et al., 2019). This observation suggests that DAB2IP may be also regulated by mechanical inputs.

1.2.6 Restoring DAB2IP expression reduces cancer aggressiveness

Different works demonstrate that restoring DAB2IP expression in DAB2IP depleted cancer cells reverts metastatic behavior and drug-resistance (see **Table 1**).

Table 1 | Effects of DAB2IP overexpression in various types of tumors

Tumor type	Effects	References
Prostate cancer	reduced tumor growth in xenografts, reduced chemoresistance in vitro	(Min et al., 2010), (Wu et al., 2013)
Bladder cancer	reduced resistance to pirarubicin in vitro	(Wu et al., 2015)
Breast cancer	reduced insulin-induced proliferation in vitro	(Valentino et al., 2017)
Pancreatic cancer	inhibition of cell proliferation, and increased sensitivity to cetuximab in vitro	(Duan et al., 2020)
Gastric cancer	impaired cell proliferation, and increased sensitivity to cisplatin in vitro	(Wang et al., 2021)
Esophageal squamous cell (ESCC) carcinoma	increased survival in ESCC patients, reduced viability in vitro and increased apoptosis after cisplatin treatment and irradiation exposure in vitro	(Tong et al., 2022)

In detail, Min et al. demonstrated that the overexpression of DAB2IP in human prostatic cancer cells reduces the expression of EMT markers in vitro models and impairs tumor growth in xenografts (Min et al., 2010). Another work indicates that the loss of DAB2IP promotes chemoresistance in prostate cancer cells by increasing the expression the anti-apoptotic factor Clusterin, whereas DAB2IP overexpressed cells display a reverse effect. Mechanistically, DAB2IP blocks the crosstalk between Wnt/b-catenin and IGF-I signaling, leading to the suppression of Egr-1 that is responsible for Clusterin expression. Speculatively, restoring DAB2IP protein levels in cancer cells might be a co-adjuvant strategy in promoting cell death after chemotherapeutic agents, via blocking Clusterin expression (Wu et al., 2013). Another evidence supports the hypothesis that DAB2IP overexpression reduces metastasis and chemoresistance also in bladder cancer by inhibiting STAT3 activation and suppressing the expression of Twist1 and its target gene P-glycoprotein, both of which are crucial for chemoresistance to pirarubicin (Wu et al., 2015). Notably, Valentino et al. demonstrated that DAB2IP overexpression reduces insulin-dependent AKT phosphorylation abolishing the increase in proliferation and invasion triggered by insulin in breast cancer cell lines (Valentino et al., 2017).
Also, overexpression of DAB2IP has been shown to decrease the Ras activity, inhibit cell proliferation, and increase sensitivity to cetuximab in pancreatic cancer cells (Duan et al., 2020).

Also, is has been reported that DAB2IP upregulation impairs cell proliferation and sensitizes gastric cancer cells to cisplatin, while DAB2IP depletion displays the opposite effects. Mechanistically, in this context DAB2IP could exert such properties by blocking the phosphorylation and activation of AKT and ERK (Wang et al., 2021). Low DAB2IP levels have been showed to correlate also with chemoresistance and decreased survival in esophageal squamous cell carcinoma (ESCC) patients; on the contrary DAB2IP overexpressed ESCC cells display less viability and higher apoptosis after cisplatin treatment and irradiation exposure. In this context the effect is elicited by DAB2IP-induced activation of the pro-apoptotic ASK1-JNK pathway in response to irradiation (Tong et al., 2022).
Taken together these evidences suggest that DAB2IP may serve as a potential prognostic biomarker and a promising target molecule for the development of new anti-cancer targeted therapies to fight potentially a broad range of cancers.

1.3 ANTI-CANCER TARGETED THERAPY

1.3.1 Small molecules in targeted cancer therapy

Despite traditional chemotherapies are the first-line treatments against cancer, they have the disadvantage to act indiscriminately both on cancer and normal cells causing a wide range of side effects. Since the approval in 2001 of the first targeted small molecule: the tyrosine kinase inhibitor (TKI) imatinib, many different targeted drugs have been developed. Targeted molecules, since are directed against a specific molecular target, present less toxicity and more effectiveness compared to chemotherapy. Patients are selected for treatment with biological targeted drugs on the basis of the presence or absence of specific biomarkers. The main targets of these drugs include protein kinases, cell receptor, epigenetic regulators, DNA damage repair enzymes, and proteasome, among others (Zhong et al., 2021)**.** Despite a wide range of molecules are identified to be altered in cancer, only a few part of these is targetable. This is mainly due by their conformational structure that often impedes the direct binding of a drug or, more frequently, by the existence of multiple biological functions belonging to the targeted molecules that hampers the efficacy and specificity of action of a drug (Bedard et al., 2020). To date, just about 50 small molecules inhibitors have been approved by the Food and Drug Administration (FDA) for oncology indications (**Figure 8**) (Bedard et al., 2020).

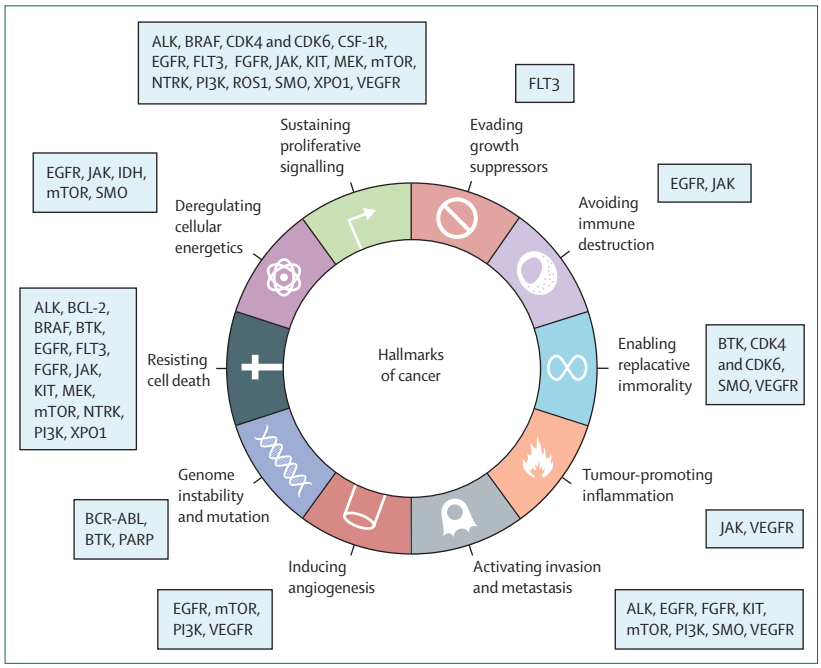

Figure 8 | Targets of approved anti-cancer small molecule inhibitors (Bedard et al., 2020).

The classic examples of molecular targets are the surface cell receptors; they are usually over-expressed or excessively activated in tumors and inhibiting molecules usually act by directly binding and inhibiting their activation.

Also, a plethora of novel therapeutic targets involved in metastasis are identified such as TGF-β, MMP and protein involved in cytoskeleton organization (Stoletov et al., 2020).

For instance, important number of molecules targeting AKT/PKB have been developed to counteract its pro-oncogenic functions. In this regard, two inhibitors, capivasertib and ipatasertib, are now being tested in phase III clinical trials (H. Hua et al., 2021).

Despite different small molecules are developed to counteract the aberrant activation of oncogenes, targeting tumor suppressor genes is more challenging; nevertheless, various small molecules that restore the onco-suppressive function of tumor suppressor genes (TSG) are now used to treat cancer patients. Usually, mutations or loss of function of tumor suppressors are correlated with drug resistance. Noteworthy, therapeutic approaches targeting ubiquitin-proteasome system are used to increase the amount of tumor suppressors overcoming drug resistance, whereas drugs targeting the mechanisms of epigenetic regulation such as DNA methylation, histone modification and chromatin remodeling are already in clinical trials (Gao et al., 2021). Moreover, evidences demonstrate that it is possible to re-activate TSGs via modulating transcription factors in order to increase cancer cells drugs sensitivity. Targeting proteins involved in the nuclear-cytoplasmic transport represents another strategy to counteract mis-localization and thus restoring functionality of TSGs (Gao et al., 2021).

1.3.2 Challenges and opportunities

To date multiple targeted drugs have been approved by FDA and many more are undergoing clinical trials for cancer treatment (Zhong et al., 2021). Despite this, a lot of challenges are still to overcome. One of the main is the acquired drug resistance. Almost all targeted drugs induce drug resistance after a period and this can be due to different mechanisms (most of them were already discussed above). Gene mutation of the target molecule is the main reason leading to anti-cancer drug resistance after targeted therapy. To overcome some of these limitations, nowadays it is become increasingly used the combination of small-molecule targeted drugs with immunotherapy. Also, recently, novel tools, such as CRISPR-Cas9 screening technology, allow to unveil mechanisms responsible for resistance to targeted cancer therapies; this opens novel opportunities for designing next-generation drugs against new targets to improve cancer treatment (Hou et al., 2022).

Another challenge in targeted therapy is represented by its low efficacy; indeed only a few portion of patients effectively respond to a specific therapy and this is demonstrated to be due by the presence

or absence of a specific gene mutation. For this reason, it is important to identify first predictive biomarkers for response to a targeted anti-cancer drug (Zhong et al., 2021).

Another limitation is that only few proteins can effectively be targetable. Recently, several small molecules (e.g. AMG510, MRTX849, JNJ-74699157, and LY3499446) have been developed to specifically target K-RAS (Uprety & Adjei, 2020). However, years of efforts have been required to render the oncogene KRAS druggable. The high binding affinity to its ligand GTP, the small size and its high flexibility render it difficult to be inhibited (Zhong et al., 2021).

Nowadays novel and implemented targeted approaches are under investigation. In this regard, the development of antibody-drug conjugate (ADC) drugs is a promising and emerging area in targeted therapy. Moreover, in the very recent years an innovative technology, called "PROTAC" has been developed. It employs small molecules that recruit target proteins for ubiquitination and degradation by the proteasome. Compared to traditional inhibitory drug, the molecular strategy used by PROTAC reduces a lot the recovery of target protein activity, resulting in a more efficient method of inhibition (Dale et al., 2021).

Importantly, an emerging class of drugs called next-generation drugs are developed by the optimization of existing drugs in order to increase their efficiency, specificity, pharmacological profile and delivery to hard-to-reach sites, as well as to reduce the develop of resistance.

Nowadays also the delivery of anticancer drugs in combination is demonstrated to increase and prolong therapeutic benefits of a single therapy by acting synergically via multiple mechanisms (Bedard et al., 2020).

1.3.3 Drug repositioning for discovering anti-cancer drugs

The high cost and long time required for new drug discovery are the main drawbacks of research and development (R&D). The process of development of new drugs is long and full of obstacles. For each new or old disease it is necessary to find out essential proteins on the bases of the pathology known as the "targets"; around them the drug will be developed (Pushpakom et al., 2018).

Thanks to recent technologies, companies can test millions of compounds in less time. However, once a potential compound is identified it requires several years and several authorizations to determine if it is sufficiently safe and efficient to be used. In the recent years, it has been increasingly used the approach of drug repositioning, a strategy that employs the use of already approved drugs for a different scope from the original medical indication (Pushpakom et al., 2018). This strategy has several advantages. First of all, the time needed to introduce a repositioned drug on the market is significantly reduced compared to those required for a new drug; this because most of the preclinical testing of safety have already been completed. Cause of regulatory affairs regarding safety and

efficacy in animal models and clinical trials the time required to develop a new drug is approximately 12-17 years, whereas drug repositioning process significantly reduces the time required: just 3-10 years are needed to develop an old drug for new treatment (Hua et al., 2020). Further, the risk of failure is lower because the drug has already been found to be sufficiently safe after testing it for the original purpose. Finally, it requires less investment because the phases I and II are almost completely abolished (Pushpakom et al., 2018). Another important advantage of using already approved drugs is that their mechanisms of action are already known as well as their molecular targets and pharmacological properties. There are several examples of drugs whose starting therapeutic indication was not cancer treatment, that now are under investigation for cancer - among them: antibiotics, antidepressants, antipsychotic drugs, cardio-vascular drugs, microbiological agents, non-steroidal and anti-inflammatory drugs (NSAIDs) (Antoszczak et al., 2020).

As regarding the approaches for drug repositioning, they might be subdivided into two big categories: computational approaches and experimental approaches, both of them are being used synergistically. Computational approaches involve systematic analysis of data of any type such as gene expression, chemical structure, genotype or proteomic data. Regarding experimental approaches they mainly involve binding assays to identify target interactions or phenotypic screening to identify compounds that show disease-correlated effects in model systems (Pushpakom et al., 2018). Experimental screening approaches are the most common ones used to uncover new targets for existing approved molecules. They require highly specialized screening facilities and libraries containing up to thousands of compounds that have reached clinical trials or are already FDA-approved. These compounds are screened by using automatic high-throughput systems to find out those that answer to a specific biological question (Cha et al., 2018).

To find out potential compounds able to target a specific molecule is fundamental to clearly, sensitively and quantitatively measure the expression levels or the activity of the endogenous protein and/or detect its localization. This requires the availability of very good antibodies, or highly sensitive phenotypes that can be adapted to a high-throughput screening format. In the absence of the above conditions, to overcome this limitation, a possible strategy is to tag the protein of interest using genome editing. This approach is described in the next chapter.

1.5 CRISPR/Cas9-MEDIATED ENDOGENOUS GENE TAGGING

1.4.1 An overview on endogenous tagging

From its first discovery CRISPR/Cas9 system has been increasingly emerge for its versatility in a broad range of applications. One of them is the insertion of desired sequences of DNA into target genomic regions in order to manipulate the product or the expression of endogenous genes or stably induce the expression of a particular protein of interest. This sort of gene editing is called 'knock-in'. For brevity, in this Thesis I will just describe a specific kind of CRISPR/Cas9-mediated knock-in, that is the gene tagging. The term 'tagging' is referred to the insertion of a tag into specific sites of the genome. The tag usually is a short sequence of DNA that encodes for a protein or a peptide that ones expressed in fusion to a protein of interest improves protein detection or purification exploiting tag-specific properties (Bukhari & Müller, 2019).

Current methods to detect and study gene expression and functions are based on ectopic protein overexpression. In this case the gene of interest is cloned in fusion to the tag under an exogenous promoter in an expression vector. Usually, this approach causes the production of high amount of protein that can cause some artifacts such as protein misfolding, false localization and aspecific protein-protein interaction. Often the endogenous gene is silenced before overexpressing the fusion protein, however, protein overexpression may not always recapitulate original protein behavior (Bukhari & Müller, 2019). For these reasons, in the last years became increasingly popular to tag endogenous gene in order to detect the protein under native conditions.

The knock-in of peptide tags is particular useful when a good antibody against a protein of interest is not available or when the endogenous protein is expressed at too low levels to be clearly detected using standard methods. There are enormous applicative potentials in CRISPR/Cas9-mediated gene tagging. For instance, it can be used to assess the expression levels of a gene of interest or to determine the subcellular localization of endogenous proteins, monitoring their movements through cellular compartments. Also, it is possible to exploit gene tagging to co-immunoprecipitate or purify a protein complex in order to identify and analyze protein-protein interactions (**Figure 9**). CRISPR/Cas9 can be also used to create transgenic animals expressing epitope-tagged genes in order to explore which tissues and/or cell types express the protein of interest (Banan, 2020).

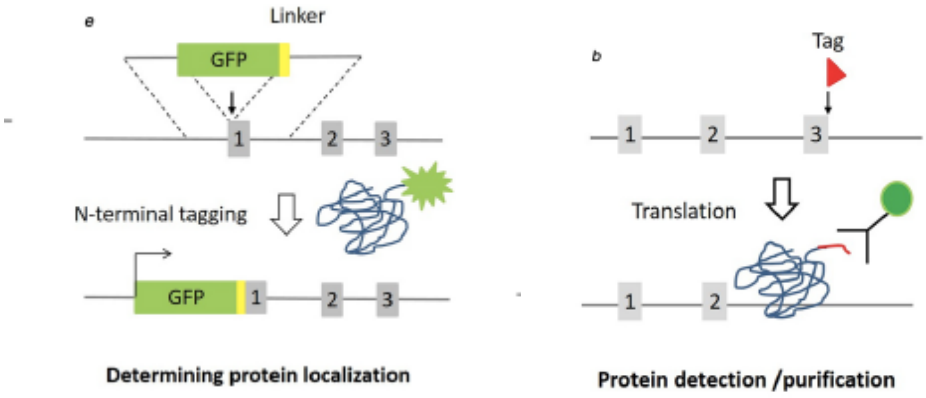

Figure 9 | Application of CRISPRS/Cas9-mediated protein tagging (Banan, 2020).

To answer different experimental needs, a wide range of tags are available:

- epitope tags (such as HA, Myc, Step, His, FLAG, V5): given their small dimensions are well suited for protein detection under native conditions without perturbing protein properties such as folding and functionalities (Banan, 2020); however, since they require the fixation and permeabilization for the recognition from specific anti-tag antibodies they do not enable protein detection in live imaging;
- auto-fluorescent proteins, such as GFP and mCherry: they are well adaptable for monitoring proteins in live cells; nevertheless, their large size could interfere with the 3D structure of the protein (Banan, 2020).
- structure domain-based tags (e.g. GST, MBP, Sumo): they are the best choices for purification through affinity techniques (Urh, 2012) (Terpe, 2003) (Banan, 2020).
- luminescent tags: they allow quantification of the expression levels of tagged proteins with high sensitivity; their enzymatic reaction enables also to monitor protein dynamics in live cells (Schwinn et al., 2018).

In the majority of cases described in literature, the tag is commonly placed at the extreme N' or C' terminus of the target protein. There are different reasons for such decision. The main reason is that the tag at protein termini usually should not interfere with the structure of native protein. Also, the ends of proteins are rarely included in active sites needful for protein functions, thus limiting possible alterations (Jarvik & Telmer, 1998). Despite this, when the tag is inserted at N' terminus, it could compromise protein expression by interfering with the promoter activity or with different transcriptional start sites. Similarly, although the tag at C' terminal end usually results in a minor impact on the structure and functionality of the protein, it is to avoid when the target gene encode for alternative C' terminal spliced isoforms. When these limitations cannot be avoided the tag can be placed in an intramolecular region close to external loop or inactive sites. Hydrophobic regions should

be avoided as they are likely to be in transmembrane domains or in catalytic hydrophobic cores. In case of intramolecular insertion, to guaranteeing the original folding of the protein, the introduction of a flexible linker between the protein and the tag is always recommended (Banan, 2020).

1.4.2 CRISPR/Cas9-HDR-mediated genome editing: advantages and limitations

CRISPR/Cas9 technology exploits the use of a bacterial nuclease (Cas9) and a target specific guide RNA (gRNA) to introduce small short DNA sequences into defined genomic loci by exploiting the two intrinsic cellular DNA repair mechanisms: the non-homologous end joining (NHEJ) and the homology-directed repair (HDR) (Doudna & Charpentier, 2014) (F. Jiang & Doudna, 2017).

Both of them present advantages and disadvantages and it could be possible to favor one mechanisms of integration respect to the other according to specific conditions. When the exogenous DNA sequence, called donor DNA, is delivered as a double-stranded DNA (dsDNA) that contains two homologous arms to the target genomic region, the sequence will be preferentially inserted exploiting the homology-directed repair pathway. HDR enables a very specific integration with less off-targets; however, it may occur just between the S-G2 phases of the cell cycle and thus it can be applied only in dividing cells (Rothkamm et al., 2003) (F. Jiang & Doudna, 2017) (Banan, 2020) (**Figure 10**).

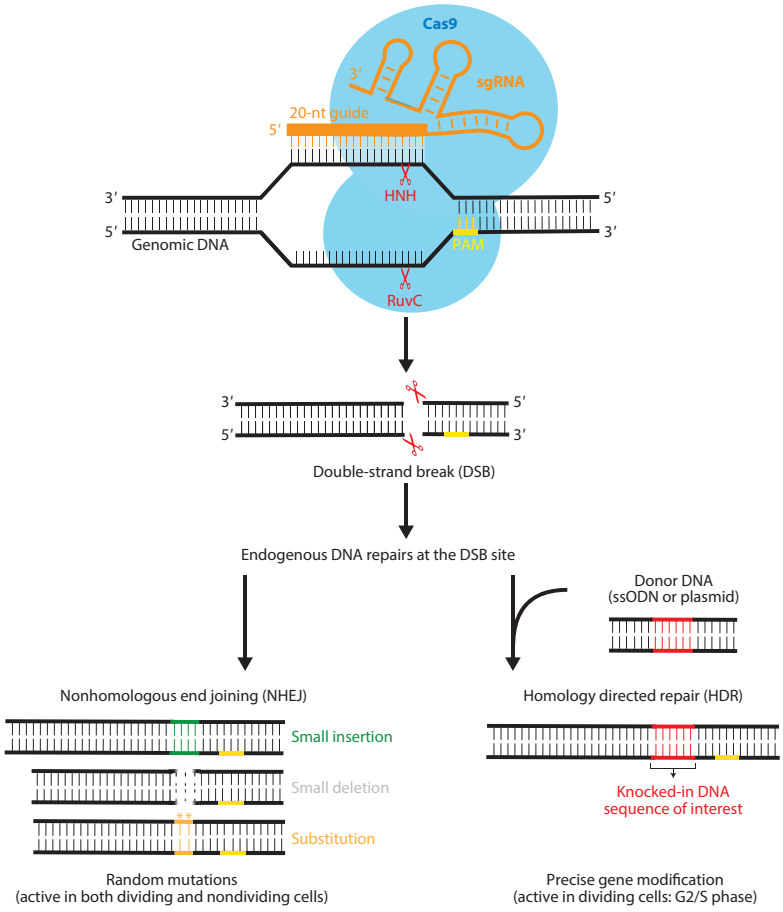

Figure 10 | DNA double-strand break (DSB) repair mechanisms (see the text for explanation) (F. Jiang & Doudna, 2017)

On the contrary, if the dsDNA donor is delivered without homology arms it will be preferably inserted via the NHEJ mechanism. This last method is more efficient because it occurs both in dividing and in non-dividing cells so that also post-mitotic cells (such as primary neurons) could be edited. Since the donor lacks the homologous sequences to the target region it is possible to use a universal template DNA for tagging any gene of interest (ubiquitous template), however the integration may occur in

dual orientations and cause more off-targets compared to HDR (Gao et al., 2019). Moreover, NHEJ is an error prone DNA repair process that may lead to the introduction of small insertion/deletion mutations at the targeted region (White et al., 2017) (F. Jiang & Doudna, 2017) (**Figure 10**).

It is possible to favor the more specific HDR-mediated integration by using cell lines deficient in some NHEJ components or using pharmacological inhibitors of NHEJ (Robert et al., 2015) (Ghetti et al., 2021) that contribute to enhance the rate of HDR-mediated repair events. However, inhibition of NHEJ is likely to be poorly tolerated by most cells, given its fundamental role in normal DNA repair. Alternatively, is possible to favor HDR by synchronizing cells in G1 phase through serum deprivation or pharmacological compounds (Koch et al., 2018) (Banan, 2020), consequently inducing the cells to enter in S-phase after the transfection and thus increasing the chances of recombination. Concerning this point, one of the crucial challenges in CRISPR/Cas9 knock-in is the development of approaches able to improve the HDR:NHEJ ratio. In particular for therapeutic applications seeking to exploit HDR and reduce or eliminate competing NHEJ is still a critical important need (Sander & Joung, 2014).

1.4.3 Delivery strategies for CRISPR components

The bacterial nuclease Cas9 can be delivered into cells as DNA, mRNA or purified protein. The choice among those methods of delivery depends among others on the cells to edit, the editing strategy, as well as availability of laboratory equipment.

The delivery of Cas9 as DNA typically requires the use of plasmids, in which often also the sequence for the target-specific gRNA is inserted (Sander & Joung, 2014). Expression vectors that incorporate the coding sequence for Cas9, gRNA and donor template are available from various commercial companies. On the contrary, when Cas9 is delivered as recombinant protein it could be pre-complexed to the gRNA forming a Cas9:sgRNA ribonucleoprotein (RNP). This last method presents reduced rick of mosaic formation and off-targets insertion due to Cas9 protein short life (24-48h); also Cas9 is immediately available for genome editing and induces less toxicity allowing higher rate of editing (S. Kim et al., 2014) (Gaj et al., 2017). Importantly, gene modification in eukaryotes cells requires the use of a Cas9 containing a nuclear localization signals (NLS) to allow nuclear shuttling (Eoh & Gu, 2019).

Traditionally the sgRNAs were delivered as plasmid or RNA in vitro transcribed; nowadays, is increasingly used to deliver sgRNAs chemically synthesized, however these are much expensive thus limiting the applications. Alternatively, a two-part gRNA can be used: it is composed by a short target specific crRNA plus a longer generic tracrRNA (the sequence required for the binding with Cas9) (Jinek et al., 2012). This ‘dual’ gRNA is cheaper – just the crRNA needs to be re-synthetized for each

new target - resistant to nuclease digestion, limits immune response and has greater stability producing enhanced targeting efficiency (Dewari et al., 2018).

As concerning the DNA donor template, it can be delivered as a single or a double stranded DNA sequence containing the desired insert (tag) - in case of HDR integration - flanked by two homologous arms of variable length to the adjacent sequence of the insertion site in the genome. DNA templates can be synthetized (up to ~100 nts), derived by plasmid DNA following molecular cloning or be PCR products. In designing them it is necessary to consider the position of each gRNA relative to the desired insertion site. It has been shown that HDR efficiency strongly decreases when the predicted site of insertion is just 5–10 bp away from the cut site (Inui et al., 2014).

To date, many strategies are available for Cas9 and CRISPR components delivery. These can be classified into physical delivery methods (e.g. microinjection, electroporation), viral delivery methods (e.g. adeno-associated virus (AAV), full-sized adenovirus and lentivirus), and nonviral vector based methods (e.g. liposomes, polyplexes, gold particles). Understanding the advantages and disadvantages of each delivery strategy is important for choosing the most appropriate for one specific application (Yip, 2020) (**Figure 11**).. In regard to nonviral approaches electroporation is the most popular delivery method. By applying pulses of electrical currents electroporation stimulates the transient opening of pores on cell membrane, permitting the delivery of cargoes into the cell. Given its high efficiency it enables to edit also difficult-to-transfect cell types such as primary cells (Yip, 2020). Electroporation of Cas9:crRNA:tracrRNA ribonucleoprotein was demonstrated to have less off-targets effects compared to plasmid-based or viral deliveries methods and be less toxic on the cells resulting in a higher rate of bi-allelic knock-in frequency (S. Kim et al., 2014) (Dewari et al., 2018).

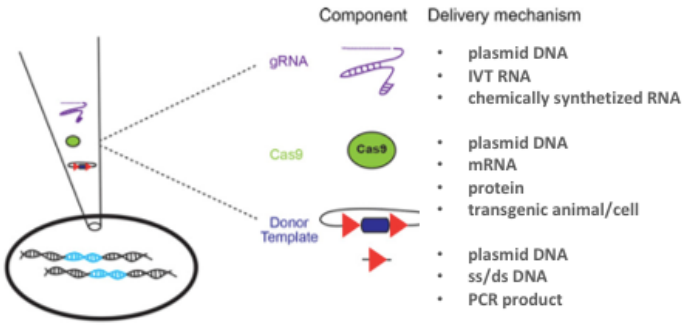

Figure 11 | Summary of delivery strategies for CRISPR components

(Adapted from Harrison et al., 2014).

AIM OF THE THESIS

In the tumor tissue malignant cells and non-transformed stromal cells constantly communicate with each other, eventually creating an environment that supports tumor growth and survival. Cell communication is finely regulated by modulators that cooperate in the regulation of proliferation, apoptosis and migration. Among them, the tumor suppressor DAB2IP, a Ras-GAP and signaling adaptor protein, modulates signal transduction in response to several extracellular stimuli, negatively regulating multiple oncogenic pathways. Accordingly, the loss of DAB2IP in tumor cells exacerbates cancer aggressiveness, promoting metastasis and enhancing chemo- and radio-resistance. Interestingly, DAB2IP is rarely mutated in cancer, but is frequently downregulated or inactivated by multiple mechanisms. Several evidences indicate that DAB2IP reactivation can reduce cancer aggressiveness in tumors driven by multiple different oncogenic mutations.

Based on these evidences, DAB2IP is a strong candidate for development of therapeutics that may increase its protein levels in cancer cells and/or in the tumor stroma, restoring its onco-suppressive role. Despite limited knowledge of the transcriptional and post-transcriptional regulation of DAB2IP, it is possible that drugs already in clinical use may directly or indirectly affect DAB2IP levels by targeting the mechanisms controlling its synthesis or turnover. Similarly, non-coding RNAs may affect DAB2IP levels and may be developed as drugs; for instance, a recently discovered class of antisense non-coding RNAs that modulate translation efficiency (SINEUPs) could be employed to increase DAB2IP expression in cancer cells.
Based on these premises, the main aim of my Thesis was to find molecules capable to increase DAB2IP levels in cancer cells. To achieve this goal, we used a “drug repositioning” approach, screening a library of FDA-approved compounds; we are convinced that even a moderate increase in DAB2IP levels may be able to limit cancer aggressiveness. Since the mechanisms of action as well as the safety profile of FDA-approved drugs are known, we hypothesize that identified DAB2IP enhancers could be potentially tested in combination to traditional chemotherapies for cancer patients, in order to increase the responsiveness to therapies.

Overall, my Thesis project can be divided in four tasks:

- The first task was to assess if an artificial increase of DAB2IP was able to counteract some cancer-related phenotypes. To do this we generated a monoclonal prostate cancer cell line homogeneously expressing ectopic DAB2IP, in order to evaluate the contribution of DAB2IP expression on prostate cancer behavior.

- Since detection of endogenous DAB2IP is technically difficult due to relatively low expression levels and poor performance of available antibodies, the second task was to generate a cell model suitable to measure DAB2IP in a sensitive and quantitative manner, applicable to a high-throughput approach. To do this we applied CRISPR/Cas9 technology to tag endogenous DAB2IP with a peptide that allow luminescence-based detection (Figure 12).
- Taking advantage of this cell model, the third task was to screen a library of FDA-approved drugs to identify those that increase endogenous DAB2IP protein levels. The screen was performed and the best compounds were validated on parental prostate cells and other cell lines (Figure 12).
- Finally, as a fourth task of the project, we started to explore the use of non-coding RNAs to increase DAB2IP translation in prostate cancer cells.

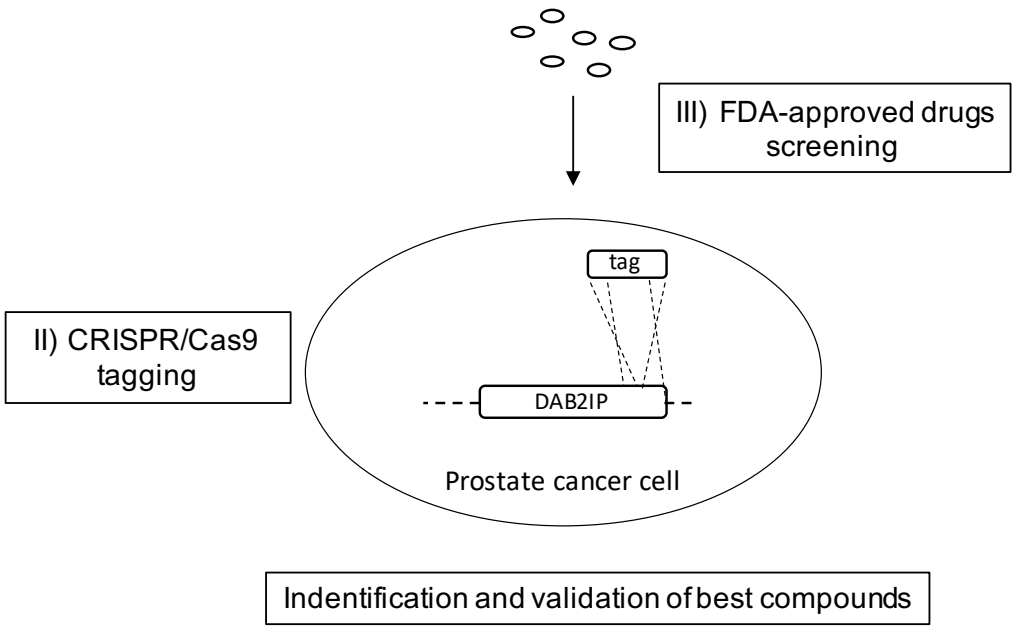

Figure 12 | Schematic representation of the screening workflow.

We tagged endogenous DAB2IP by using CRISPR/Cas9 gene editing in order to measure protein levels variation in a high-throughput contest. FDA-approved molecules were screened using edited cells to find out those that modulate DAB2IP levels.

MATERIALS AND METHODS

2.1 Cell Culture

The following human cell lines were used: immortalized retinal pigmented epithelium hTERT-RPE1, non-small cell lung carcinoma H1299, metastasis-derived prostate adenocarcinoma cell lines PC3 and DU145, breast cancer cell line MCF7, umbilical vein endothelial primary cells HUVEC. hTERT-RPE1 cells were provided by Prof. Luca Fava (CIBIO-Trento). hTERT-RPE1 cells were cultured in DMEM-F12 (1:1) [Euroclone, ECM0728L, ECM0135L] supplemented with 10% Foetal bovine serum (FBS) [OptiClone Serum, ECS0183L, Euroclone], 100 U/mL penicillin and 100 µg/mL streptomycin (pen/strep) solution [Euroclone, ECB3001]. H1299 cells were cultured in RPMI (ECM2001L, Euroclone) supplemented with 10% FBS, and pen/strep solution. PC3 were cultured in DMEM-F12 (1:1) [Euroclone] supplemented with 10% FBS, pen/strep solution, MEM NonEssential Aminoacids [ECB3054D, Euroclone], and Sodium Pyruvate (1 mM), [ECM9542D, Euroclone]. DU145 were cultured in EMEM [LOBE12611F, Euroclone], supplemented with 10% FBS and pen/strep solution. MCF7 were cultured in EMEM [LOBE12611F, Euroclone], supplemented with 10% FBS, pen/strep solution, and human insulin 10ug/ml [Sigma, I2643]. HUVECs, kindly provided by Dr. Roberta Bulla and IRCCS Burlo Garofolo - Trieste, were isolated by collagenase treatment and cultured in HESFM medium (Life Technologies, 11111044) supplemented with 10% FBS, epidermal growth factor (EGF 10 ng/ml), fibroblasts growth factor 2 (FGF2 20 ng/ml) and pen/strep solution. Cells were cultured at 37°C in a humidified incubator with 5% CO_2.

2.2 Drug treatments

Cells were treated with FDA-approved drugs included in the Prestwick Chemical library, that were purchased from GreenPharma. For validation experiments, cells were treated with Thiostrepton CAS-1393-48-2-Calbiochem, purchased from Sigma-Aldrich. In all experiments cells were treated with drugs or with an equivalent volume of DMSO for 36 hours, unless otherwise indicated.

2.3 Transfections

Transfection of pcDNA3-hDAB2IP-HiBiT in H1299 was performed using Lipofectamine 2000 (Invitrogen), following manufacturer's instructions. Transfection of pCS2 SINEUPs in PC3 was performed using Lipofectamine 3000 (Invitrogen), following manufacturer's instructions (SINEUPs sequences in **Table 3**). For knockdown experiments, cells were transfected the same day of plating (384-well plates) or 24 hours after plating (6-well plates). For siRNA experiments, cells were transfected with 50nM siRNA (384-well plates) or 40nM siRNA (6-well plates) or 3nM miRNAs

mimics (6-well plates) using Lipofectamine RNAiMax (Invitrogen), following manufacturer's instructions. Cells were processed after 48 hours, except when differently specified. DAB2IP silencing was performed using a mix of siDAB2IP A and siDAB2IP B. hTERT-RPE1 cells were transfected twice.

Sequence of siRNAs/miRNA used:

siRNA/miRNA	Sequence	Purchased from
Control siRNA	Unknown	All Star negative control (1027281, Qiagen)
siDAB2IP A	GGAGCGCAACAGUUACCUG	Eurofins MWG
siDAB2IP B	GGUGAAGGACUUCCUGACA	Eurofins MWG
hsa-miR-149-3p	AGGGAGGGACGGGGGCUGUGC	Dharmacon

2.4 Retroviral Transduction

For generation of prostatic cancer cells stably expressing ectopic hDAB2IP, low confluence (~20%) 293GP packaging cells, stably expressing retroviral gag and pol proteins, were transfected by calcium-phosphate precipitation. Briefly, cells were plated the day before the transfection in 10 cm^2 dishes in DMEM with 10% FBS and antibiotics. Each different virus was produced by co-transfection of 10 μg of the vector of interest and 5 μg of pEnv encoding vector. After 8 hours, medium was changed and cells were incubated at 37°C. After 48 hours the virus-containing medium was filtered (0.45 μm filter) and supplemented with 10% FBS and polybrene (8 ug/ml). The culture medium of target cells growing at low confluence (~ 30-40%) was replaced by the appropriate viral supernatant and incubated at 37°C for 24 hours. After 48 hours from infection, cells were selected with puromycin (0.5 μg/ml) and kept under selection for the entire experiment. Retroviral constructs encoding DAB2IP and DAB2IP-targeting Short Harpins (shDAB2IP) are described in the Results.

2.5 Immunofluorescence

Cells were seeded on glass coverslips in 6-well plates with 2ml of medium. After 24 h cells were fixed with 4% paraformaldehyde (PFA) for 15 min, permeabilized with 0.5% Triton X-100 in phosphate buffered saline (PBS) solution for 10 min, followed by 30 min blocking in 3% bovine serum albumin (BSA) in PBS. Cells were then stained for 2 hours at 37°C with the primary antibodies (list of primary antibodies in **Table 2**), diluted in blocking solution (BSA 3% in PBS). Cells were washed with PBS and incubated for 2 hours, at room temperature, with the following secondary antibodies: Goat anti-Mouse Alexa Fluor-488 (green) [A11001, LifeTech], Goat anti-Rabbit Alexa Fluor-488 (green) [A11008, LifeTech], or Goat anti-Rabbit Alexa Fluor-568 (red) [A11011, LifeTech]. Cell nuclei were further stained with 1 μg/ml Hoechst (LifeTech). After 3 final PBS

washes, followed by one ddH2O wash, the coverslips were mounted on glass slides with ProLong Gold Antifade Reagent [Invitrogen, P36934]. Mounted coverslips were stored at 4°C in the dark.

2.6 RNA expression analysis

Total RNA was extracted with TRIFAST II [EMR517100, Euroclone] using a standard protocol. For RT-qPCR, 500 ng of total RNA was reverse transcribed with iScript Advanced cDNA Synthesis Kit (mRNA) [1725038, Biorad]. Real-time PCR was performed using iTaq Universal SYBR Green SMX 5000 [1725124, Biorad] on a CFX96 Real-Time PCR System [Biorad].
Primer sequences were as follows:

Target	Sequences 5'→3':
hDAB2IP	Fw: CACATCACCAACCACTAC Rv: TCCACCTCTGACATCATC
MMP9	Fw: GCCGCCTTTGGACACGCACGACGT Rv: GCAGGACGGGAGCCCTAGTC
ANGPT1	Fw: AGCGCCGAAGTCCAGAAAAC Rv: TACTCTCACGACAGTTGCCAT
ADRB2	Fw: TACCAGACCCTGCTGACCAAGA Rv: AGTCACAGCAGGTCTCATTGGC
CD13 (APN)	Fw: GCTGTTTGACGCCATCTCCTAC Rv: GTTCTGGTAGGCAAAGGTGTGG
H3	Fw: GTGAAGAAACCTCATCGTTACAGGCCTGGT Rv: CTGCAAAGCACCAATAGCTGCACTCTGGAA

2.7 Analysis of hDAB2IP isoforms

For assessing the expression of predicted C'-terminal splice isoforms of hDAB2IP, 500 ng of total RNA was reverse transcribed with iScript Advanced cDNA Synthesis Kit (mRNA) [1725038, Biorad]. PCR reactions were done using Taq DNA Polymerase [201203, Qiagen] on a MiniAmp™ Thermal Cycler [Thermo Fisher], using the following 50 µL PCR reaction:

Reagents	Volume (µL)
Buffer 10X	5
dNTPs (10 mM)	1
Primer Fw (10 µM)	2.5
Primer Rv (10 µM)	2.5
Taq Polymerase	0.25

DNA (~ 10 ng/µL)	5
Water	33.75

PCR reactions were carried out with the settings listed below:

Cycle Step	Temperature	Time	Cycles
Initial Denaturation	95°C	2min	1
Denaturation	95°C	1min	30
Annealing	60	1min	
Extension	72°C	30sec	
Final extension	72°C	7min	1
	4°C	∞	

Primer pairs designed to distinguish the alternative splicing isoforms (see **Figure 14**) are as follows:

Target	Sequences 5'→3':
hDAB2IP C-terminal unspliced	Fw: ATCAGCAGGTTGATGTCCGT Rv: TGCAATTTGGTGGGGTTGGT
hDAB2IP C-terminal spliced	Fw: TCAGCAGGTTGATGTCCGTG Rv: TGCGCACGCTCAACTTAAAA

2.8 Protein expression analysis

Cells were lysed in 2X SDS Sample buffer (125 mM Tris-HCl at pH 6.9, 4% SDS, 20% Glycerol, 3% β-mercaptoetanol). Samples were sonicated 10 sec at 20% potency and boiled at 95°C for 5 min. 10-20 ug of lysates were loaded in polyacrylamide gels and resolved by SDS-PAGE in BioRad Mini-Protean® Tetra System. Proteins were electroblotted on Protran 0.2 nitrocellulose membranes [GE Healthcare, 10600001] using a semidry transfer system for 10 min at 1.3 A, 25 V. Membranes were blocked for at least 1 hour at room temperature in 5% skim milk PBST (0,1% Tween-20 in PBS) and then incubated overnight at 4°C with primary antibody diluted in 5% skim milk PBST (**see Table 2**). Membranes were washed three times in PBST and left in agitation in PBST 3 times for 10 min. Then were incubated for 1 hour at 4°C with horseradish peroxidase (HRP)-conjugated secondary antibody diluted 1:4000 in 5% skim milk PBST. Membranes were washed again as described above and kept in PBS before detection. Protein detection was performed by chemiluminescence using Liteablot Extend [EMP013001, Euroclone] for DAB2IP and c-Myc, and with ECL [32209; Thermo Scientific] for normalization markers. Chemiluminescent signal was impressed on Hyperfilm ECL [Amersham]. The following secondary antibodies were used:

Antigen	Conjugation	Species	Company	Clone	Dilution
Anti-Mouse IgG	HRP	Goat	Bethyl, A90-516P	Polyclonal	1:4000
Anti-Rabbit IgG	HRP	Goat	Bethyl, A120-201P	Polyclonal	1:4000

2.9 DAB2IP C-terminal-HiBiT reporter: construct generation

To evaluate the applicability of the HiBiT tag (Promega) in detecting DAB2IP protein levels we cloned HiBiT in fusion to hDAB2IP in an expression vector. C-terminal-HiBiT reporter was obtained by cloning the C-terminal end of hDAB2IP in fusion to HiBiT in the pcDNA3-Myc-hDAB2IP plasmid (provided by Sidney Yu, University of Hong Kong). The plasmid was digested with AscI and XbaI and ligated with C-termDAB2IP-linker-HiBiT obtained from PCR reaction using the following primers (Eurofins MWG):

Primers	Sequences 5'→3':
Forward primer (AscI-hDAB2IP FW)	ACCTCCGAGGGCGCGCCA
Reverse primer (XbaI-HiBiT-hDAB2IP REV)*	ACCACCTCTAGA**CTA**HiBiTGCCGCTGCTGCC TTTCAGCTGGGTCAGGGCACTC

*Reverse primer is composed as follows:

- 21nt ORF C-terminal hDAB2IP
- linker (GSSG) + HiBiT
- **Stop codon**
- XbaI site
- additional bases (6bp)

The following PCR mix (50 µL/reaction) was utilized to amplify the insert:

Reagents	Volume (µL)
HF Phusion Buffer 5X	10
dNTPs (10 mM)	1
Primer Fwd (10 µM)	2,5
Primer Rev (10 µM)	2,5
Phusion Polymerase (2 U/µL)	0,5
DNA (2 ng/µL)	1
DMSO	1,5

Water	31

PCR reactions were carried out with the thermocycler settings listed below:

Cycle Step	Temperature	Time	Cycles
Initial Denaturation	98°C	30 sec	1
Denaturation	99°C	10 sec	30
Annealing	69°C	10 sec	
Extension	72°C	30 sec	
Final extension	72°C	7 min	1
	4°C	∞	

Obtained plasmid was transformed into DH5-alpha [NEB]. Colonies were screened for ampicillin resistance and insert size by restriction enzyme digestion. Correctness of insertion was checked by Sanger Sequencing, using Eurofins pcDNA3 reverse standard primer.

2.10 crRNAs: design and synthesis

Except for PCR primers (Eurofins), all the synthetic nucleic acids were purchased from Integrative DNA Technologies (IDT). For CRISPR-Cas9 knock-in gene tagging, crRNAs were designed using three online tools, providing as search base an 80–100 bp genomic sequence retrieved from Ensembl Genome Browser and centered around the preferred editing site:

1. IDT Custom Alt-R® CRISPR-Cas9 guide RNA (https://eu.idtdna.com/site/order/designtool/index/CRISPR_CUSTOM)
2. CRISPOR (http://crispor.tefor.net/)
3. GPP sgRNA Designer (https://portals.broadinstitute.org/gpp/public/analysis-tools/sgrna-design).

crRNAs were chosen by comparing the on-target and off-target scores calculated by all three of the tools listed above. crRNAs are usually selected privileging the proximity of the Cas9 cut site to the editing target site: max 5-10 bp when possible. In case of crRNAs targeting C-terminal regions they were designed to cut as close as possible to the stop codon of the mRNA of interest. The cut site of DAB2IP_intramolecular localizes in an intramolecular non-catalytic region, next to a Serine-rich region (hydrophilic).

The following table reports lists the guides together with their PAM sequence (NGG):

crRNA	Sequence	PAM Sequence
DAB2IP_intramolecular	GTGATTGAGAACGATCTTTC	CGG

DAB2IP_ nonspliced (Q5VWQ8-2)	AGCAATTGTTAACCTGCCTG	AGG
DAB2IP_ spliced (Q5VWQ8-5)	TTTCTAATGCATACTGTGAA	AGG
DAB2IP_ C-terminal of both isoforms	CCCTGACCCAGCTGAAAGAG	AGG

2.11 V5 and HiBiT Single Strand DNA Donors: design and synthesis

To perform HDR-driven gene editing reactions, 150 bp ca. single stranded donor DNAs (Ultramer® DNA Oligos, IDT) were synthesized. Each donor included two symmetric flanking regions (50 bp ca. each) providing left and right homology arms, and a central region for the desired knock-in sequence. The knock-in sequence encoded a short flexible linker (Gly-Ser) followed by the chosen small epitope, e.g. V5 (GKPIPNPLLGLDST). Ultramer® DNA Oligos were designed using the online tool Dharmacon Edit-R HDR Donor Designer-oligo (https://horizondiscovery.com/en/dharmacon). Single stranded DNA donors were designed with the insertion site as close as possible to the predicted editing site, because the HDR rate decreases significantly when the template insertion is just 5-10 bases away from the cut site. Moreover, the donor was designed in such a way that the correct insertion disrupts the gRNA recognition site, thus preventing Cas9 nuclease activity towards the genomic locus after integration of the desired edit. The Ultramer DNA Oligos are described in **Figures 16 and 18.**

2.12 RNP Assembly and Electroporation

The procedure was exactly as described in Ghetti et al., 2021. Cas9 was delivered as recombinant protein because of its higher efficiency and lower chance of off-targets effects, compared to plasmid-based or viral delivery methods. gRNAs were assembled by mixing together 1:1 crRNA (100 µM) and tracrRNA (100 µM) [Alt-R® CRISPR-Cas9 tracrRNA, IDT, 1072533] to a final concentration of 50 µM. The mixture was heated at 95°C for 5 min and then cooled at room temperature. To prepare RNPs, gRNA (150 pmol) was incubated with Cas9 protein (120 pmol) at room temperature for 20 min. DPBS was added to reach the final volume of 5 µL. gRNAs can be stored at -20°C for 1 year, while RNP can be stored at 4°C for 1 month or at -80°C for 2 years in ready-to-use aliquots.
For the electroporation reaction, cells were detached by trypsinization and resuspended in complete medium. Cells were centrifuged 400xg for 5 min and washed twice with DPBS. $2x10^5$ (DU145 and RPE), or $1.5x10^5$ (PC3) cells/reaction were harvested and resuspended in 20 µL of complete:

- P3 electroporation buffer [P3 Primary Cell 4D-Nucleofector™ X Kit S, Lonza, V4XP-3032] (hTERT-RPE1).
- SE electroporation buffer [SE Cell Line 4D-Nucleofector™ X Kit S, Lonza, V4XP-3032] (PC3 and DU145).

Then 5µL of RNP were added to the mixture together with 1,2 µL of Alt-R® Cas9 Electroporation Enhancer (100µM) [IDT, 1075916]. 120 pmol of single stranded donor DNAs (100 µM) [Ultramer® DNA Oligos] were introduced.

The mixture was then transferred in 16-well Nucleocuvette StripsTM [Lonza] (25 µL/well). Cells were electroporated using the 4D-NucleofectorTM [Lonza, AAF-1002B] using the following programs:

- EA-104 for hTERT-RPE1,
- DS-137 for PC3,
- CA-137 for DU145.

10 min after electroporation, 75 µL of complete medium with or without NU7441 (1µM) were added to nucleofected wells and cells were transferred into new 12-well plate to allow for recovery. Each well was filled with pre-warmed complete medium with or without NU7441 (1µM). 24h after electroporation the medium was replaced with fresh medium with NU7441 (1µM). 48h post-nucleofection the culture medium was removed and replaced with fresh and complete medium without drug.

2.13 Generation of monoclonal cell lines

For generation of genetically homogenous edited clonal cells, nucleofected or transduced cells were seeded with a density of 0,5 cell/well or 1 cell/well in a 96-well plate previously filled with 200 µL/well of complete medium. Cells were incubated for at least 2 weeks before expansion and characterization. At least 24 isolated monoclonal lines per condition were characterized by immunoblotting and genomic PCR (see 2.14).

2.14 Genomic DNA analysis

In order to assess the allelic status of isolated V5 and HiBiT positive clones, we designed PCR primers to amplify small regions (300-400 bp) around the insertion site. Synthesized oligos [Eurofins] are reported below:

Locus	Forward Primer	Reverse Primer
hDAB2IP intramolecular_419bp (V5)	GAGGTCACACCTGCCTCTTG	AACCTATAGCATCACCTCCTCT
hDAB2IP C-terminal_340bp (HiBiT)	TACCTTCTCTTGCCAGCTGC	GGTAGCTTCCTCCCTCCTCA

Genomic DNA was extracted from bulk samples 72h post electroporation, or from positive monoclonal cell lines, using a commercial DNA extraction kit [Zymo Research, ZYD3024] following

the protocol for cultured cells. DNA was quantified using NanoDrop spectrophotometer and diluted to 10 ng/μL working concentration. PCR reactions were carried out following the same thermocycler settings listed above (see Section 2.7), except for the extension time that was changed according to the length of amplicons.

PCR products were run in a 2% agarose gel to allow a clear separation between wild type and knock-in amplicons. Correct integration was checked by Sanger sequencing of PCR products of some homozygous clones using the respective reverse primer.

2.15 High Throughput Screening

For the screening experiment, PC3-HiBiT cells (4.0×10^3 per well) were seeded on white opaque 384-well microplates [Perkin Elmer, 6007690], 24 hours later 1280 FDA-approved & EMA-approved drugs [Prestwick Chemical Library®] were transferred robotically from library stock plates (1mM in DMSO) to the plates containing the cells; control (DMSO) was added to columns 1, 2, 23 and 24 of each plate. Cells were processed 36h after addition of drugs. Briefly, medium was aspirated with Plate washer BioTek 405, leaving 10μL of medium. 10μL of CellTiterFluor reagent (Promega) (2X) was added to the cells, and cells were incubated for 30 min at 37°C, 5% CO_2. CellTiterFluor reagent is a non-lytic fluorescence-based assay that measures the relative number of viable cells in culture, and it is compatible with other luminescence assays. Cell viability was measured in order to normalize the HiBiT-DAB2IP levels for fluctuations in the number of cells, due to variable pipetting or to drug toxicity. Fluorescence was detected using EnVision multimode plate reader with dual monochromator [PerkinElmer]. Immediately after, 40μL of NanoGlo Lytic reagent (Promega) (2X) was added on the cells prior incubated with the CellTiterFluor, without removing reagent. Cells were incubated for 10 min at room temperature and luminescence was detected with EnVision multimode plate reader. Luminescence values were normalized on fluorescence readings. Screening was performed once, at 10μM drug concentrations; final concentration of DMSO in the culture medium was 1% (v/v). The screening was performed at the ICGEB High-Throughput Screening Facility (https://www.icgeb.org/high-throughput-screening-equipment/).

2.16 Assays to measure luciferase (DAB2IP-HiBiT expression) and viability

In order to assess the minimal effective dose of drugs required for phenotypic assays, cells were plated in triplicate in the presence of escalating drug concentrations. In detail, cells were plated in white opaque 96-well microplates [PerkinElmer, 6005680] one day before treatment. 36h after addition of drugs (unless otherwise indicated), medium was removed and 40μl of CellTiter-Fluor Cell Viability Assay reagent (1X) [G6081, Promega] was added to cells (2X reagent was diluted in an equal volume

of medium). Cells were mixed briefly by orbital shaking and incubated at 37°C, 5% CO_2 for 30 min. Fluorescence was detected using a multimode plate reader ($400nm_{Ex}/505nm_{Em}$). Next, 40µl of Nano-Glo HiBiT Lytic Detection reagent (2X) [N3040, Promega] were added to wells, plates were mixed briefly by orbital shaking and incubated at room temperature for 10 min before luminescence detection. Fluorescence and Luminescence were measured using EnVision multimode plate reader [PerkinElmer].

The half-maximal Effective Concentration (EC_{50}) value was defined as the drug concentration at which there was a 50% (respect to the maximum value) increase or decrease in DAB2IP levels (ratio luminescence/fluorescence). The IC_{50} value was defined as the drug concentration at which there was a 50% decrease in cell viability (fluorescence). Data were analysed using Prism 7.0 (GraphPad), and EC50 and IC50 values were calculated by nonlinear regression analysis using the dose–response (variable slope) equation.

2.17 Colony formation assays

In order to assess the effects of drugs on cell proliferation, the capability of cells to form colonies was measured. Briefly, cells were seeded at a density of 5000 cells per 6 cm diameter plate, and incubated for 24 hours in 10% FBS-supplemented culture medium. Cells were treated with drugs at EC_{50} concentration changing the medium every 48 hours. After 10 days, cells were fixed in 4% PFA and stained with crystal violet [C-6158, Sigma] for 45 min. Plates were photographed and colony formation efficiency was calculated by measuring the % of colonies covered area over whole dish area. The areas were measured using ImageJ software.

2.18 Transwell invasion assays

In order to assess the effects of drugs on the capabilities of cells to degrade extracellular matrix and invade surrounding tissues, logarithmically growing cells were pre-treated in high serum (10% FBS) with various drugs (EC_{50} concentration) or DMSO for 24 hr. Subsequently, cells were trypsinized and counted, and $9x10^5$ cells were reseeded in 24-well PET inserts (8 µm pore size, Falcon) coated with BD Matrigel [BD Bioscience], in low serum medium (0.1% FBS) with or without drugs. The lower chamber was filled with high serum medium (10% FBS) without drug. After 18h, cells that were able to degrade matrigel and to pass through the filter were fixed in 4% PFA, stained with 0.1% crystal violet, and counted. Invasion was scored by counting cells in 5 random non-overlapping microscope fields at 100X magnification.

2.19 Wound healing assays

In order to assess the effect of drugs on cell migration, we monitored the capability of cells to fill the space created by a "wound" in a monolayer. Cells were grown to confluency and a scratch was made with a pipette tip to create an incision-like gap. The scratch area was photographed at defined time points, and cell migration was quantified and expressed as average rate of closure of the scratch. In detail, cells were plated on 96-well plates in presence of Hoechst (0,2 μg/ml) [LifeTech] and cultured to 90% confluence. Cells were scraped with a sterile pipette tip, and treated with drugs (or DMSO) at EC50 concentration; wound closure was followed for 48 hours. Images of live cells were automatically acquired with PerkinElmer Operetta every 12 hours. The width of the scratches was measured using ImageJ. Migration distances, M(t), were calculated as followed:

$$M(t) = \text{width}(0) - \text{width}(t),$$

where width (t) is the wound width at time t and width (0) is its initial width.

2.20 Statistical analysis

All the results are expressed as mean ± SEM. Values of $p<0.05$ were considered statistically significant. For statistical comparison of two groups, unpaired, two-tailed Student's t-test was used; for the comparison of three or more groups, one-way ANOVA followed by Dunnett's post-hoc test was used, as indicated in figure legends and text. The number (n) of independent experiments is indicated in the figures or figure legends. Data were analyzed using Prism 7.0 (GraphPad).

Table 2 | List of primary antibodies used

Antigen	Species	Company	Dilution IF	Dilution WB
V5-tag	Rabbit (monoclonal)	Cell Signaling, 13202	1:500	1:5000
DAB2IP	Rabbit (polyclonal)	Abcam, ab87811	1:250	
DAB2IP	Rabbit (polyclonal)	Bethyl, A302-440A		1:4000
Myc-tag	Mouse (monoclonal)	9E10 hybridoma supernatant	1:1	1:100
HSP90	Mouse (monoclonal)	Santa Cruz, sc-13119		1:8000
Actin	Rabbit (polyclonal)	Sigma, A2066		1:8000
Tubulin	Mouse (monoclonal)	Sigma, T5168		1:8000

Table 3 | List of SINEUP sequences that were cloned in pCS2 plasmids (XhoI-HindIII)

miniSINEUP	Sequence
hDAB2IP.001 (-40/+4 M1)	CTCGAGGCATCAGATGGGACCTGTCACAGGTGCCCCACCACCAG GCTTTCATCTGCAGAATTCGCCCTTCAGTGCTAGAGGAGGTCAG AAGAGGGCATTGGATCCCCCAGAACTGGAGTTATACGGTAACCT CGTGGTGGTTGTGAACCACCATGTGGATGGATATTGAGTTCCAA ACACTGGTCCTGTGCAAGAGCATCCAGTGCTCTTAAGTGCTGAG CCATCTCTTTAGCTCCAAGCTT
hDAB2IP.002 (-14/+4 M1)	CTCGAGGCATCAGATGGGACCTGTATCTGCAGAATTCGCCCTTC AGTGCTAGAGGAGGTCAGAAGAGGGCATTGGATCCCCCAGAACT GGAGTTATACGGTAACCTCGTGGTGGTTGTGAACCACCATGTGG ATGGATATTGAGTTCCAAACACTGGTCCTGTGCAAGAGCATCCA GTGCTCTTAAGTGCTGAGCCATCTCTTTAGCTCCAAGCTT
hDAB2IP.003 (-40/+4 M2)	CTCGAGCCATGCTGAGGTCCAGCGCCTCCACCGCACTGCTGGGG CTGAGCATCTGCAGAATTCGCCCTTCAGTGCTAGAGGAGGTCAG AAGAGGGCATTGGATCCCCCAGAACTGGAGTTATACGGTAACCT CGTGGTGGTTGTGAACCACCATGTGGATGGATATTGAGTTCCAA ACACTGGTCCTGTGCAAGAGCATCCAGTGCTCTTAAGTGCTGAG CCATCTCTTTAGCTCCAAGCTT
hDAB2IP.004 (-14/+4 M2)	CTCGAGCCATGCTGAGGTCCAGCGATCTGCAGAATTCGCCCTTC AGTGCTAGAGGAGGTCAGAAGAGGGCATTGGATCCCCCAGAACT GGAGTTATACGGTAACCTCGTGGTGGTTGTGAACCACCATGTGG ATGGATATTGAGTTCCAAACACTGGTCCTGTGCAAGAGCATCCA GTGCTCTTAAGTGCTGAGCCATCTCTTTAGCTCCAAGCTT

hDAB2IP.005 (-40/+4 M1 V3)	CTCGAGACATGCTGCCGCCCGCCGGGCACCGGGCCGGGCCTGGG CGCGCTATCTGCAGAATTCGCCCTTCAGTGCTAGAGGAGGTCAG AAGAGGGCATTGGATCCCCCAGAACTGGAGTTATACGGTAACCT CGTGGTGGTTGTGAACCACCATGTGGATGGATATTGAGTTCCAA ACACTGGTCCTGTGCAAGAGCATCCAGTGCTCTTAAGTGCTGAG CCATCTCTTTAGCTCCAAGCTT
hDAB2IP.006 (-14/+4 M1 V3)	CTCGAGACATGCTGCCGCCCGCCGATCTGCAGAATTCGCCCTTC AGTGCTAGAGGAGGTCAGAAGAGGGCATTGGATCCCCCAGAACT GGAGTTATACGGTAACCTCGTGGTGGTTGTGAACCACCATGTGG ATGGATATTGAGTTCCAAACACTGGTCCTGTGCAAGAGCATCCA GTGCTCTTAAGTGCTGAGCCATCTCTTTAGCTCCAAGCTT

RESULTS

This section will present the results obtained during my PhD period. I focused on two major projects that will be described and discussed as separate sections.

The first is described in PART I and is divided in two different tasks:

The first task involved the generation of a stably edited cell line, using CRISPR/Cas9 system, that was used for the small molecules high-throughput screening. The technical approach will be described in detail, taking into considerations also the workflow of a prior procedure as support to the successful strategy.

The second task is still ongoing, and I will present in detail the results obtained so far about the identification and characterization of molecules affecting DAB2IP levels.

To start I will do a brief digression about proof-of-concept evidences that I obtained to evaluate and confirm the feasibility of the research project.

Finally, as a side project, I briefly explored the use of RNA therapeutics in increasing DAB2IP levels. This work is still in progress and is described in PART II.

PART I

OVEREXPRESSING DAB2IP IN HUMAN PROSTATE CANCER CELLS REVERTS AGGRESSIVENESS AND METASTATIC BEHAVIOR

3.1 DAB2IP over-expression reduces prostate cancer cell viability, proliferation and invasion

To explore the effect of DAB2IP up-regulation on cancer cells behavior we stably expressed human DAB2IP in human prostate cancer PC3 cells, a cell line that expresses low levels of DAB2IP. We transduced PC3 with a retrovirus encoding epitope-tagged hDAB2IP, and selected from the bulk of infected cells those single clones displaying the lowest levels of ectopic DAB2IP protein (Figure 13A-D). Next, we used one such clone (clone 10) to perform cell viability, proliferation, migration and matrigel invasion assays, in order to assess the impact of DAB2IP overexpression on known DAB2IP-related phenotypes.

Cell viability was monitored by CellTiterFluor assay. Proliferation was assessed by colony formation, an in vitro assay based on the ability of a single cell to grow into a colony (Franken et al., 2006). Migration was evaluated by wound-healing assays; invasion properties were assessed by transwell matrigel invasion assays.

Interestingly, we observed that increased DAB2IP levels slightly reduce cell viability (Figure 13E), but significantly decrease the proliferative (Figure 13F) and migratory (Figure 13G) capabilities of PC3 as confirmed by colony formation assay and wound healing assay, respectively. Invasion assays showed that augmenting DAB2IP levels counteracts the capability of prostate cancer cells to degrade an extracellular matrix (Figure 13H). Together, these results confirm earlier evidences obtained in various tumor cells types (Chen et al., 2019) (Feng et al., 2022) and support the hypothesis that increasing DAB2IP levels may counteract the pro-oncogenic behavior of prostate cancer cells. Therefore, since DAB2IP is rarely mutated or deleted in cancer, but is preferentially inactivated by epigenetic silencing or post-transcriptional mechanisms, this gene is a strong candidate for development of anti-cancer drugs and/or RNA-based therapeutics that may increase its protein levels in cancer cells, or in cells of the tumor microenvironment.

Figure 13

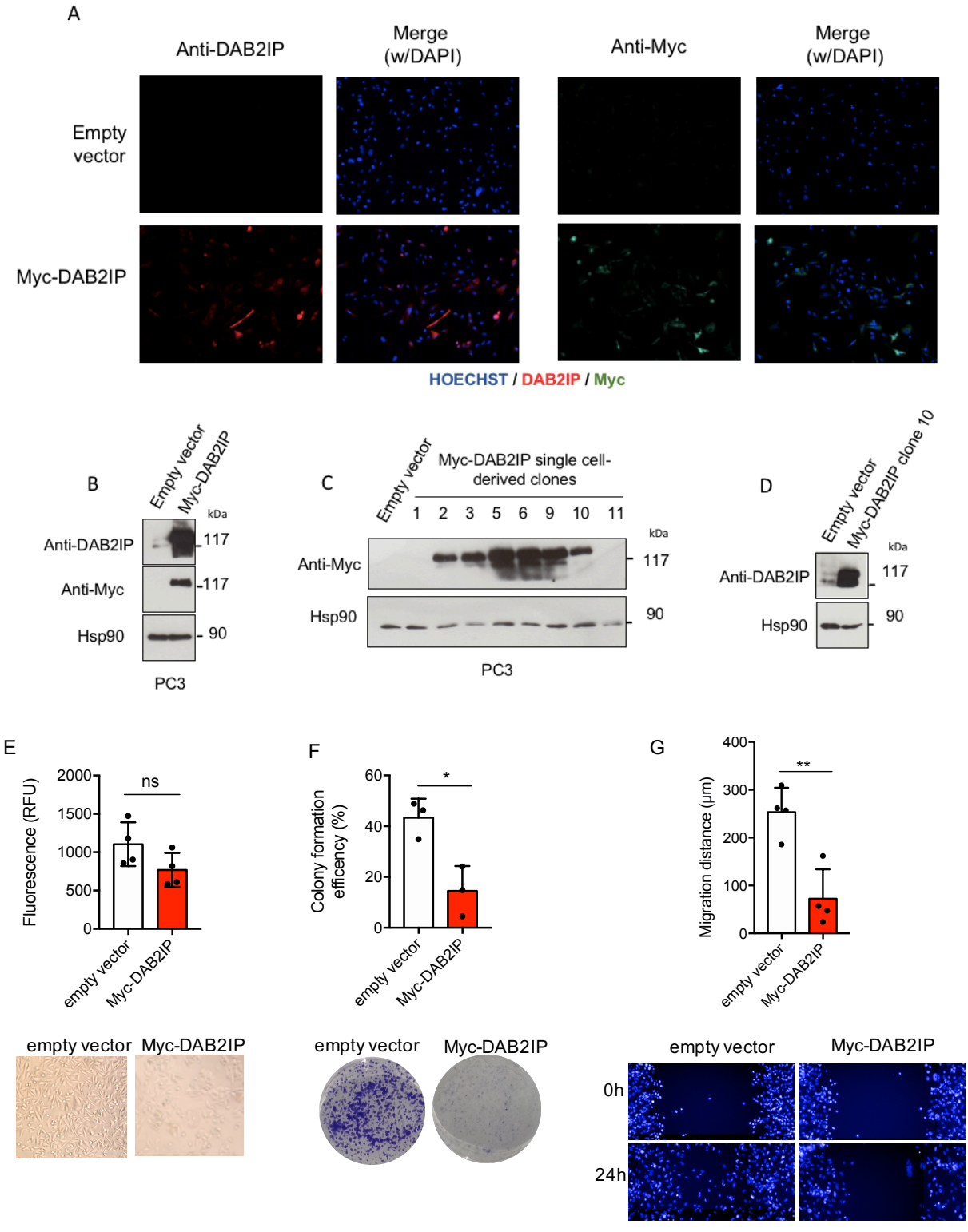
A
Anti-DAB2IP
Merge (w/DAPI)
Anti-Myc
Merge (w/DAPI)
Empty vector
Myc-DAB2IP
HOECHST / DAB2IP / Myc
B
Empty vector
Myc-DAB2IP
kDa
Anti-DAB2IP
117
Anti-Myc
117
Hsp90
90
PC3
C
Empty vector
Myc-DAB2IP single cell-derived clones
1 2 3 5 6 9 10 11
kDa
Anti-Myc
117
Hsp90
90
PC3
D
Empty vector
Myc-DAB2IP clone 10
kDa
Anti-DAB2IP
117
Hsp90
90
E
Fluorescence (RFU)
2000
1500
1000
500
0
ns
empty vector
Myc-DAB2IP
F
Colony formation efficency (%)
60
40
20
0
*
empty vector
Myc-DAB2IP
G
Migration distance (µm)
400
300
200
100
0
**
empty vector
Myc-DAB2IP
empty vector
Myc-DAB2IP
empty vector
Myc-DAB2IP
empty vector
Myc-DAB2IP
0h
24h

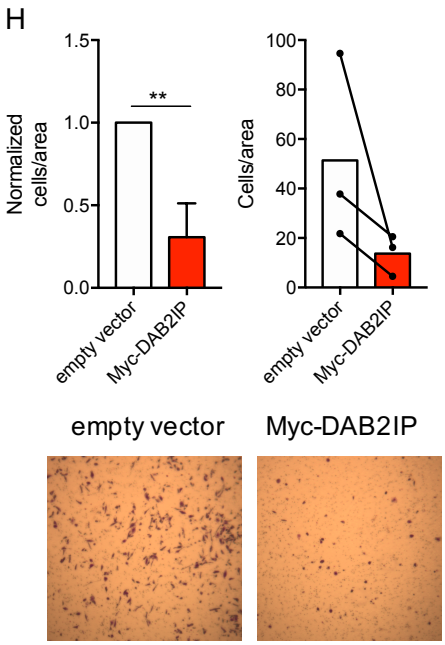

Figure 13 | DAB2IP over-expression reduced prostate cancer cell viability, proliferation and invasion. **A)** Representative images of PC3 cells infected with pLPC Myc-hDAB2IP or empty vector as control. Cells were fixed and stained with either anti-DAB2IP (red) or anti-Myc (green) antibodies. Nuclei were stained with Hoechst (blue). **B)** Bulk PC3 cells infected with pLPC Myc-hDAB2IP express high levels of DAB2IP protein. DAB2IP was detected with the indicated antibodies. Hsp90 was blotted as loading control. **C)** Clonal cell lines display variable levels of DAB2IP expression. DAB2IP was detected using an antibody against Myc tag. **D)** Expression levels of DAB2IP in PC3 clone 10. DAB2IP was detected using an antibody against DAB2IP. **E)** DAB2IP over-expression inhibits cell proliferation. Viability of PC3 (clone 10) or PC3 vector control cells was measured with CellTiterFluor (Promega) 48h after plating an identical number of cells. Rapresentative brightfield images are also shown. **F)** DAB2IP over-expression inhibits cell proliferation. An identical number of PC3 (clone 10) or PC3 control cells were plated at low density and cultured for 10 days. Petri dishes were photographed after crystal violet staining (representative pictures are shown), and colony formation efficiency was quantified using ImageJ (cells covered area/dish area). **G)** DAB2IP over-expression reduces cell migration. PC3 (clone 10) or PC3 vector control cells were plated at high confluence and scraped, scratch closure was followed for 24 hr. Migration distance was quantified using ImageJ as indicated in Materials and methods. Representative images of cells at time 0h and 24h after scratching. **H)** DAB2IP expression reduces prostate cancer cells ivasion. Invasion assays were performed in low serum using PC3 (clone 10) or PC3 vector control cells. Graphs summarize the number of migrated cells per area, normalized to control (left) or non-normalized (right). Representative images of migrated cells, fixed and stained with crystal violet, are also shown. Migrated cells are the mean of 5 random non-overlapping fields at 100X magnification. Results are represented as mean ± SD of n=4 (E) or n=3 (F,H) indipendent experiments or n=4 wells per condition (G); ** P<0.01; * P<0,1; unpaired Student's t-test.

GENERATION OF CRISPR/Cas9-MEDIATED DAB2IP-EPITOPE TAGGED CELL LINES FOR DETECTING ENDOGENOUS PROTEIN LEVELS VIA A HIGH-THROUGHPUT APPROACH

3.2.1 Characterization of hDAB2IP protein isoforms and tagging strategy

To discover potential drugs or RNA therapeutics that can modulate DAB2IP levels, it is necessary to be able to detect the amount and dynamics of the endogenous DAB2IP protein with sensitive, quantitative and high-throughput assays. Unfortunately, this is difficult due to the relatively low expression levels of the protein and the lack of good antibodies to detect it under non-denaturing conditions – so that currently the most reliable detection of DAB2IP is by western blot.

To overcome these limitations, we decided to tag endogenous DAB2IP in human cell lines using CRISPR/Cas9 genome editing.

As proof of feasibility, we started by tagging endogenous DAB2IP in hTERT-RPE1 cells, a diploid non-transformed human epithelial cell line already used successfully for efficient CRISPR/Cas9-mediated gene tagging (Ghetti et al., 2021).

The human DAB2IP gene encodes for multiple transcript variants, corresponding to different proteins. Ideally, the tag should be inserted in a position conserved in all isoforms, and with no impact on the structure/function of the protein, guaranteeing a faithful and accurate detection of endogenous DAB2IP under physiological conditions. Available RNA sequences in public databases, and CAGE analysis in multiple cells and tissues, indicate that DAB2IP has at least four different transcriptional start sites (TSS), with multiple transcripts, and at least three N-terminal variants of the protein; moreover, alternative splicing generates two possible C-terminal variants (**Figure 14A**).

Given the complexity of multiple variants, we decided to target the central region of the protein (a hydrophilic and not catalytic region between the GAP domain and the PER domain), which is conserved in all possible isoforms.

We also decided to target the two alternative C-terminal ends of the protein; in fact, tagging at the C-terminus, immediately upstream of the stop codon, usually has minimal impact on structure and function of the protein. As a preliminary experiment, we analyzed expression of the alternative C-terminal variants of DAB2IP in our model cell lines. Performing RT-PCR with primers designed to distinguish spliced and unspliced transcripts, we found that RPE1 cells express both DAB2IP isoforms (**Figure 14B-C**). Using the same approach we observed that both C-terminal variants of DAB2IP are co-expressed in several normal and transformed cell lines (**Figure 14C**). Note that in THP-1 monocytic leukemia cells none of the isoforms could be detected, in line with the notion that DAB2IP is not expressed in blood (https://www.gtexportal.org/).

Figure 14

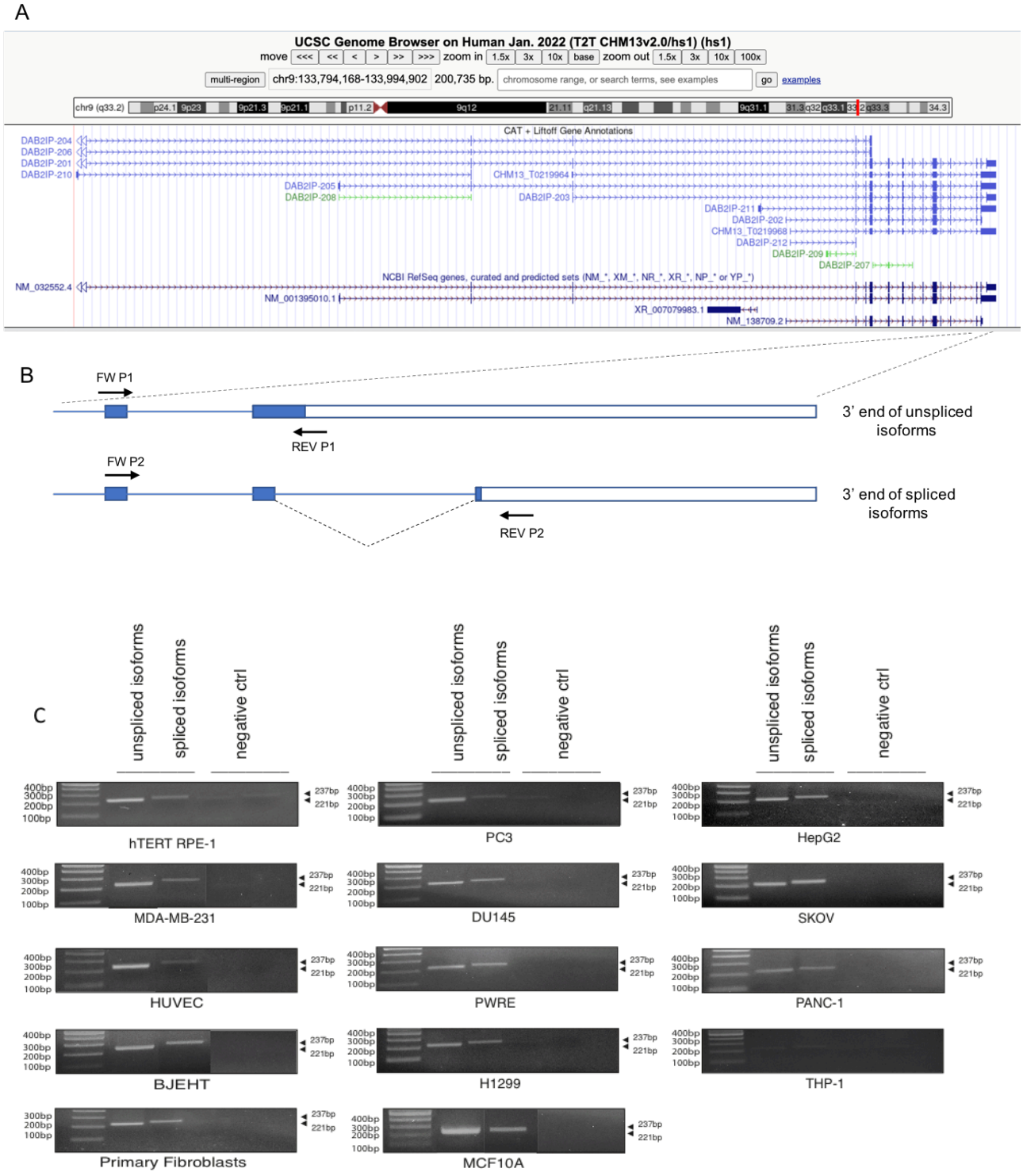
A
UCSC Genome Browser on Human Jan. 2022 (T2T CHM13v2.0/hs1) (hs1)
CAT + Liftoff Gene Annotations
DAB2IP-204
DAB2IP-206
DAB2IP-201
DAB2IP-210
CHM13_T0219964
DAB2IP-205
DAB2IP-208
DAB2IP-203
DAB2IP-211
DAB2IP-202
CHM13_T0219968
DAB2IP-212
DAB2IP-209
DAB2IP-207
NCBI RefSeq genes, curated and predicted sets (NM_*, XM_*, NR_*, XR_*, NP_* or YP_*)
NM_032552.4
NM_001395010.1
XR_007079983.1
NM_138709.2
B
FW P1
REV P1
3' end of unspliced isoforms
FW P2
REV P2
3' end of spliced isoforms
C
unspliced isoforms
spliced isoforms
negative ctrl
400bp
300bp
200bp
100bp
237bp
221bp
hTERT RPE-1
PC3
HepG2
MDA-MB-231
DU145
SKOV
HUVEC
PWRE
PANC-1
BJEHT
H1299
THP-1
Primary Fibroblasts
MCF10A

Figure 14 | Human DAB2IP is expressed with two C-terminal variants in multiple cell lines. A) Schematic representation of predicted hDAB2IP isoforms (UCSC Genome Browser). **B)** Scheme of primers used to detect the unspliced (above) (NM_138709.2) or the spliced (below) isoforms (NM_032552.3). REV P1 primer amplifies only the unspliced variant, because it is designed to recognize a sequence within the intron. REV P2 primer amplifies efficiently only the spliced variant, although it could theoretically produce also a PCR amplicon of 1371 bp in the unspliced variant. Lines represent introns, and boxes exons. The filled boxes represent the translated sequence (ORF), while the open boxes represent untranslated 3' UTR regions. **C)** hTERT RPE-1 and multiple normal and transformed cell lines express both C-terminal variants. Total RNA extracted from the indicated cell lines was retrotranscribed and amplified using primers designed to distinguish alternative spliced DAB2IP isoforms as described in B. RT-PCR products were run in 2% agarose gel. PCR reactions without cDNA were run as negative controls. Note: some electrophoresis images are cropped.

3.2.2 CRISPR/Cas9 gene editing for DAB2IP tagging with V5 epitope

We chose to tag DAB2IP with V5 because of its small size (~1kDa), predicted to have a minimal impact on the folding and functionality of the fusion protein. We reasoned that V5 detection with a highly specific monoclonal antibody could allow a "semi-quantitative" analysis of DAB2IP levels and localization pattern, with better sensitivity and lower background than commercially available polyclonal antibodies (data not shown).

Several papers demonstrate that delivery of Cas9 as recombinant protein pre-complexed with single guide RNA (sgRNA) provides higher genome editing efficiency with fewer off-targets insertions (Kim et al., 2014) (Dewari et al., 2018). Accordingly, we used recombinant Cas9 protein pre-complexed with sgRNA; ribonucleoprotein (RNP) complexes were electroporated into cells together with a single stranded donor DNA (ssDNA) containing the V5 sequence flanked by two homology arms corresponding to the target genomic locus (**Figure 15 and 16A**). To increase the proportion of HDR events, we treated cells with NU7441, an inhibitor of DNA-dependent protein kinase (DNA-PK), an enzyme involved in the non-homologous end joining (NHEJ) DNA repair pathway (**Figure 15**) (full protocol in Ghetti et al., 2021).

With this approach, we successfully tagged the three different regions of the DAB2IP gene, as assessed by immunoblotting for the V5 epitope. The higher efficiency was obtained with the sgRNAs targeting the 'intramolecular' site (**Figure 16C**).

Gene-specific integration was confirmed by the absence of V5 expression after DAB2IP silencing (**Figure 16D**). Effective tagging was also confirmed by immunofluorescence of endogenous V5-DAB2IP in edited RPE-1 cells (**Figure 16E**). Immunofluorescence with anti-V5 antibody in heterogenous bulks suggests a punctate cytoplasmatic distribution for DAB2IP in RPE-1 cells, with no enrichment in specific organelles under normal conditions. Moreover, localization seems not to differ between the two alternative C-terminal variants of DAB2IP.

Given the high efficiency of V5 integration in cells transfected with the 'intramolecular' sgRNA, we selected single clones by monitoring expression of V5-tagged DAB2IP by immunoblotting (**Figure 17A-B**). At least 20 positive lines were examined in order to exclude clone-specific artifacts. V5-positive clones by immunoblotting were then analyzed by PCR, amplifying the target genomic sequence with primers that produce amplicons of about 400 bp (**Figure 17C**) that allow to discriminate a small upshift derived by V5 integration (about 50 bp). The ratio between homozygote (single upper band) and heterozygote (double-band) clones was almost equal. The correct insertion was further confirmed by Sanger sequencing of the PCR product of four putative homozygous clones (clones 2, 7, 17, 22 in **Figure 17C**).

Immunofluorescence analysis of monoclonal cells lines compared to parental cells suggested that V5-DAB2IP signal may be specific, and confirmed a cytoplasmic dotted distribution (**Figure 17D**). However, in all immunofluorescence experiments the V5 signal was very weak, requiring long exposure times. Moreover, transfection of a DAB2IP specific siRNA did not induce a clear loss of V5 staining compared to control cells (data not shown), suggesting that the immunofluorescence signal may be non-specific. I performed different protocols for antigen retrieval, but with negative results. Based on these observations, we believe that the detection of endogenous DAB2IP by immunofluorescence is primarily limited by the low expression levels of the protein, although we cannot formally exclude that the V5 epitope is masked by the 3D folding of the protein.

Aiming at identifying small molecules able to increase expression levels of DAB2IP, the difficulty in detecting endogenous V5-tagged DAB2IP by immunofluorescence excluded the possibility to perform the screening using high-content microscopy. Thus, we selected an alternative system to detect endogenous DAB2IP in a more sensitive and quantitative way by exploiting a luciferase-based approach: the HiBiT System.

Figure 15

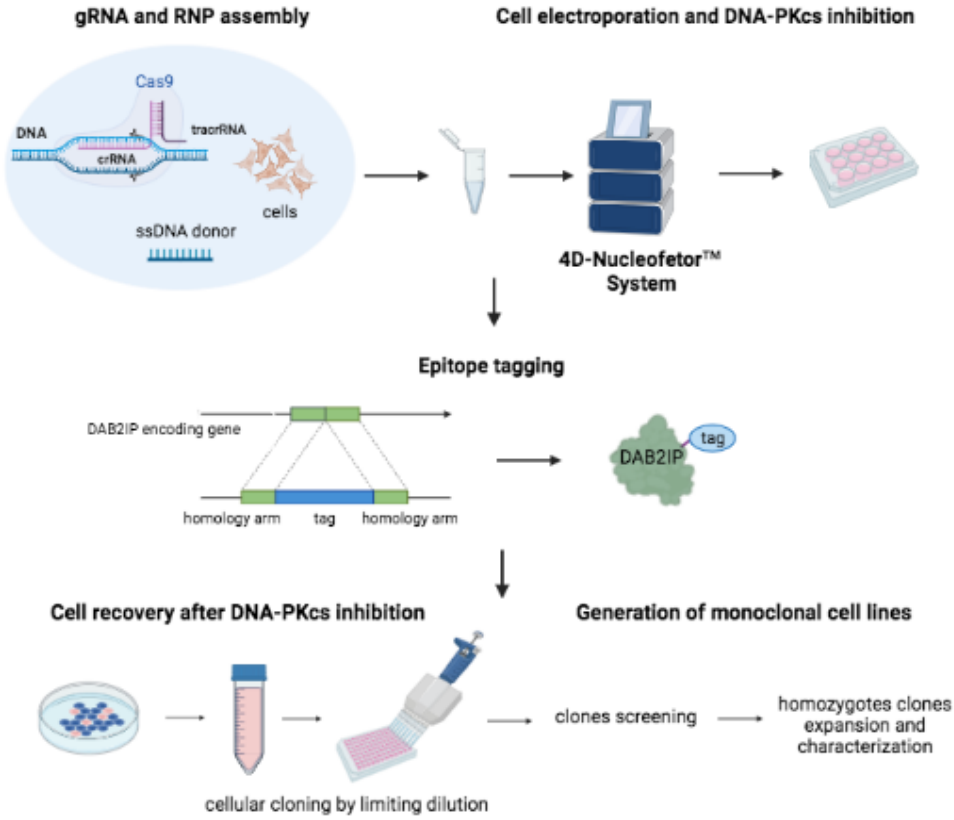

Figure 15 | Workflow of CRISPR/Cas9 ribonucleoprotein-mediated knock-in generation. See the results for details (Adapted from Ghetti et al., 2021, created with BioRender.com)

Figure 16

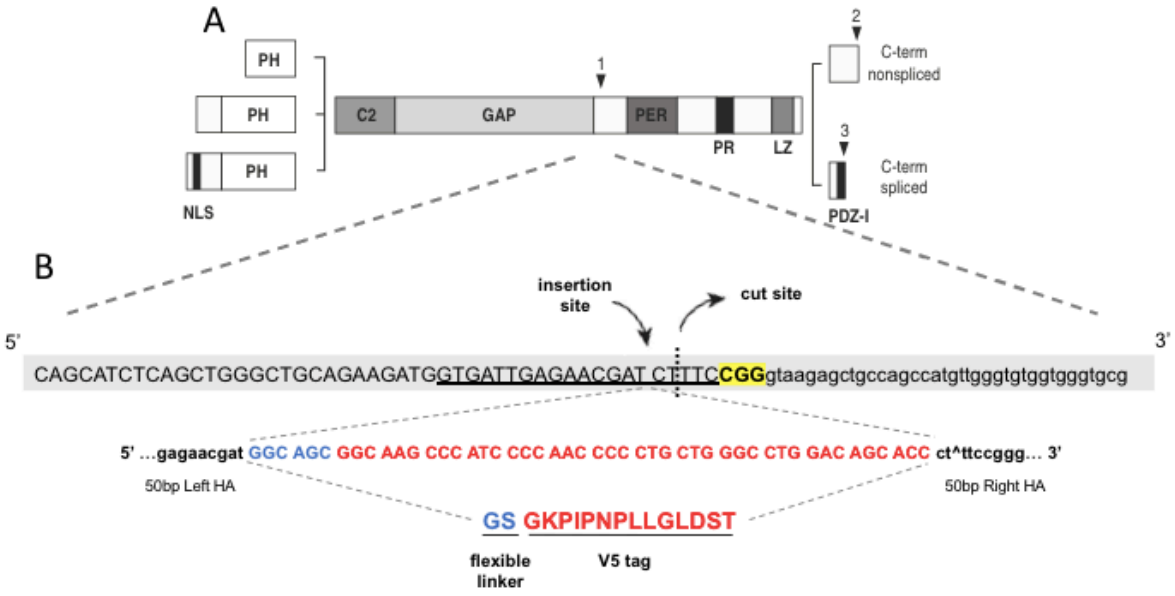
A
PH
PH
PH
NLS
C2
GAP
PER
PR
LZ
1
2
C-term nonspliced
3
C-term spliced
PDZ-I
B
insertion site
cut site
5'
3'
CAGCATCTCAGCTGGGCTGCAGAAGATGGTGATTGAGAACGAT CTTTCCGGgtaagagctgccagccatgttgggtgtggtgggtgcg
5' ...gagaacgat GGC AGC GGC AAG CCC ATC CCC AAC CCC CTG CTG GGC CTG GAC AGC ACC ct^ttccggg... 3'
50bp Left HA
50bp Right HA
GS GKPIPNPLLGLDST
flexible linker
V5 tag

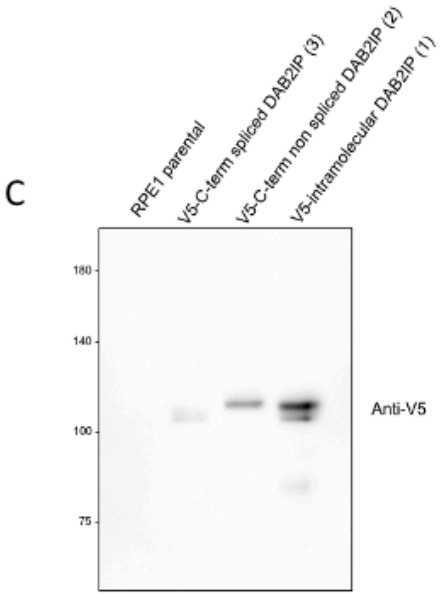
C
RPE1 parental
V5-C-term spliced DAB2IP (3)
V5-C-term non spliced DAB2IP (2)
V5-intramolecular DAB2IP (1)
180
140
100
75
Anti-V5

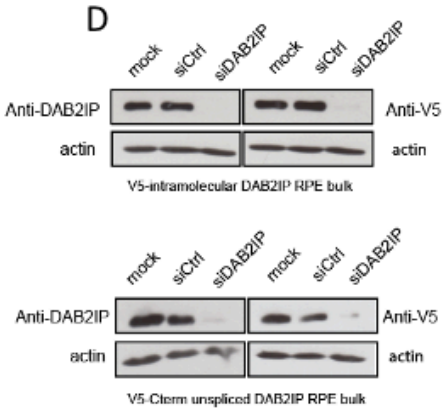
D
mock
siCtrl
siDAB2IP
mock
siCtrl
siDAB2IP
Anti-DAB2IP
Anti-V5
actin
actin
V5-intramolecular DAB2IP RPE bulk
mock
siCtrl
siDAB2IP
mock
siCtrl
siDAB2IP
Anti-DAB2IP
Anti-V5
actin
actin
V5-Cterm unspliced DAB2IP RPE bulk

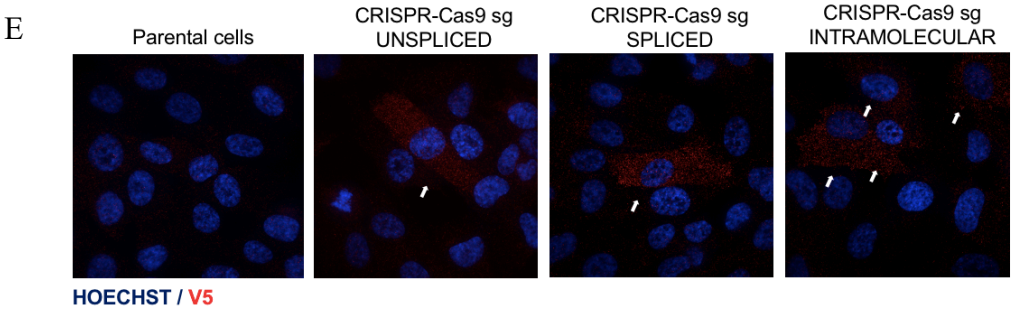
E
Parental cells
CRISPR-Cas9 sg UNSPLICED
CRISPR-Cas9 sg SPLICED
CRISPR-Cas9 sg INTRAMOLECULAR
HOECHST / V5

Figure 16 | CRISPR/Cas9-mediated DAB2IP tagging in RPE1 cells. A) Structure of human DAB2IP predicted isoforms. Arrows indicate tagging sites: (1) 'intramolecular' site; (2) C-terminal of unspliced isoform (NM_138709.2); (3) C-terminal of spliced isoform (NM_032552.3). **B)** Schematic representation of intramolecular insertion site. Upper part: the genomic sequence coding for the intramolecular region of hDAB2IP protein. Uppercase letters represent exon sequence whereas lowercase letters intron sequence. Underlined sequence represents the guide recognition site in the target sequence, with the PAM sequence in yellow. The vertical dotted line indicates the predicted cut site. The insertion site was arbitrarily positioned 1 bp away from the cut site, i.e., at the closest possible junction between two codons. In the lower part, codons (above) and the corresponding translation (below) composing the insert are reported: blue capital letters refer to the flexible linker followed by V5-tag (in red). 50 bp LHA or RHA = 50 base pairs Left Homology Arm or Right Homology Arm (figure and figure legend are adapted from Ghetti et al., 2021). **C)** Bulk electroporated RPE-1 cells were analyzed by immunoblotting with anti-V5 monoclonal antibody, revealing a specific signal in line with the expected DAB2IP molecular weight (117 kDa). **D)** DAB2IP silencing abrogates the expression of V5-epitope in bulk electroporated RPE- 1 cells. Cells were transfected with DAB2IP-specific siRNA for 48h. Endogenous DAB2IP was detected with anti-V5 or anti-DAB2IP antibodies as indicated, with actin as loading control. **E)** Endogenous V5-DAB2IP localization in edited RPE-1 cells. Immunofluorescence of V5-DAB2IP in bulk nucleofected cells corresponding to three different insertion sites, compared to parental RPE1 cells. Arrows indicate V5-positive cells. Cells were fixed in 4% PFA and stained for V5 (red). Nuclei were stained with Hoechst (blue).

Figure 17

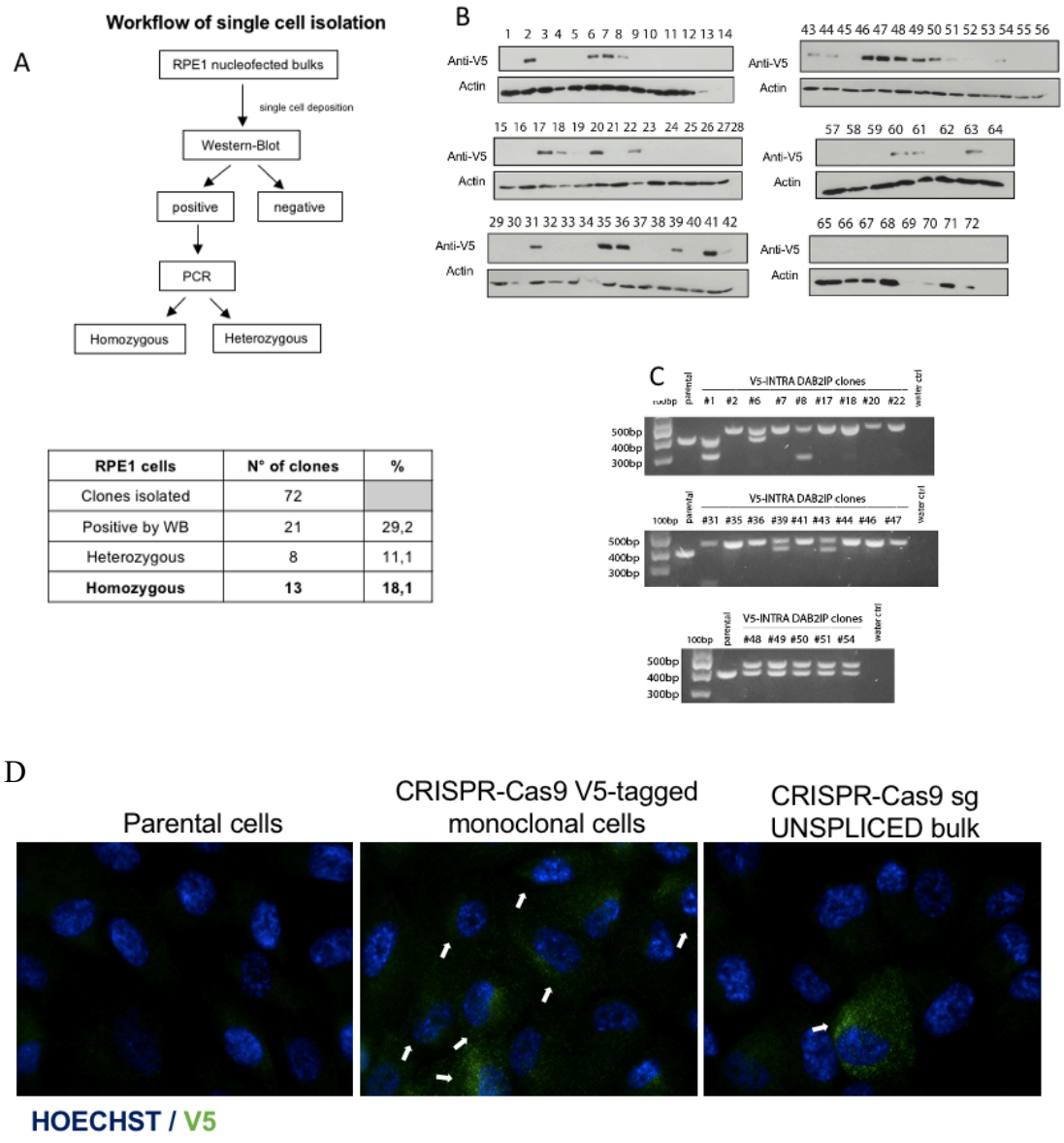

RPE1 cells	N° of clones	%
Clones isolated	72	
Positive by WB	21	29,2
Heterozygous	8	11,1
Homozygous	**13**	**18,1**

Figure 17 | Isolation of V5-DAB2IP positive RPE-1 clonal cell lines. A) Pipeline of single cell isolation (top) and summary of resulting cell lines (bottom). **B)** Immunoblotting of V5 expression in 72 different clones (intramolecular tagging). Actin was blotted as loading control. **C)** Genotyping of monoclonal cell lines. Genomic DNA was amplified using primers designed to produce ca. 400 bp amplicons with a clear upshift (of 48bp) in case of V5 integration. Lower bands detected in some clones can be explained as partial deletions of the target sequence after Cas9-induced DNA nicks. PCR products were run in 2% agarose gel. RPE1 parental genomic DNA was amplified as control. **D)** Immunofluorescence of endogenous V5-tagged DAB2IP in a monoclonal line (intramolecular V5 insertion), compared to parental RPE1 cells and a heterogenous bulk (V5 in green).

3.2.3 Endogenous DAB2IP tagging with HiBiT

HiBiT is an 11 amino acid peptide, commercialized by Promega, that complements with the major subunit of NanoLuc (LgBiT) to reconstitute a functional luciferase enzyme; in presence of the substrate and excess LgBiT, the luminescence intensity is directly proportional to the amount of HiBiT-tagged protein in the cell lysate.

We designed sgRNA and donor template exploiting the same approach used for V5-tagging. However, this time, to tag all possible DAB2IP variants, but to avoid the potential disadvantages of an intramolecular tag (i.e. protein misfolding or tag masking), we planned insertion of the HiBiT peptide followed by an exogenous stop codon, immediately upstream of the last splice donor site, in order to translate the same C-terminally tagged DAB2IP protein from both alternatively spliced mRNAs (**Figure 18A-B-C**).

To verify whether the tag inserted in such position would be available for efficient interaction with the LgBiT subunit, we cloned the HiBiT peptide in fusion to DAB2IP in a mammalian expression vector, in the same exact position of the predicted endogenous tagging (**Figure 18D**). Luminescence was readily detected in transfected cells after lysis and incubation with LgBiT and furimazine, with very low background, indicating that the C-terminal HiBiT peptide in fusion to DAB2IP maintains its functionality (**Figure 18E**).

Since strong evidences indicate that DAB2IP reactivation in prostatic cancer counteracts metastasis and chemoresistance in vitro and in vivo models (Min et al., 2010) (Wu et al., 2013), we chose to edit PC3 and DU145 human prostate cancer cell lines; the two cell lines differ for DAB2IP expression levels as well as for p53 status (mutant p53 is a negative regulator of DAB2IP), rendering them proper for exploring mechanisms of drug-mediated DAB2IP modulation in cancer. To tag endogenous DAB2IP we nucleofected the two cell lines using the same protocol used for RPE-1. Bulk nucleofected cells were analyzed first by luciferase assay (**Figure 19A**), and then by PCR on genomic DNA, confirming the successful integration of the HiBiT-tag into the target region (**Figure 19B**). Specificity of the tagging was evaluated by siRNA-mediated silencing of DAB2IP, and by transfection of miR-149-3p, a DAB2IP-targeting miRNA previously identify in our laboratory (**Figure 19C-D**). The reduction of luminescence signal after both siRNA and miRNA transfection is in line with those observed by western blot and confirms that the system is well applicable to measure variations in DAB2IP protein levels. Both PC3 and DU145 cells positive for HiBiT insertion were selected as single clones to obtain reporter cell lines with homozygous DAB2IP tagging. In the first round of screening, HiBiT positive clones were selected by luminescence; positive clones were then analyzed by genomic PCR to identify homozygous insertions (**Figure 19E-F**). The correct HiBiT

insertion in selected homozygous clones was finally confirmed by Sanger sequencing (data not showed).

Figure 18

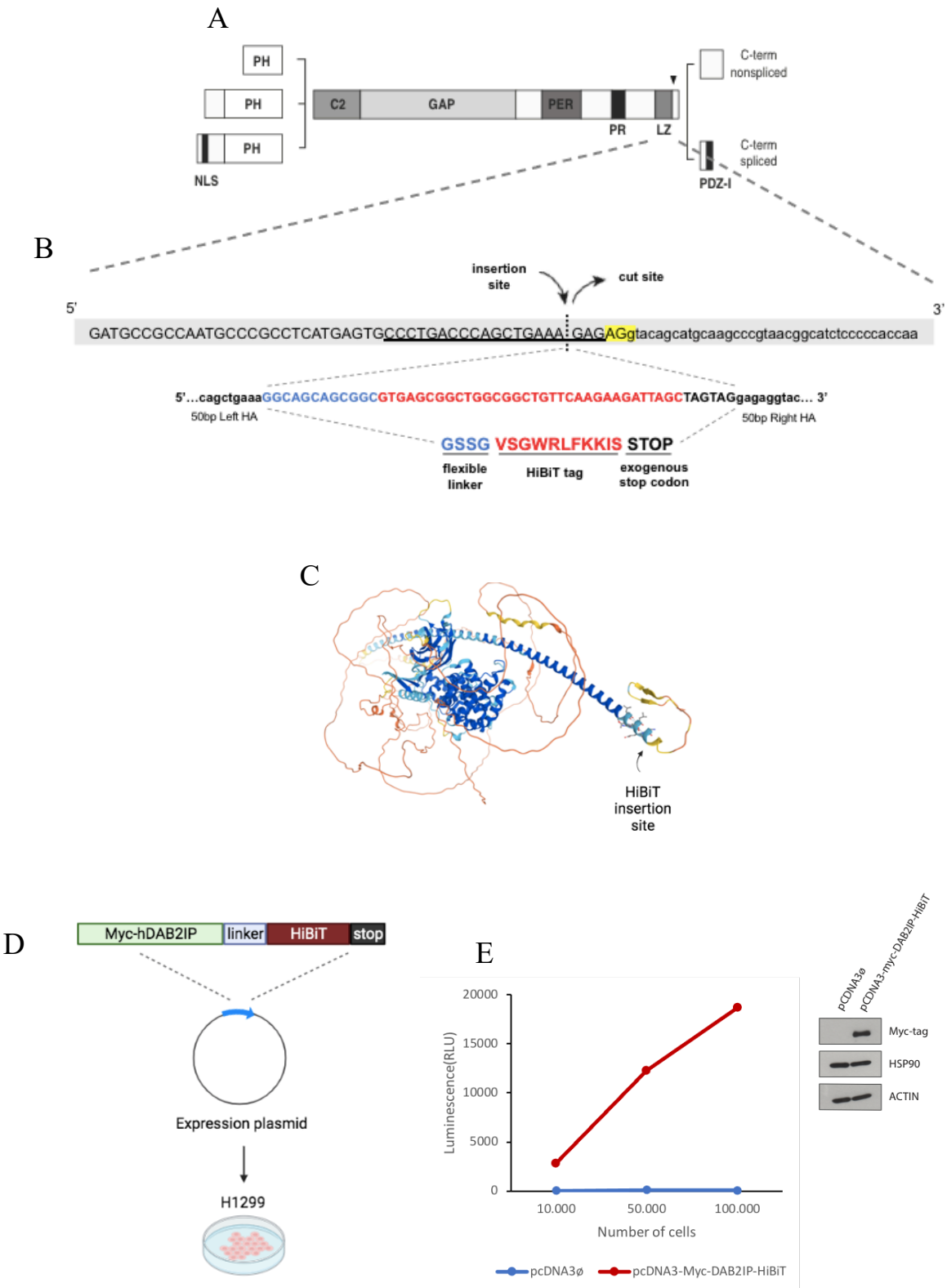

Figure 18 | DAB2IP tagging with HiBiT. A) Schematic representation of hDAB2IP C-terminal insertion site. **B)** Upper part: the genomic sequence coding for the C-terminus of hDAB2IP protein. Uppercase letters represent exon sequence whereas lowercase letters intron sequence. Underlined sequence represents the guide recognition site in the target sequence, with the PAM sequence in yellow. The vertical dotted line indicates the predicted cut site. The insertion site was arbitrarily positioned in correspondence of the cut site at junction between codons. In the lower part, codons (above) and the corresponding translation (below) composing the insert are reported: blue capital letters refer to the flexible 4 Gly/Ser linker followed by HiBiT-tag (in red) and two additional exogenous stop codons (in black). 50 bp LHA or RHA = 50 base pairs Left Homology Arm or Right Homology Arm C-terminal insertion site and donor ssDNA sequence. Below, the donor ssDNA sequence. Lowercase letters: left and right homology arms; uppercase letters: inserted HiBiT peptide sequence, with corresponding translation below. Uppercase black letters indicate two added exogenous stop codons. (figure and figure legend are adapted from Ghetti et al., 2021). **C)** Predicted 3D structure of hDAB2IP as computed by AlphaFold (https://alphafold.ebi.ac.uk/entry/Q5VWQ8) (Varadi et al., 2022) with the site of insertion of the HiBiT tag. **D-E)** H1299 cells were transfected with pCDNA3 myc-hDAB2IP-HiBiT plasmid. **D)**, encoding a DAB2IP fusion protein identical to the endogenous tagged product. An empty pCDNA3 plasmid was transfected as a negative control. Variable numbers of transfected cells were transferred 24h later in 96-well plates, and Luciferase assay was performed **(E).** Western blot confirmed expression of the transfected fusion protein.

Figure 19

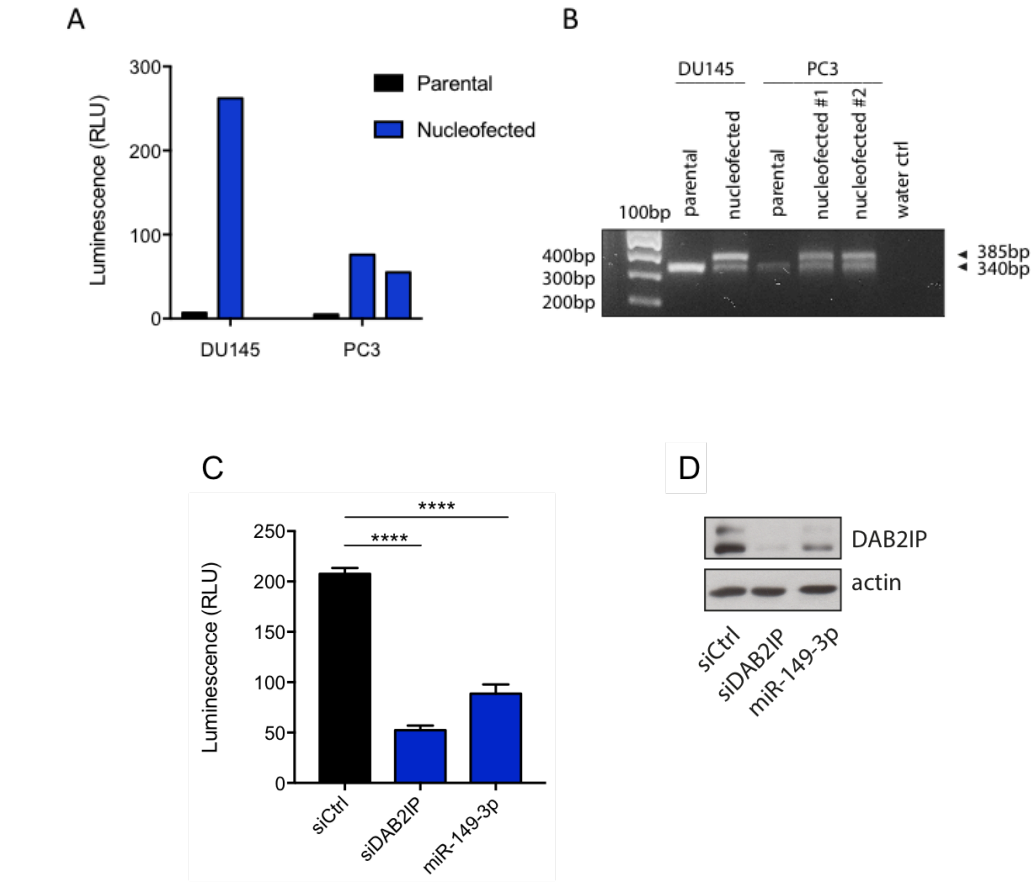

E

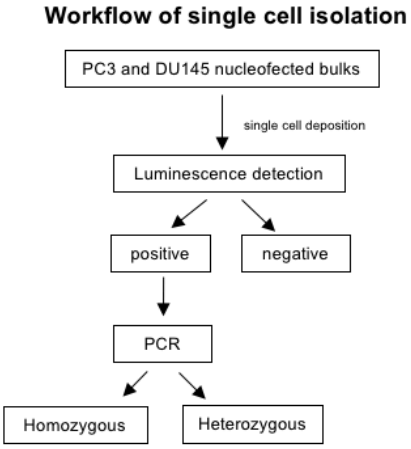

F

PC3 cells	N° of clones	%
Clones isolated	76	
Positive to luminescence	31	40,7
Heterozygous	16	21,1
Homozygous	**15**	**19,7**

DU145 cells	N° of clones	%
Clones isolated	55	
Positive to luminescence	31	56,4
Heterozygous	20	36,3
Homozygous	**11**	**20,0**

Figure 19 | Endogenous DAB2IP tagging with HiBiT and isolation of monoclonal reporter cell lines. A) Bulk HiBiT nucleofected cells are positive to luminescence. An identical number of the indicated cells were lysed and incubated with LgBiT and furimazine substrate before luciferase detection. Note: PC3 were nucleofected using two different electroporation programs, generating two bulk cell lines. **D)** Bulk HiBiT nucleofected cells display edited target sequence. Genomic DNA was amplified using primers designed to produce ca. 350 bp amplicons with a clear upshift in case of HiBiT integration. PCR products were run in 2% agarose gel. Parental genomic DNAs were amplified as control. **C-D)** DAB2IP knockdown reduces HiBiT-DAB2IP levels. Bulk nucleofected PC3 cells were transfected with DAB2IP siRNA or with DAB2IP-targeting miR-149-3p for 48 hours before luminescence reading (Data are mean ± SD; n=3 wells per condition; **** $P<0.0001$; one-way ANOVA with Dunnett's post hoc). **D)** Western blot confirmed modulation of DAB2IP protein levels. Actin was blotted as a loading control. **E)** Pipeline of PC3 and DU145 HiBiT positive single cell isolation. **F)** Summary of cell lines obtained, with the rate of heterozygous and homozygous tagging.

IDENTIFICATION AND CHARACTERIZATION OF SMALL MOLECULES THAT RESTORE THE TUMOR SUPPRESSIVE FUNCTION OF DAB2IP IN CANCER

3.3.1 High-throughput screening set-up

To screen for molecules that may potentially restore DAB2IP protein levels, we decided to use the more metastatic PC3 cells. In fact, PC3 display lower expression levels of DAB2IP respect to DU145, thus rendering them more suitable to isolate compounds that potentially increase protein levels. We therefore performed the screening on a selected PC3-HiBiT clone.

To normalize luciferase activity for fluctuations in the number of cells, due to variable pipetting or to drug toxicity, we simultaneously quantified viable cells using a fluorescence-based assay that does not require cell lysis (CellTiterFluor, Promega). To test the feasibility and the accuracy of this approach, we plated different numbers of PC3-HiBiT cells and measured cell viability and DAB2IP-HiBiT levels. As reported in **Figure 20A-B** the intensity of both fluorescence (viability) and luminescence (DAB2IP levels) correlated with the number of plated cells, as expected, displaying a constant luminescence/fluorescence ratio **(Figure 20C)**.

To confirm that the assay was able to measure endogenous DAB2IP variations, we silenced DAB2IP in PC3-HiBiT and DU145-HiBiT cells. We observed a striking reduction of luminescent signal, demonstrating that it is specific for DAB2IP (**Figure 20D-E**). The silencing of Ubiquitin C (UBC), predicted to induce cell death, was performed to control how the assay would respond under conditions of non-specific cell toxicity. As shown in **Figure 20,** knockdown of UBC was not very toxic in PC3 but strongly reduced viability in DU145. In both cell lines, the reduction of fluorescence (viability) was not paralleled by a corresponding decrease in luciferase activity (DAB2IP levels), and the lum/fluo ratio was augmented by UBC depletion (**Figure 20D-E**). Although we cannot exclude that UBC depletion might actually increase DAB2IP protein levels (a specific experiment would be required to test this hypothesis), results suggest that the lum/fluo ratio is indeed a reliable measure of endogenous DAB2IP levels, but fluctuations in cell viability must be carefully taken into account when evaluating putative hits.

Importantly, the drop in luciferase after siRNA-mediated DAB2IP knockdown reasonably excludes that the HiBiT tag might have been randomly inserted (in frame) in any other protein.

Figure 20

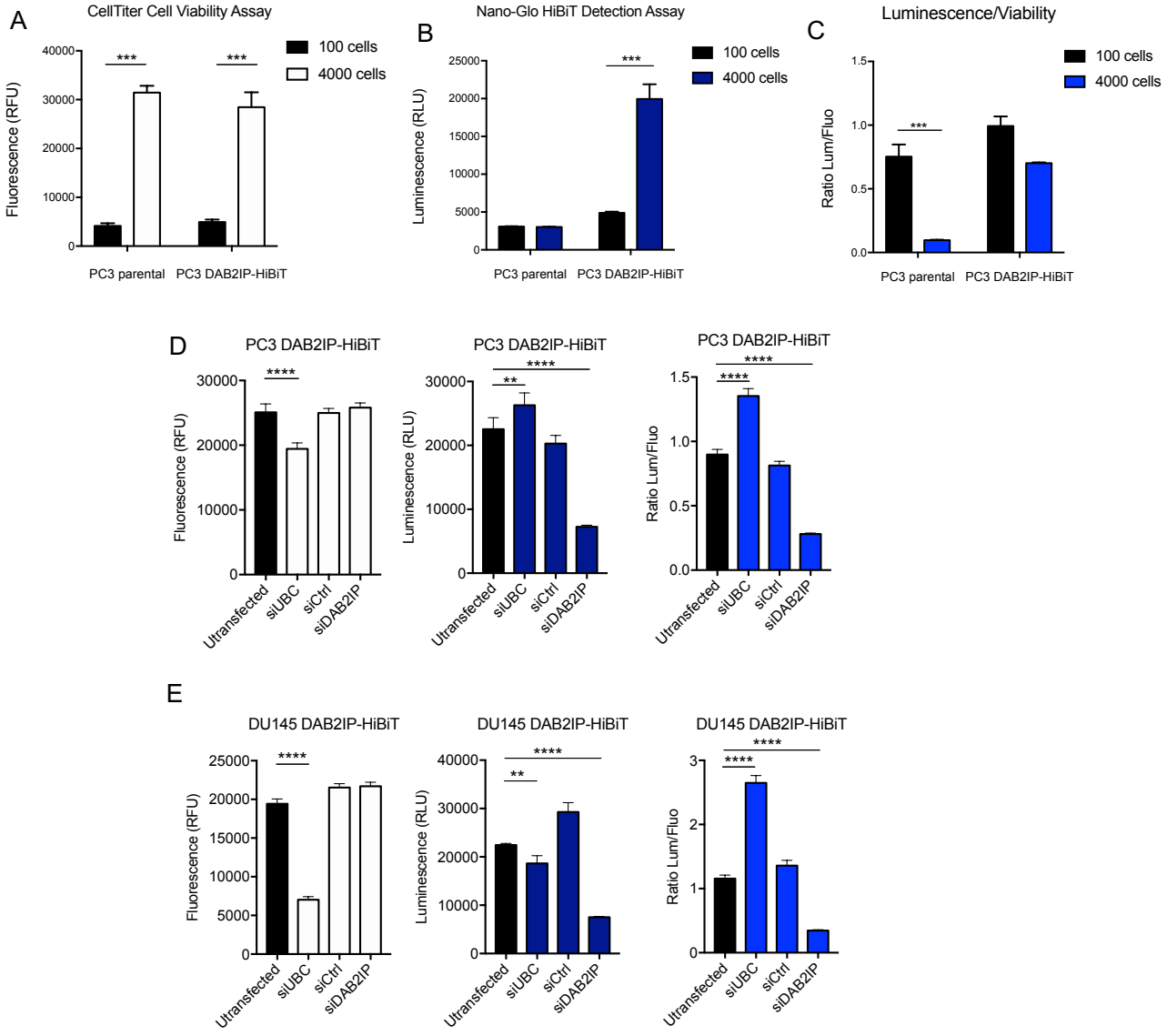
A
CellTiter Cell Viability Assay
Fluorescence (RFU)
100 cells
4000 cells
***
***
PC3 parental
PC3 DAB2IP-HiBiT
B
Nano-Glo HiBiT Detection Assay
Luminescence (RLU)
100 cells
4000 cells
***
PC3 parental
PC3 DAB2IP-HiBiT
C
Luminescence/Viability
Ratio Lum/Fluo
100 cells
4000 cells
***
PC3 parental
PC3 DAB2IP-HiBiT
D
PC3 DAB2IP-HiBiT
Fluorescence (RFU)
****
Utransfected
siUBC
siCtrl
siDAB2IP
PC3 DAB2IP-HiBiT
Luminescence (RLU)
****
**
Utransfected
siUBC
siCtrl
siDAB2IP
PC3 DAB2IP-HiBiT
Ratio Lum/Fluo
****
****
Utransfected
siUBC
siCtrl
siDAB2IP
E
DU145 DAB2IP-HiBiT
Fluorescence (RFU)
****
Utransfected
siUBC
siCtrl
siDAB2IP
DU145 DAB2IP-HiBiT
Luminescence (RLU)
****
**
Utransfected
siUBC
siCtrl
siDAB2IP
DU145 DAB2IP-HiBiT
Ratio Lum/Fluo
****
****
Utransfected
siUBC
siCtrl
siDAB2IP

Figure 20 | Screening set up. A) Fluorescence intensity from viability assay correlates with the number of cells. The indicated numbers of PC3 (parental) and PC3-HiBiT (edited to express DAB2IP-HiBiT) cells were plated in 384 well-plates. 24h after, cells were incubated with the CellTiterFluor (Promega) reagent and fluorescence was detected using a plate reader**. B)** Luminescence intensity (DAB2IP levels) correlates with the number of PC3 HiBiT cells. After fluorescence detection, the same cells were incubated with NanoGlo lytic reagent (Promega) and luminescence was measured. **C)** The ratio of Luminescence (DAB2IP levels) on fluorescence (viability) reduces the artifacts due to different cells number. **D-E)** siRNA mediated DAB2IP depletion reduces luminescence. PC3-HiBiT cells (D) and DU145-HiBiT cells (E) were reverse transfected with the indicated siRNAs in 384 well-plates. 72h after transfection, cells were incubated first with CellTiterFluor and then Nanoglo lytic reagent to measure viability and DAB2IP-HiBiT levels. Results are represented as mean ± SD of 3 wells per condition; ** $P<0.01$; *** $P<0.001$; **** $P<0.0001$; Multiple t-tests (A,B,C) or one-way ANOVA with Dunnett's post hoc (D,E).

3.3.2 High-throughput luminescence and fluorescence-based screen identifies molecules able to modulate DAB2IP expression levels

The high-throughput, fluorescence and luminescence-based screen was performed in the PC3-HiBiT cell line using a library composed by a collection of 1280 compounds FDA and EMA-approved (https://www.prestwickchemical.com). Each compound was added at 10μM final concentration to the culture medium in 384-well plates. Several wells in each plate were treated with the same volume of DMSO as negative controls. After 36h, cells were incubated with CellTiterFluor non-lytic reagent and fluorescence was measured in a plate reader. Subsequently, the same cells were incubated with NanoGlo lytic reagent to measure HiBiT-dependent luminescence (**Figure 21A**).

For each drug, the luminescence/fluorescence ratio was normalized to control DMSO-treated cells and expressed as Z-score. Positive hits were selected among compounds displaying significant variation in the Lum/Fluo ratio Z-score. According to the demonstrated tumor suppressive activity of DAB2IP, we decided to select compounds that either increased/decreased or did not change luminescence (Lum), independently by their effect on cell viability (Z-score Fluo) (**Figure 21B**).

According to these criteria, we selected 9 compounds, 6 upregulators and 3 downregulators, that are summarized in **Figure 21C**.

Figure 21

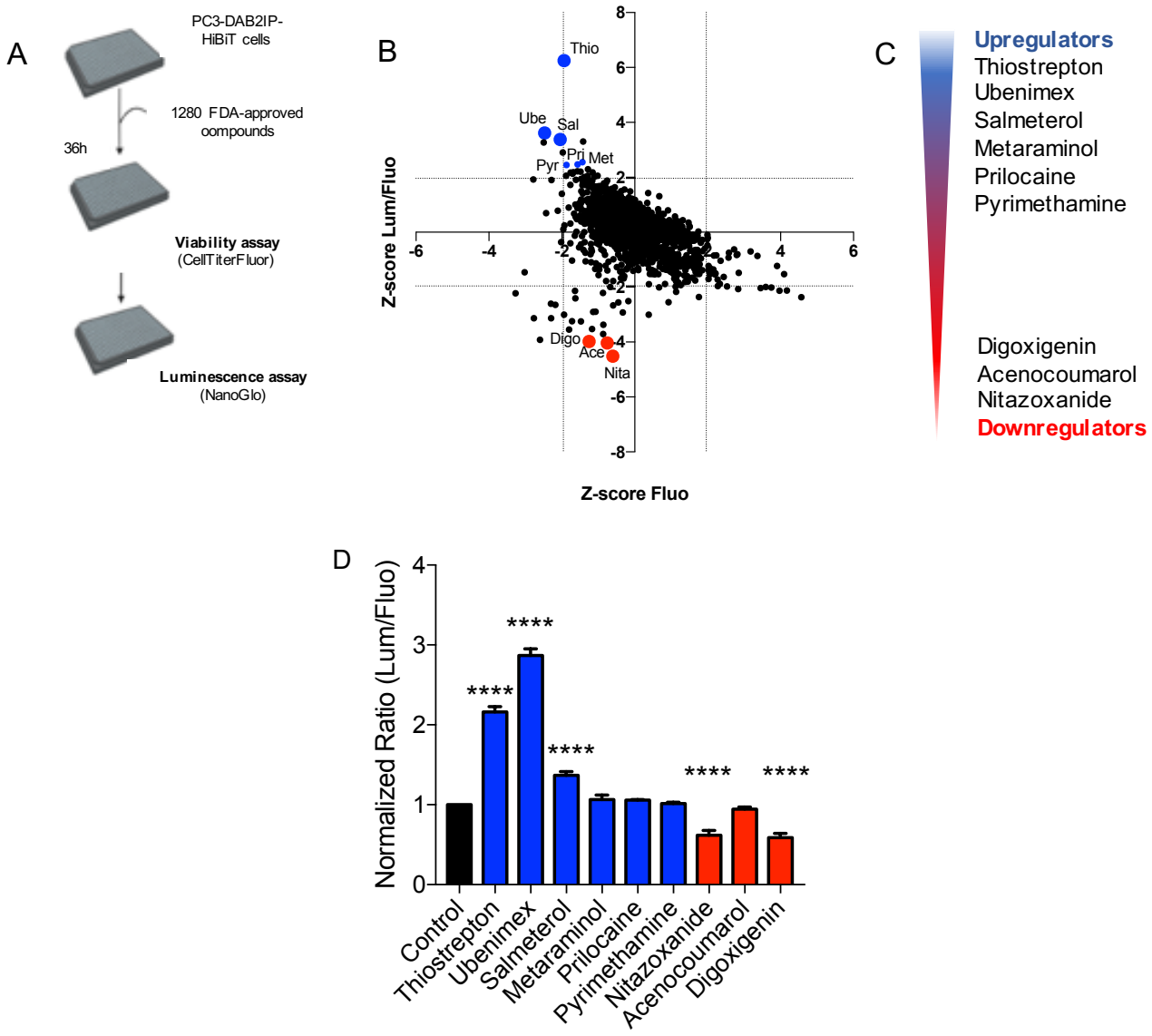

Figure 21 | Identification of FDA-approved drugs modulating DAB2IP protein levels. A) Schematic representation of the high-throughput screening procedure. PC3-HiBiT cells were seeded in 384-well plates and 24h later 1280 FDA-approved compounds were added to cells at 10 µM final concentration. 36h after treatment, cells were incubated with CellTiterFluor first, and then with NanoGlo lytic reagent. Fluorescence and luminescence readouts were acquired separately. The screening was performed one time. **B)** The graph shows the Z-score of Luciferase (DAB2IP levels) over fluorescence (cell viability) (Y-axis), plotted over the Z-score of fluorescence (viability) (X-axis). P-values of 0.05 were used as thresholds: hits were selected among compounds falling outside of the P-value on the Y-axis. **C)** List of selected drugs modulating DAB2IP levels. **D)** Histogram summarizes the Lum/Fluo ratio measured with PC3-HiBiT cells seeded in 96-well plates and treated for 36h with the indicated compounds at 10 µM concentration (n = 3 wells per dose; data are mean ± SD; **** P<0.0001; one-way ANOVA with Dunnett's post hoc).

3.3.3 Validation of the screening hits

Based on the screening results, we decided to separately validate the effects of the selected drugs on luminescence/fluorescence ratio. As shown in **Figure 21D** among upregulators only one antibiotic **(**thiostrepton), one anti-leukemic (ubenimex) and one antiasthmatic (salmeterol) confirmed their ability to increase DAB2IP levels; whereas among selected downregulators, one antihelmintic (nitazoxanide) and one steroid (digoxigenin) confirmed their action.

None of these compounds can be referred within a specific class of drugs. Briefly, thiostrepton is mainly known as a proteasome inhibition, ubenimex is a non-selective inhibitor of aminopeptidases, salmeterol is an agonist of beta-2 adrenergic receptor, and nitazoxanide is an inhibitor of pyruvate:ferredoxin oxidoreductase (PFOR) (further information are in discussion section).

To corroborate the effect of the identified DAB2IP modulators, we tested them on the other edited prostate cancer cell line, DU145-HiBiT, obtaining rather consistent results (**Figure 22A-B)**. Finally, we monitored the effects of the 6 selected compounds in PC3-HiBiT by immunoblotting. As shown in **Figure 22C**, the variations in DAB2IP protein levels reflected the variations in lum/fluo ratio (**Figure 22A-C**), confirming the screening results.

Next, we investigated the effects of duration of the treatments on DAB2IP. We treated PC3-HiBiT and DU145-HiBiT cells with 10μM drug concentration and measured fluorescence and luminescence at different time-points. We observed that both thiostrepton and nitazoxanide showed a time-dependent effect on DAB2IP levels, with the higher effect at 36h of treatment. On the contrary the other compounds showed efficacy already after 6h, and their effect remained almost constant at later time points (**Figure 23A-B**). Given these observations, we decided to use 36h as treatment end-point with all the drugs, in most of the following studies.

The above experiments, plus a series of additional observations by us and by others (not shown) brought us to temporary set aside two of the downregulator drugs, acenocoumarol and digoxigenin, because of controversial effects and high toxicity, respectively.

To further validate the results, we treated cells with variable drug dilutions in order to define the half-maximal effective concentration (EC50). As shown in **Figure 24,** thiostrepton and salmeterol displayed similar half-maximal effective concentration values of 3.4 μM, whereas ubenimex had an EC50 of 2.9 μM. Among downregulators, nitazoxanide showed a half-maximal effective concentration (EC50) of 2.3 μM. As regarding the drug effects on viability, almost all drugs did not show high toxicity effects, with half-maximal inhibitory concentration (IC50) (viability) clearly above the half-maximal effective concentration (**Figure 24)**.

Unexpectedly, ubenimex showed a strong impact on viability. However, it is possible that ubenimex, acting as inhibitor of aminopeptidases (Chen et al., 2011), might interfere with the endogenous

protease activity that is measured by the CellTiterFluor reagent, and therefore could underestimate cell viability. Indeed, phase-contrast images of cells treated with ubenimex revealed that the drug did not significantly affect cell viability (respect also to the other compounds) – in clear contrast to the fluorescence-based viability assay (**Supplemental Data Figure 32**).

To exclude clone-specific artifactual effects of the drugs on CRISPR-edited PC3 and DU145 cells, we tested the putative hit compounds on the respective non-edited parental cell lines. As shown in Figure 25A, the effects of drugs on DAB2IP expression in parental PC3 cells are comparable to those observed in the PC3-HiBiT clone. In DU145, the effects were mostly confirmed, with the exception of thiostrepton, that unexpectedly reduced DAB2IP levels (Figure 25B). It should be noted that this result is in stark contrast with the Lum/Fluo results obtained with the DU145-HiBiT clone.

Interested to understand the controversial effect of thiostrepton in the two cell lines, we treated DU145-HiBiT with escalating concentrations of thiostrepton and measured luminescence and viability after 36 hours. In contrast to PC3 (see Figure 24), in DU145 thiostrepton half-maximal effective concentration, and half-maximal inhibitory concentration (viability) values were very similar: 4.5μM for EC50 and 5.8μM for IC50 (Figure 26A). This indicates that thiostrepton is much more toxic for DU145 than PC3 cells, as also confirmed by phase contrast microscopy of treated cells (Figure 26B-C). High toxicity could therefore explain the apparent downregulatory effect of thiostrepton on endogenous DAB2IP in parental DU145 cells when detected by immunoblotting (Figure 25B). However, this supposition does not explain the obvious increase of luminescent signal induced by thiostrepton in DU145-HiBiT cells (see Figure 26D). The cause of this apparently paradoxical effect of thiostrepton remains an open question (see discussion section).

Another discrepancy between the screening and the validation experiments regards the effects of salmeterol in DU145. In fact, the drug has minimal effects on the Lum/Fluo ratio in DU145-HiBiT cells (see Figure 22B and 23A), however it induces a significant upregulation of DAB2IP protein in parental unedited DU145 cells (Figure 25B). The easiest explanation for this observation would be that the selected DU145-HiBiT clone is somehow different than the parental cells. Another possible explanation is that salmeterol acts through a mechanism that involves the C-terminal aminoacids of DAB2IP, that are altered by the HiBiT fusion.

Figure 22

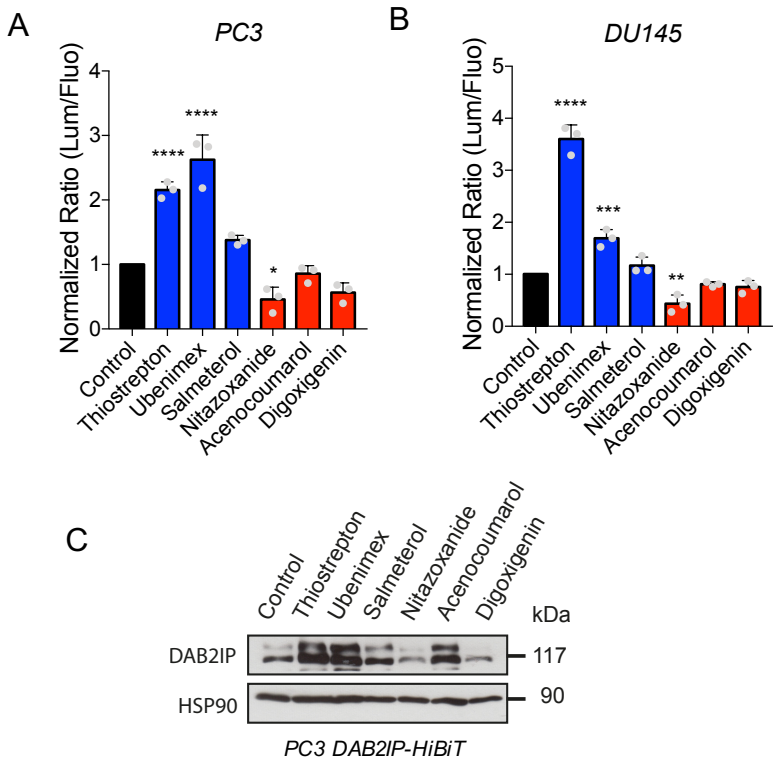

Figure 22 | Further validatiton of selected hits. A-B) Analysis of the Lum/Fluo ratio of PC3-HiBiT cells (A) and DU145-HiBiT cells (B) treated for 36h with 6 hit compounds (10 µM) or DMSO. (Results are represented as mean ± SD of n=3 indipendent experiments; **** P<0.0001; *** P<0.001; ** P<0.01; * P<0,1; one-way ANOVA with Dunnett's post hoc). **C)** Western blot analysis of endogenous DAB2IP detected in PC3-HiBiT cells treated as in A. HSP90 was blotted as loading control.

Figure 23

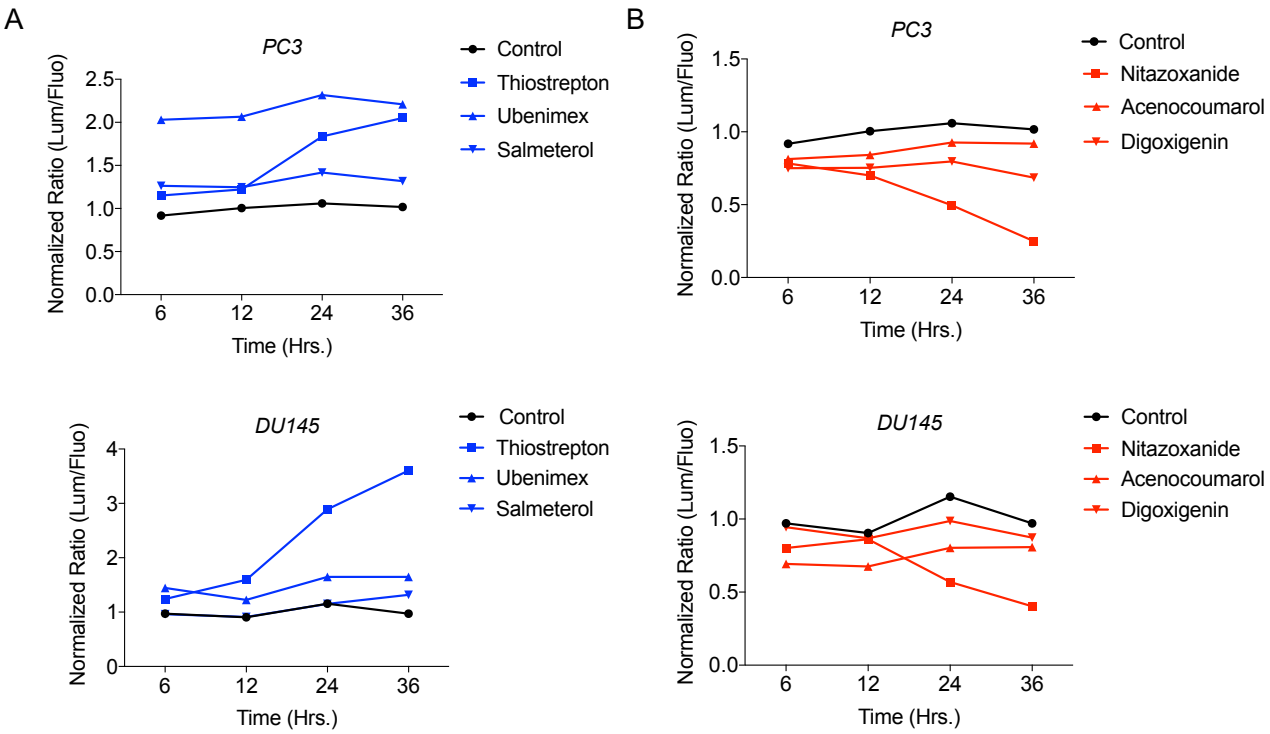

Figure 23 | Time-course of the effect of hit drugs on the Lum/Fluo ratio. The graphs show the Lum/Fluo ratio in PC3-HiBiT cells (above) and DU145-HiBiT cells (below) treated with 3 upregulator drugs **(A)** and 3 downregulator drugs (**B).** Cells were plated in 96-well plates and 24h later drugs were added at 10 µM. Fluorescence and luminescence were detected at the indicated time points. Measurements are the mean of 3 wells per condition.

Figure 24

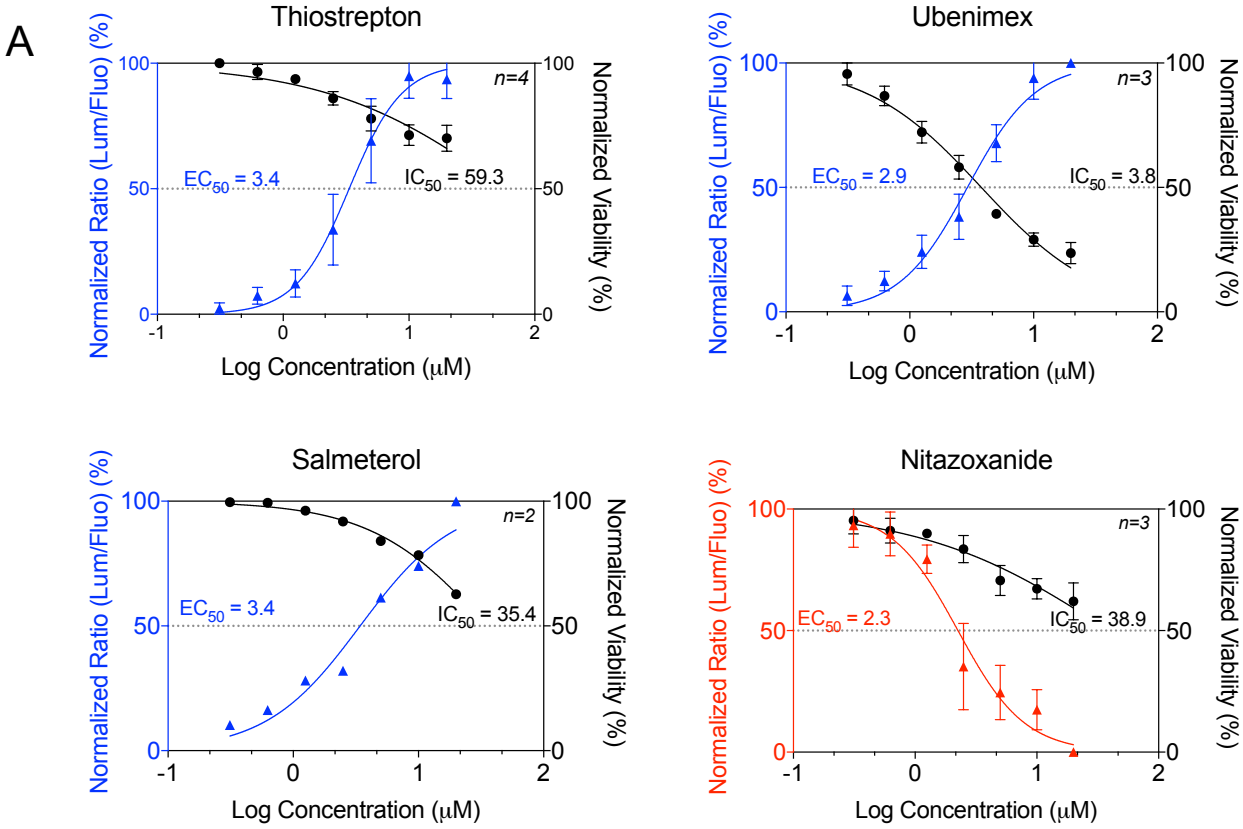

Figure 24 | Dose–response curves of the best candidate drugs. The graphs summarize the effect on DAB2IP levels (i.e. the lum/fluo ratio) and the effect on viability (i.e. fluorescence) of different doses of the indicated drugs in PC3-HiBiT. For each drug, the half-maximal effective concentration (EC50) and half-maximal inhibitory concentration (IC50) are also indicated. Cells were plated in 96-well plates and 24h later the compounds were added for 36h. Data are mean (of n indipendent experiments as indicated in figure) ± SD.

Figure 25

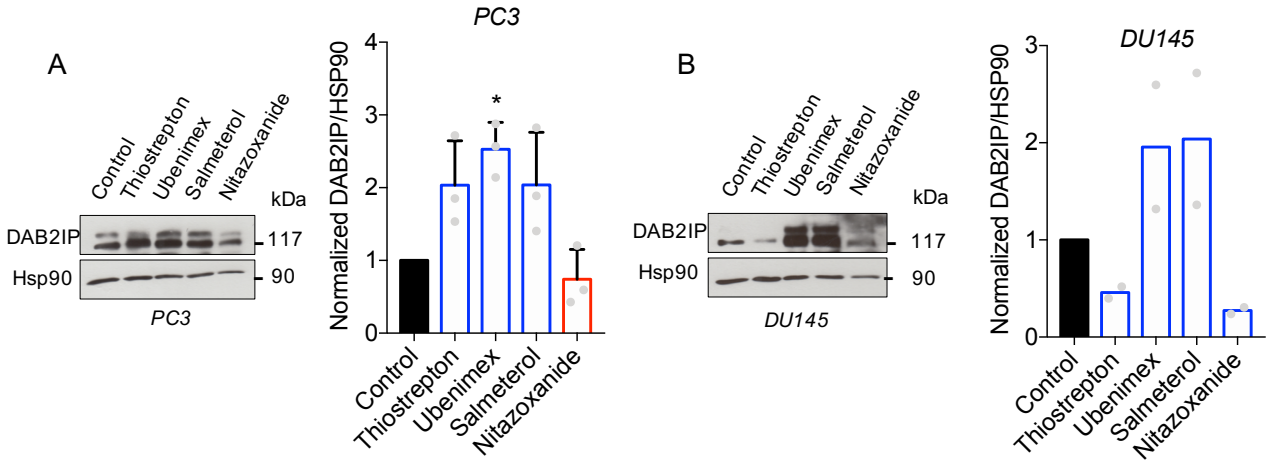

Figure 25 | Effects of candidate drugs on non-edited parental prostate cancer cell lines. A) Thiostrepton, ubenimex and salmeterol increase DAB2IP protein levels, whereas nitazoxanide decrease DAB2IP levels in PC3. Cells were treated with the indicated drugs (10uM) or DMSO (control) for 36h. DAB2IP was detected by immunoblotting, with HSP90 as loading control. On the left panel, a representative blot; on the right, quantification of relative DAB2IP/HSP90 levels as measured by densitometry on autoradiographic film (Data are mean ± SD, n=3; * P<0,1; one-way ANOVA with Dunnett's post hoc). **B)** Thiostrepton and nitazoxanide decrease DAB2IP protein levels, whereas ubenimex and salmeterol increase DAB2IP levels in DU145. Cells were treated and analyzed exactly as in A (Data are mean ± SD, n=2).

Figure 26

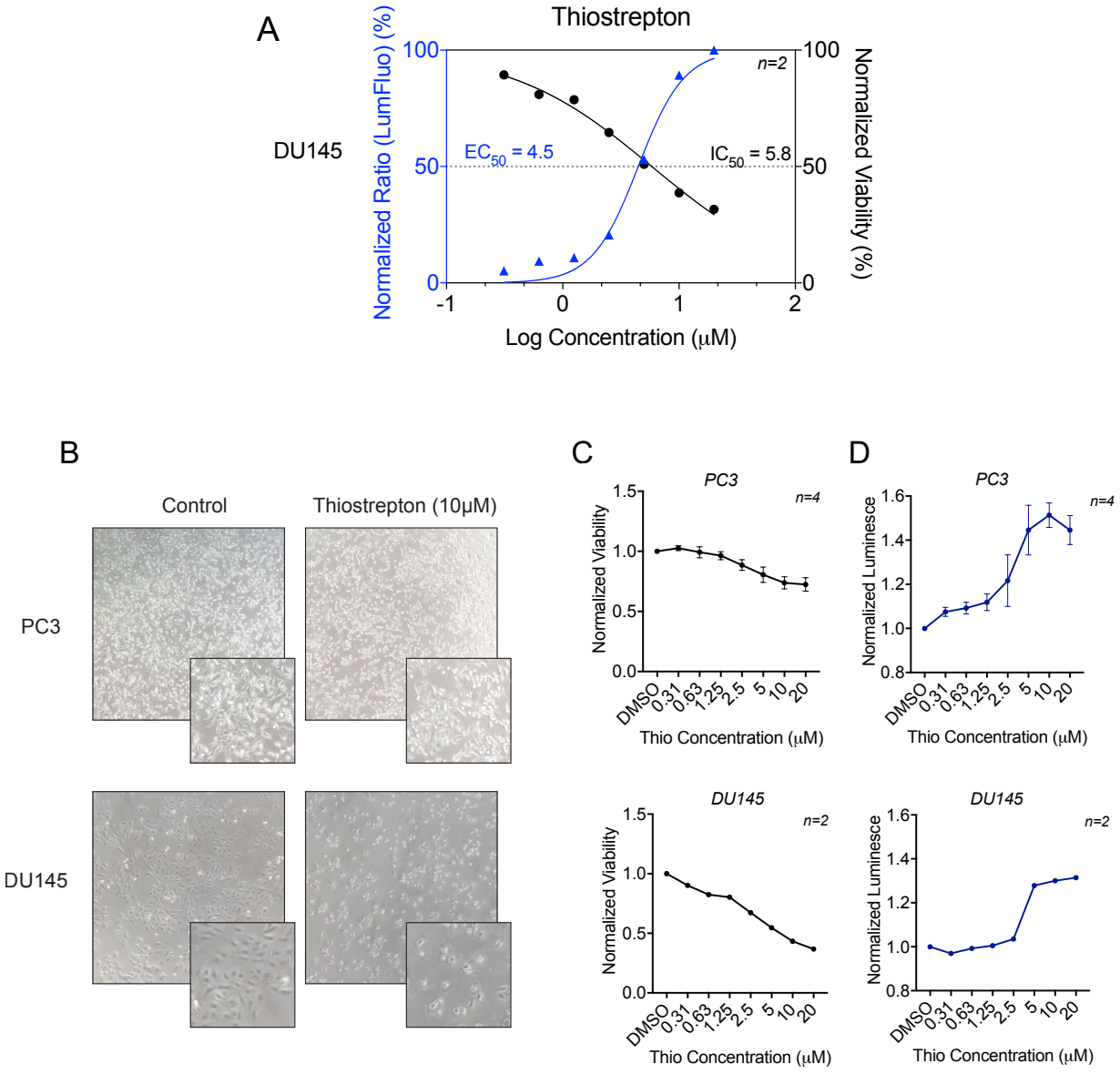

Figure 26 | Effect of thiostrepton in PC3 and DU145. A) Dose–response effect of thiostrepton in DU145 cells. The graph shows the effects of different doses of thiostrepton on Lum/Fluo ratio (DAB2IP levels) and Fluo (cell viability) in DU145-HiBiT cells. Cells were seeded in 96-well plates and treated for 36h (mean ± SD, n=2). **B-C)** Thiostrepton differentially impacts viability in PC3 and DU145. **B)** Representative images of cells treated with 10 uM thiostrepton for 24h. **C)** Graphs summarize viability (CellTiterFluo) of PC3 (above) and DU145 (below) treated with different concentrations of thiostrepton as in A. **D)** Thiostrepton increases luminescence in a dose-dependent manner in both PC3 and DU145. Graphs summarize luminescence (DAB2IP-HiBiT) in PC3 (above) and DU145 (below) treated with thiostrepton as in A. In C and D values are normalized on control. The number of n independent experiments are indicated in figure.

3.3.4 DAB2IP-upregulator drugs act via post-transcriptional mechanisms

To understand the possible mechanisms underlying drug-induced DAB2IP modulation, we investigated whether their action occurred at the transcriptional level. Interestingly, we observed that all upregulator drugs did not change significantly the mRNA levels of DAB2IP, neither in PC3 nor in DU145, suggesting that they may act on protein stability or turnover. On the contrary, the downregulator nitazoxanide clearly reduced DAB2IP mRNA levels, indicating that it probably interferes with its transcription **(Figure 27A-B)**. Curiously, thiostrepton reduced also DAB2IP mRNA in DU145, further supporting the hypothesis that such downregulation may be an artifact caused by the high sensitivity of this cell line to the drug.

Figure 27

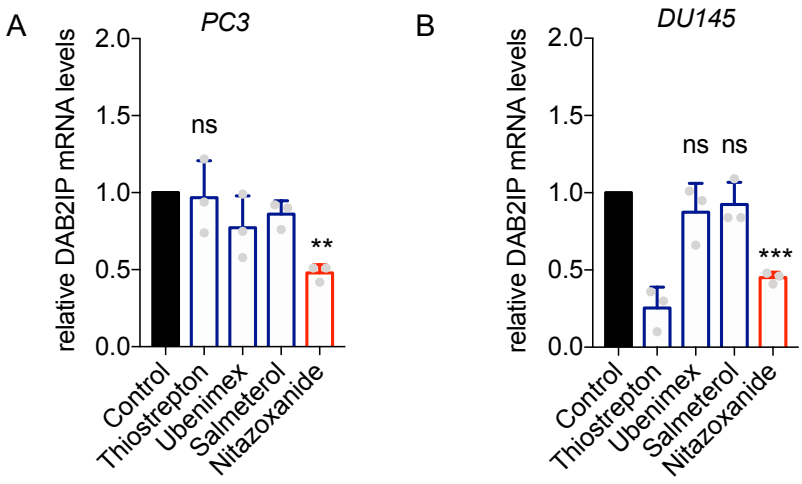

Figure 27 | Effects of candidate drugs on DAB2IP mRNA levels. Upregulator drugs do not increase DAB2IP mRNA levels, whereas nitazoxanide reduces DAB2IP transcript levels. PC3 **(A)** and DU145 **(B)** cells were treated with indicated drugs (10uM) or DMSO for 36h. Expression levels of DAB2IP were measured by RT-qPCR. Values were normalized on histone H3 and compared to DMSO-treated controls (mean ± SD; n = 3; ** P<0,01; *** P<0,001; one-way ANOVA with Dunnett's post hoc).

3.3.5 Some candidate drugs display a similar effect on additional cells

Aiming to corroborate our data, we extended our analysis to additional cancer cell lines. Thus, we treated the breast cancer MCF7 cells with the identified upregulator drugs and detected DAB2IP variation by immunoblotting. As shown in **Figure 28A** all the three molecules increase DAB2IP protein levels, confirming results obtained in PC3 cells. Importantly, also in these cells the drugs do not alter significantly DAB2IP mRNA levels, supporting a post-translational mechanism of action (**Figure 28B**).

Previous studies reported a correlation between DAB2IP depletion in vascular endothelial cells and enhanced tumor growth and metastasis in mouse models of melanoma and breast cancer (Ji et al., 2015), suggesting that DAB2IP in endothelial cells contributes to curb dissemination of tumor cells. We therefore asked whether DAB2IP upregulator drugs could have an effect on non-transformed endothelial cells. Thus, we tested our compounds on HUVECs. Interestingly, preliminary experiments suggest that ubenimex and salmeterol promote the increase of DAB2IP levels also in HUVECs (**Figure 28C**). In line with previous data, also in HUVEC the drug-mediated DAB2IP upregulation occurred at post-transcriptional level (**Figure 28D**).

In contrast, thiostrepton induced a decrease of both DAB2IP protein and mRNA levels in HUVEC (**Figure 28C-D**), as already observed in DU145. The opposing effect of thiostrepton in different cell lines leads us to suppose that this drug may act on DAB2IP in a cell type or tissue-specific manner; in this regard, a significant difference in toxicity in different cell types may play a crucial role (see discussion section).

Figure 28

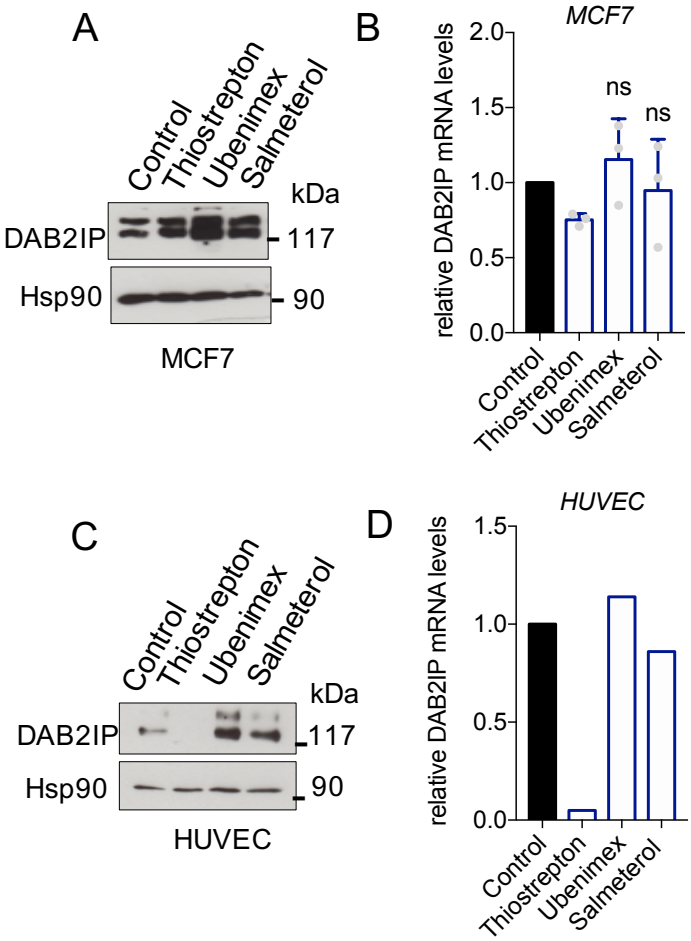

Figure 28 | Effects of upregulator drugs on breast cancer cells and non-transformed endothelial cells. **A)** Thiostrepton, ubenimex and salmeterol increase DAB2IP levels in MCF7. Cells were treated with the indicated drugs (10uM) or DMSO for 36h. DAB2IP protein levels were measured by immunoblotting with HSP90 as loading control. **B)** MCF7 were treated as in A, and expression levels of DAB2IP were measured by RT-qPCR. Values were normalized on histone H3 and compared to DMSO-treated controls (mean ± SD; n = 3; one-way ANOVA with Dunnett's post hoc). **C-D)** Thiostrepton decreases DAB2IP levels, while ubenimex and salmeterol increase DAB2IP in HUVECs. Cells were treated and analyzed as in A and B. Data refer to a single experiment.

3.3.6 Effects of DAB2IP-upregulator drugs on cellular phenotypes associated to tumor aggressiveness

To investigate if the identified DAB2IP-upregulators are able to counteract pro-oncogenic phenotypes we performed wound healing assays with PC3 cells with and without treatments. We performed our experiments treating cells with the respective EC50 drug concentration, in order to use the minimal effective concentration and limit any toxicity-dependent effects.

We interestingly observed that all drugs reduced the migration capabilities of these cells (reduced closure of wound) (**Figure 29A-B**), in line with the effects observed in PC3 cells after DAB2IP ectopic overexpression (**Figure 13G**).

Previous studies reported that endothelial specific DAB2IP knockdown causes an increase of vascular inflammation and remodeling (Zhang et al., 2018). Mechanistically, DAB2IP prevents angiogenesis by counteracting VEGF signaling by directly binding the phosphotyrosine residues within the activation loop of VEGF-Receptor 2 (Zhang et al., 2008). We therefore asked if the identified upregulator molecules, by enhancing DAB2IP, may affect the behavior of endothelial cells. In this case, we excluded thiostrepton because of its contrasting role in HUVECs; thus, we tested ubenimex and salmeterol on HUVECs and measured transcriptional expression of pro-angiogenic markers such as Matrix Metalloproteinase 9 (MMP9) and Angiopoietin (ANGPT1). Interestingly, we observed a decrease of their expression after treatments with both drugs (**Figure 29C**), indicating a potential role of these compounds in counteracting a DAB2IP-related phenotype.

Given the multiple possible actions of any drug, we asked to what extent the observed effects are actually dependent on the increase of DAB2IP protein levels. To this aim, we tested if depletion of DAB2IP could rescue the effects of DAB2IP-upregulator drugs on prostate cancer cell behavior.

First of all, we set up another assay to test a typical oncogenic behavior that is negatively modulated after DAB2IP overexpression: transwell matrix invasion assay (Min et al., 2010) (Di Minin et al., 2014) (Bellazzo et al., 2018) (Feng et al., 2022). Our experiments indicated that all three DAB2IP upregulator molecules reduced the matrigel invasiveness of PC3, confirming that these drugs modulate a DAB2IP-related phenotype.

Most importantly, silencing of DAB2IP partially reduced the action of these drugs in counteracting PC3 invasion, indicating that DAB2IP is involved in the drug-mediated anti-invasive effects (**Figure 30A-B**). Although further experiments are needed to confirm these results, the data indicate that the onco-suppressive effect of these drugs may be at least in part dependent on DAB2IP. Interestingly, the more potent DAB2IP-dependent effect seems to be observed after salmeterol treatment, suggesting a potential tight relation between salmeterol action and DAB2IP upregulation.

Figure 29

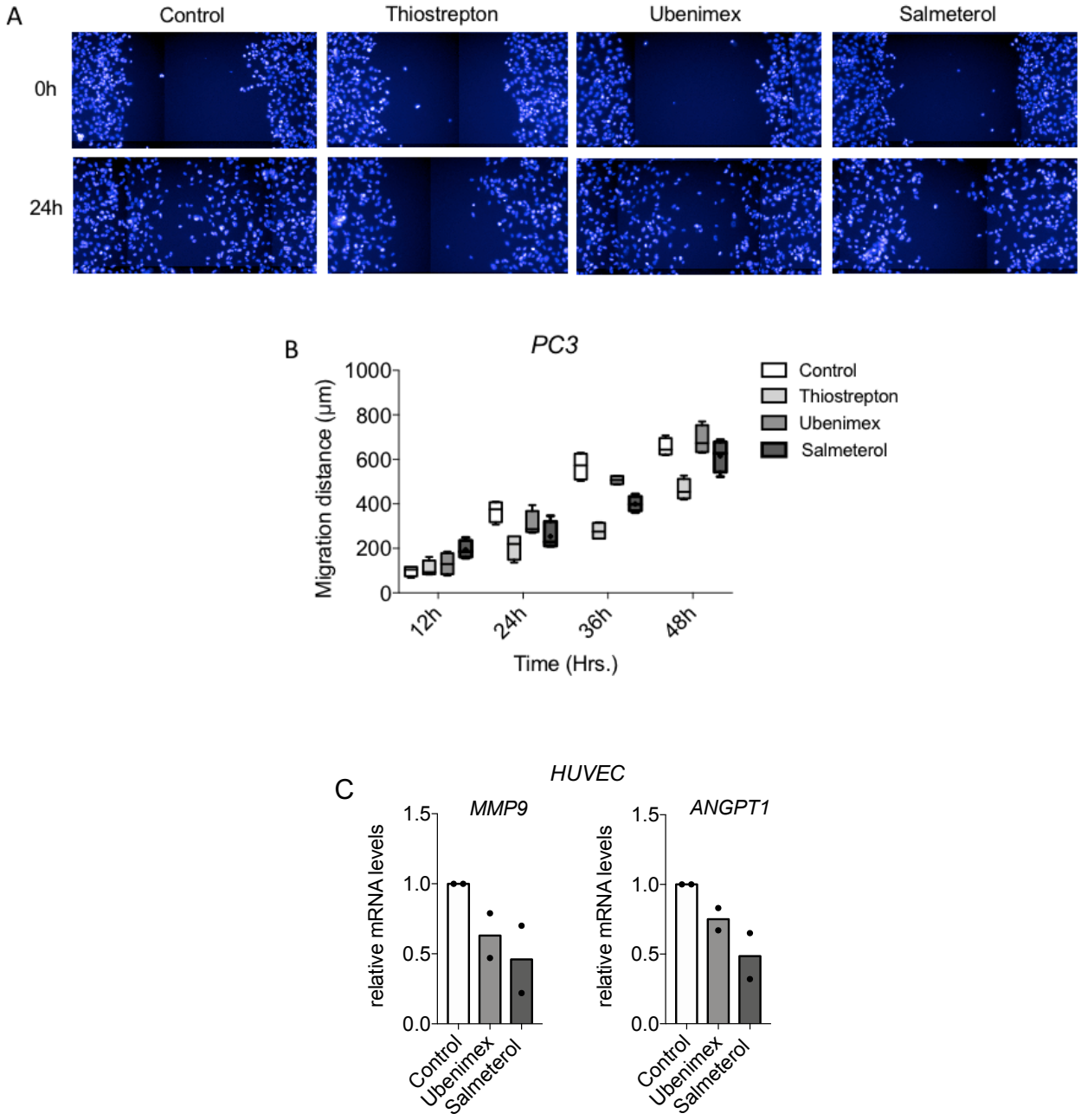

Figure 29 | Effects of upregulator drugs on cancer-associated cell phenotypes. A-B) Ubenimex, thiostrepton and salmeterol inhibit prostate cancer cell migration. PC3 cells were grown until 90% confluence, then a central region was scraped off with a sterile tip and cells were treated with drugs at the EC50 concentration, or with DMSO as control. Wound closured was checked at the indicated time-points. **A)**

Representative images of cells at time 0h and 24h after scratching. **B)** Graph summarizes the migration distance of cells at the indicated time-points. Images of live cells were automatically acquired with PerkinElmer Operetta. The width of the scratches was measured using ImageJ. Migration distances were calculated as indicated in Materials and Methods. Measures refer to 4 distinct scratches for each condition. Data refer to a single experiment. **C)** Ubenimex and salmeterol reduce the expression of pro-angiogenic markers in HUVECs. Cells were treated with the indicated drugs at 10uM concentration for 36h. Expression levels of MMP9 and ANGPT1 were measured by RT-qPCR. Values were normalized on histone H3 and compared to DMSO-treated controls (mean ± SD; n = 2; replicates refer to HUVECs isolated from two indipendent samples).

Figure 30

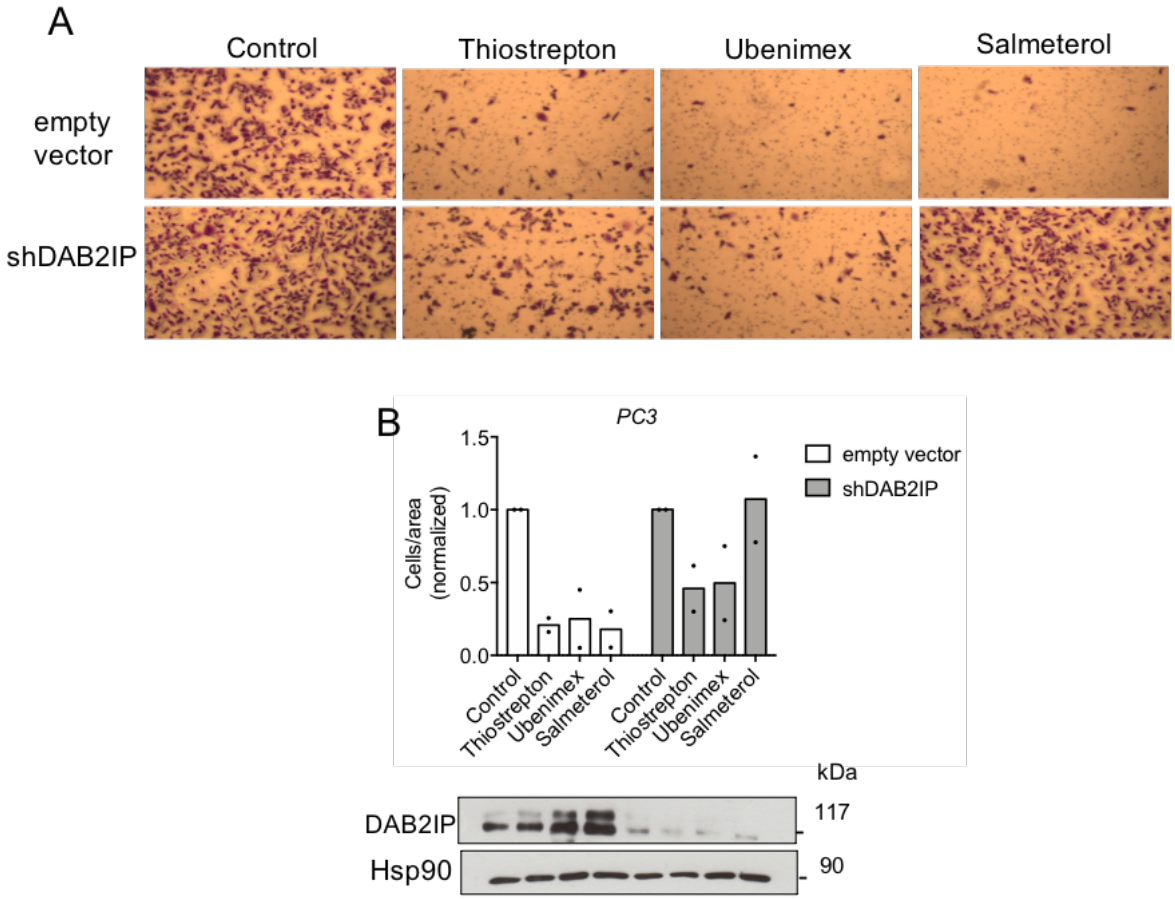

Figure 30 | The anti-invasive properties of upregulator drugs are reduced after DAB2IP depletion.
A-B) DAB2IP loss affects the invasiveness of cells in response to drug treatments. PC3 cells stably expressing a shRNA directed to the 3′UTR of DAB2IP, or empty pRS vector as control, were pre-treated with indicated drugs (at EC50 concentration) or DMSO as control for 24h, then transwell invasion assays were performed in low serum medium in the presence of drugs. **A)** Representative images (40X magnification) of migrated cells fixed and stained with crystal violet. **B)** Graph summarizes migrated cells per area. Migrated cells are the mean of 5 random non-overlapping microscope fields at 100X magnification (single experiment) (mean ± SD; n = 2). Depletion of DAB2IP was checked by western blot.

3.3.7 The molecular targets of ubenimex and salmeterol are differentially expressed in our cell models

To understand the molecular mechanisms underlying drug-induced DAB2IP upregulation, we started asking whether the effects of the drugs on DAB2IP may be mediated by their established canonical targets. Thus, we measured relative gene expression of aminopeptidase N (APN or CD13) and beta-2 adrenergic receptor (ADRB2), the two principal targets of ubenimex and salmeterol, respectively, in our cell models. Performing real-time RT-PCR we found that PC3 cells clearly express APN mRNA, whereas DU145, MCF7 and HUVECs have much lower levels (Figure 31A). Based on this analysis, the observed effect of ubenimex on DAB2IP seems not to correlate with APN expression; such a result implicates that Aminopeptidase N is likely not involved, suggesting that alternative mechanisms, or other cellular aminopeptidases, could be implicated. This consideration is based on RNA expression, and will need to be confirmed by analysis of APN protein levels.

As regarding salmeterol, its main target ADRB2 is expressed in cancer cell lines (more abundant in PC3), but is extremely low in HUVECs (100-fold less then PC3) (Figure 31B). Considering that salmeterol has an evident effect in HUVEC (Figure 28C), we cannot exclude that the action of salmeterol on DAB2IP is mediated by a mechanism that does not involve the beta-2 adrenergic receptor. Even in this case, analysis of ADRB2 protein is needed to support or contradict this hypothesis.

Overall, a significant amount of further studies will be required to investigate the mechanism of action of these drugs on DAB2IP levels.

Figure 31

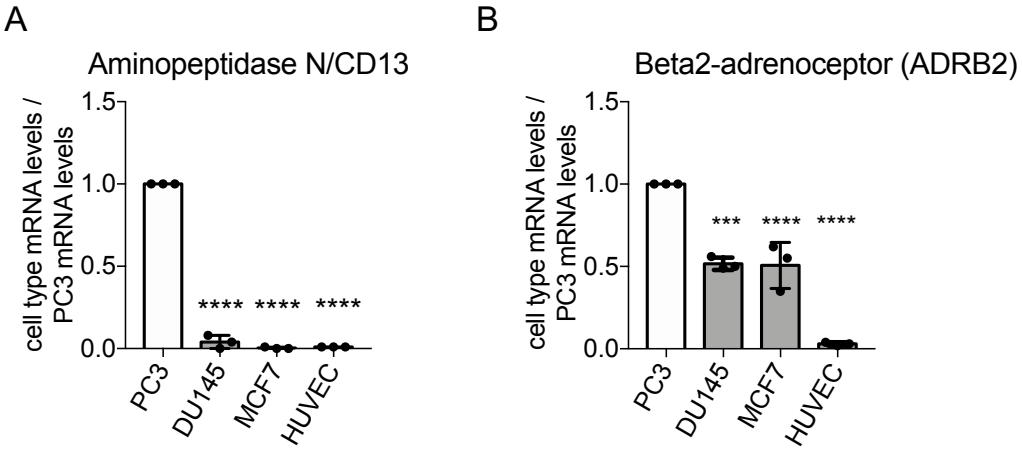

Figure 31 | Expression of CD13 (ANPEP, aminopeptidase N) and ADRB2 in our cell models.

A) CD13 is much more expressed in PC3 than in all other cell lines. **B)** ADRB2 is variably expressed in cancer cell lines but very low in HUVEC. mRNA levels of CD13 and ADRB2 were measured by RT-qPCR. Data were normalized on histone H3 and compared to PC3 (mean ± SD; n=3; **** P<0.0001; *** P<0.001; one-way ANOVA with Dunnett's post hoc).

Supplemental Data Figure 32

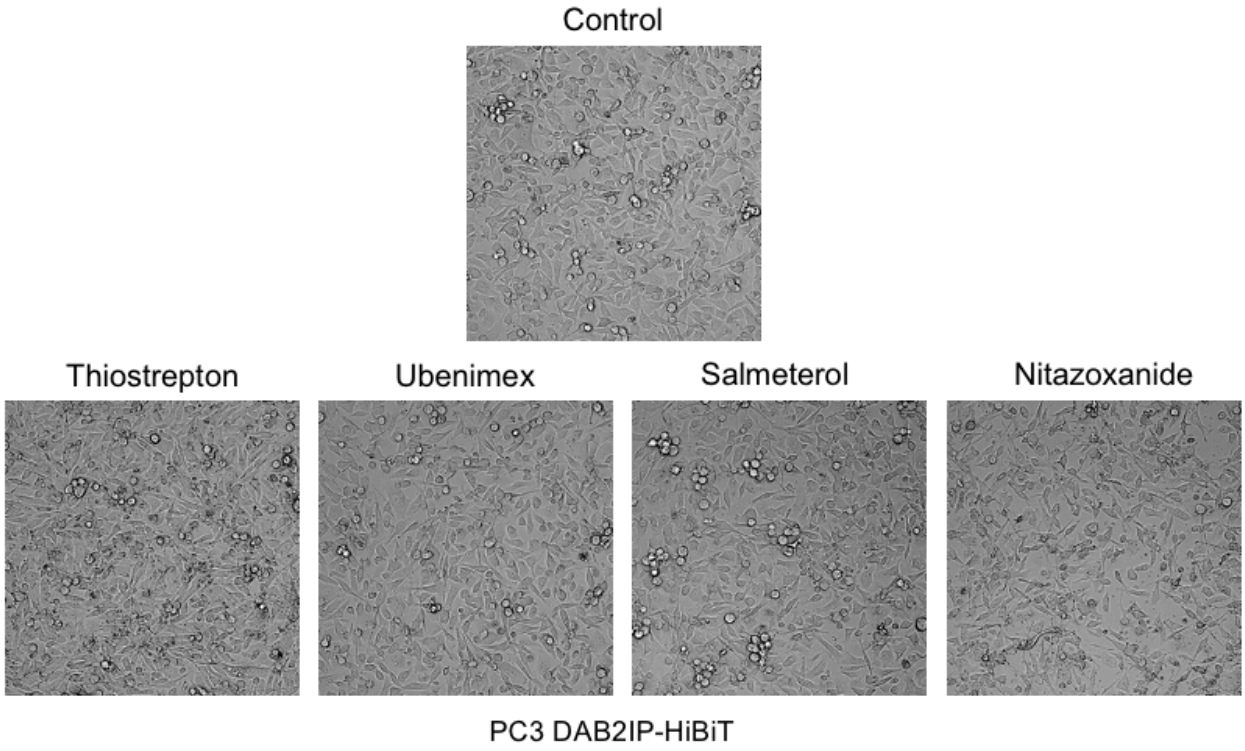

Supplemental Data Figure 32 | Effects of candidate drugs on PC3 morphology. PC3-HiBiT cells were seeded in 96 well-plates and treated with indicated drugs (10uM) for 24h. Phase-contrast images were automatically acquired with PerkinElmer Operetta on live cells. Images were first flatfield-corrected. Representative fields are shown.

DISCUSSION

3.4.1 An overview on identified drugs

Thiostrepton

Thiostrepton (thio) is an antibacterial drug approved by EMA and FDA for the treatment of bacterial infections in animals. Mechanistically, thio acts as a translation inhibitor, abrogating the binding of GTPase elongation factors to the 23S ribosome of procariotic cells (Bailly, 2022).

However, since its first discovery, different therapeutic activities have been associated to thiostrepton. For instance, thio has been reported to exerts antimalarial effects by disrupting protein synthesis in the apicoplast genome of Plasmodium falciparum (Bailly, 2022). More relevantly, many different studies have highlighted its capacity in reducing cancer cell proliferation and tumor growth (Qureshi et al., 2018). Anti-proliferative properties of thiostrepton in human cancer cells have been mainly associated to the drug-mediated down-regulation of protein expression and activity of the oncogenic transcription factor Forkhead box M1 (FoxM1). Molecular simulations indicate that thio directly inhibits FoxM1 in breast cancer by increasing the stability of the hydrogen bonds in the binding region between FOXM1 and DNA, resulting in transcription inhibition (Kongsema et al., 2019). FoxM1 is frequently over-expressed and fully activated during development and progression of solid tumors, notably for breast cancers, while its expression is often very reduced, if not totally abrogated in normal cells. FoxM1 is described as a target of choice for the development of novel anticancer drugs; the selective inhibition of FoxM1 by thio restores cell apoptosis but also suppresses proliferation, transformation ability and angiogenesis in many different types of cancer cells, such as laryngeal squamous carcinoma (L. Jiang et al., 2015), colon cancer (Ju et al., 2015), gastric cancer (S.-X. Liu et al., 2022), melanoma (Shuxi Qiao et al., 2012), and other solid tumors cell types. Also, the targeting of FoxM1 by thio was found to reduce the proliferation of B-cell and T-cell acute lymphoblastic leukemia (Kuttikrishnan et al., 2021) (B. Zhang et al., 2014) (Jian-Yong Wang et al., 2015) (Buchner et al., 2015). Interestingly, the negative regulation of FoxM1 by thio and analogues is associated with a reduced anchorage-independent growth of cancer cells (Radhakrishnan et al., 2006) (Kwok et al., 2008). Very recently, thio has been shown to induce ferroptosis in pancreatic cancer cells though the activation of STAT3/GPX4 signaling (W. Zhang et al., 2022).

Another mechanism of action of thio is that it inhibits proteasome activities (Schoof et al., 2010) leading to the accumulation of ubiquitinated proteins (Sandu et al., 2014). This event causes a proteotoxic stress, producing a huge upregulation of heat shock proteins, increased oxidative stress, and endoplasmic reticulum (ER) stress response in cancer cells; all these effects contribute to induce apoptotic cell death (Shuxi Qiao et al., 2012).

In some models, the antitumor activity of thio alone is relatively weak compared to approved anticancer drugs, but it is significantly enhanced in case of drug combinations. For instance, thio has revealed synergistic activity with the proteasome inhibitor bortezomib in prostate and liver cancer (Pandit & Gartel, 2010) (M. Wang et al., 2012), the tubulin-binders docetaxel and paclitaxel in advanced prostate cancer and triple-negative breast cancer (H. Yu et al., 2020) (C. Huang et al., 2019) (N. Yang et al., 2019), the thymidylate synthase inhibitor 5-fluorouracil (T. Xie et al., 2016) (Varghese et al., 2019) and the DNA-alkylating drug cisplatin in different cancers (Lin et al., 2013), among others. Interestingly, thio has been showed to increase mucosal absorption of macromolecules, by attenuating tight junctions-barrier function in epithelial intestinal cells, thus enhancing their permeability (Watari et al., 2017).

Another notable action of thio is its ability to reduce drug resistance of cancer cells. For instance, it enhances the sensitivity to the PARP inhibitor olaparib in ovarian cancer by mediating FOXM1 inhibition and the consequent reduced expression of HR genes, such as BRCA1 and RAD51 (Fang et al., 2018). Also, via inhibition of the FOXM1/RAF-MEK-ERK pathway, thio has been shown to reduce paclitaxel resistance in pancreatic cancer cells (C. Huang et al., 2019). Also, direct or indirect thio-mediated inhibition of FoxM1 has been shown to sensitize various tumor types to radiation-induced cell death (Lee et al., 2018). Finally, some evidences report the ability of thio in increasing autophagy thus enhancing immunogenic chemotherapy in vivo (Kepp & Kroemer, 2020) (Y. Wang et al., 2020).

Curiously, the tumor suppressor p53 is a negative regulator of FoxM1 (Gartel, 2014); normal cells, that express a wild type p53 protein, appear indeed to be more resistant to thio action (Halasi et al., 2009).

Perhaps the main pitfall in clinical use of thiostrepton lies in its non-solubility in water (Bailly, 2022). The drug is partially soluble in solvents like DMSO or chloroform, and this complicates the handling of the pharmaceutical ingredient. This is the reason why today the drug is only used topically. Specific formulations have been developed to facilitate the systemic delivery and bioavailability of thio, with the aim to get the approval for use in human (Bailly, 2022). For instance the encapsulation into micelles, liposomes and other micro/nano-structures has been shown to improve the drug delivery and potentiate the anti-cancer properties in mouse models of breast cancer (M. Wang & Gartel, 2011). Also, liposome-encapsulated thiostrepton shows a higher potential in reducing FOXM1 levels and impairing cell viability in MCF-7 cells compared to the free drug, and this may be a potential delivery system to improve efficacy of this drug in breast cancer (Wongkhieo et al., 2021). Currently, considerable effort has gone into the development of more soluble thiostrepton derivatives using chemical synthesis and bioengineering approaches (Bailly, 2022).

Ubenimex

Ubenimex (ube) is a competitive protease inhibitor. The drug was isolated from Streptomyces olioореticuli in 1976 and to date is approved in Japan for the treatment of acute non-lymphocytic leukemia and lung cancer under the name Bestatin. In the USA the drug is currently in Phase II for the treatment of pulmonary arterial hypertension and lymphedema. Although ube has been demonstrated to reach therapeutic efficacy and survival benefit in acute myeloid leukemia (AML) and lymphomas; it is still under clinical trials for the treatments of multiple solid tumors (Scornik & Botbol, 2001) (Chen et al., 2011) (Barnieh et al., 2021).

Ube is a non-selective protease inhibitor; it is known to inhibit at least 12 different aminopeptidases, including aminopeptidase B (APB), aminopeptidase N (APN or CD13), leucine aminopeptidase (LAP), methionine aminopeptidases (MetAP) and leukotriene A4 hydrolase, among others (Chen et al., 2011). Aminopeptidases are essential for protein maturation, activation, and stability as well as in the degradation and regulation of hormonal and nonhormonal peptides (Chen et al., 2011). Altered activity of aminopeptidases is associated with multiple diseases, such as aging, cancer, cystic fibrosis, hypertension, neurodegeneration, and leukemias, among others. Different aminopeptidases regulate different physiological and pathological mechanisms. For example, APB is involved in inflammatory processes, tumorigenesis, and type II diabetes, while APN exerts a role in angiogenesis and degradation of extracellular matrix, thus facilitating tumor survival and invasion (Chen et al., 2011). Among the aminopeptidases targeted by ube, aminopeptidase N (aka CD13), plays an important role in tumor progression, and is considered a major target for novel anti-cancer drug development (Wickström et al., 2011).

Different pharmacological properties have been associated to ube. First of all, it exerts a broad effect on the immune system both in vitro and in vivo. In detail, it can enhance T-cell proliferation, differentiation of T-cell precursors into CD4+ cells and activate monocytes. It also promotes the secretion by macrophages of pro-inflammatory cytokines IL-1, IL-6, IFNγ, and TNFα, as well as growth factors GM-CSF and G-SCF (Scornik & Botbol, 2001).

The inhibition of aminopeptidase N is at least in part responsible for ubenimex antitumor effects, acting at different levels. Ube can restrain cancer indirectly, by stimulating the immune system to reject the tumor (Scornik & Botbol, 2005), or can direct inhibit proliferation of tumor cells.

Another antitumor effect of ube is the inhibition of tumor invasion (Scornik & Botbol, 2001). Mechanistically, ube-mediated inhibition of invasion of breast cancer cells is associated to a reduction of E-cadherin-dependent cell adhesion, and this effect correlates with inhibition of APN (Fujioka et al., 1995). Accordingly, high APN expression in melanoma cells enhances their invasive and metastatic behavior (Fontijn et al., 2006). In fact APN participates in the degradation of collagen type

IV, a major component of the tumor extracellular matrix, suggesting a possible explanation of its active role in tumor invasion and metastasis (Saiki et al., 1993). Recently, ube has been reported to suppress the migration and invasion capabilities of gastric cancer cells by inhibiting the MAPK pathway (X. Liu et al., 2021). Ube also exerts anti-angiogenic properties. In tissue culture, it inhibits the formation of new capillary structures by human umbilical vein endothelial cells (HUVECs); in mice models, intraperitoneal administration of ube in melanoma xenografts reduced the number of vessels near the primary tumor mass (Chen et al., 2011) (Barnieh et al., 2021). Not surprisingly, in endothelial cells, both APN mRNA and protein are upregulated in response to hypoxia and/or pro-angiogenic growth factors such as bFGF, TNFα, and VEGF. The neo-angiogenesis role of APN has been shown to be essential to tumor growth, and various APN inhibitors have exhibited promising anti-angiogenic activities (Barnieh et al., 2021).

ANP is also a key player in multidrug resistance (MDR) in cancer treatments. Interestingly, ANP inhibition by ube is capable to resolve MDR; in detail, the combination of bestatin with cisplatin or 5-fluorouracil, has been demonstrated to reverse MDR in gastric, non-small lung and hepatocellular carcinoma cells, via inhibiting PI3K/AKT/NF-κB and mTOR axis (Guo et al., 2017) (Guo et al., 2020) (Wan et al., 2020). Again, the combined therapy of ube with the chemotherapeutic pemetrexed hinders the progression of lung adenocarcinoma cells by inhibiting the JAK2-STAT3 signaling pathway (Q. Chen et al., 2022).

From a mechanistic point of view, APN has two types of activities: i) enzyme-dependent and ii) enzyme-independent. Regarding the first, APN can cleave the N terminus of numerous cytokines, hormones, and chemokines and can trim peptides that bind to MHC II. Regarding the enzyme-independent activity, accumulation ANP on the cell surface induces tyrosine cross-phosphorylation of APN, that promotes the activation of various oncogenic signaling pathways that involve protein kinases such as Src, FAK and ERK, and other components of the Ras/MAPK and PI3K pathways (Subramani et al., 2013). In addition, APN interacts with FcgRs and enhances phagocytosis by increasing the level and duration of Spleen-associated tyrosine kinase (Syk) phosphorylation. Finally, APN is a cell surface receptor for different cytokines and chemokines, thus acting as a signal transductor for different pro-oncogenic pathways such Ras/MAPK and PI3K (C. Lu, Amin, & Fox, 2020).

Several APN inhibitors are at various stages of pre-clinical and clinical investigations, however no APN inhibitor is currently approved for anti-cancer treatment in Europe or USA. Considering the multi- and broad-functional spectrum of APN in various physiological processes, its inhibition is consider very likely to cause unexpected complications and toxicities (Barnieh et al., 2021). Again, the contrasting functions of APN in various cancers and different stages also raises concerns about

APN inhibition as an anti-cancer strategy. All together these evidences explain the long delay in the FDA approval of ubenimex for clinical use (Chen et al., 2011).

Salmeterol

Salmeterol (sal) is a highly selective long-acting beta-2 adrenergic agonist (LABA) that is currently prescribed for the treatment of asthma and chronic obstructive pulmonary disease (COPD).
Salmeterol is similar in structure and mechanisms of action of the better known salbutamol (Adams & Nguyen, 2022). Salmeterol's benzene moiety reflects the structure of catecholamine and occupies the active site of beta-2 adrenergic receptor (ADRB2). The ADRB2 is a member of the G-protein coupled receptor (GPCR) family. GPCRs have long been overrepresented as targets for drug therapy with about 30-50% of drugs acting via GPCRs either directly or indirectly (Elia et al., 2015). ADRB2 are ubiquitously expressed but are particularly abundant in smooth muscle tissue.
The particular site of binding of sal to the beta-2 adrenergic receptors, allows the molecule to stably remain at the receptor site and continually engage and disengage with the receptor, therefore providing a longer duration of action compared to analog compounds, such as salbutamol. Salmeterol, by activating ADRB2, stimulates intracellular adenyl cyclase to catalyze the conversion of adenosine triphosphate to cyclic-3',5'-adenosine monophosphate (cAMP). Increased cAMP levels induces the activation of protein kinase A (PKA) that inhibits myosin light chain kinase resulting in relaxation of bronchiolar smooth muscle, bronchodilation and increased bronchial airflow (Adams & Nguyen, 2022).
β2-adrenoceptor agonists can affect different cellular processes. For instance, they can regulate the immune system via beta-2 adrenergic-dependent pathways. Specifically, agonists of ADRB2 has been shown to reduce the percentage of CD4 and CD8 T cells, as well as the cytotoxicity of both CD8 T and NK cells in vitro (Zalli et al., 2015). However, ADRB2 expression has been shown to positively correlate with immune cells infiltration in breast cancer (Wei et al., 2021) and in lung adenocarcinoma (L. Ji et al., 2022), indicating it as a potential protective gene in cancer. Low ADRB2 expression, in fact, correlates with poorer overall survival of lung cancer patients (L. Ji et al., 2022). Also, inhibitors of ADRB2 are reported to reduce inflammation in cell renal carcinoma (Albiñana et al., 2022).
Although beta-2 receptor is the main target of sal, there are evidences for an ADRB2-independent action of sal in inducing apoptosis in B-chronic lymphocytic leukaemia cells. In this case, the action of salmeterol did not require cAMP synthesis, but involved a Ca^{2+}-dependent mechanism (Mamani-Matsuda et al., 2004).

Salmeterol is not currently used directly for treatment of cancers and few studies describe its effects on cancer cells; on the contrary, various evidences suggest a role of beta-2 adrenergic receptor signaling in the progression and metastasis of cancer, thus indicating ADRB2 as a potential target for cancer therapy (J. Yu et al., 2007).

For the sake of brevity, here I just describe in detail the role of ADRB2 signaling in prostate cancer. The prostate is highly enriched in β-adrenergic receptors (Braadland et al., 2015). There are controversial evidences regarding the role of ADRB2 in prostate cancer development. To begin, collective evidences fail to indicate whether adrenergic signaling is beneficial or disadvantageous for prostate cancer patients. Both stimulatory and inhibitory effects of adrenergic stimulation on proliferation have been observed in cell lines studies. In this regard, Yu and colleagues have shown that the expression level of ADRB2 changes during the metastatic process of prostate cancer (J. Yu et al., 2007). Despite up-regulation of ADRB2 is observed in malignant compared to benign prostate tissue (Ramberg et al., 2008), a decrease in ADRB2 expression is observed in aggressive relative to moderate prostate cancer (J. Yu et al., 2007). Interestingly, knockdown of ADRB2 was shown to induce EMT in benign prostatic epithelial cells. Expression analyses have revealed that ADRB2 knockdown cells upregulate mesenchymal markers. Indeed, ADRB2 knockdown cells, as well as cells treated with an ADRB2 antagonist, show increased ability to migrate and invade. Conversely, treatment with ADRB2 agonists, reduces invasion in prostate cancer cells (J. Yu et al., 2007).

However, different and opposite effects have been observed after chronic exposure to ADRB2 agonists both in vivo and in vitro, such as neuroendocrine differentiation, metastasis, angiogenesis, and apoptosis-resistance, indicating that adrenergic signaling promotes prostate cancer progression (Braadland et al., 2015).

From a clinical point of view, during androgen deprivation therapy of prostate cancer patients, low β-adrenergic activity, and down-regulation of ADRB2 mRNA, respectively, have been reported (Ramberg et al., 2008). Although ADRB2 is up-regulated in malignant cells, the expression levels seem to decrease during progression; also ADRB2 is inversely correlated with PSA recurrence (J. Yu et al., 2007). In metastatic prostate cancer, the situation is more complex as both high and low levels of ADRB2 have been observed (Ramberg et al., 2008) (J. Yu et al., 2007). Given controversial evidences, more data are needed to understand the role of ADRB2 in development of castration-resistant prostate cancer (Braadland et al., 2015).

Regarding the signaling downstream to ADRB2 in prostate cancer, the main effector appears to be PKA. Active PKA translocates to the nucleus and phosphorylates cAMP responsive element binding protein (CREB), which induces the expression of neuroendocrine markers and both pro- and anti-apoptotic proteins (e.g. BAD and BCL2). Also, PKA promotes the activation of PI3K/AKT/p70S6K

signaling that converges in the activation of HIF-1α and up-regulation of VEGF expression. Furthermore, PKA may inhibit the Ras homolog family member A (RhoA) and Rho-associated protein kinase (ROCK) pathway (Braadland et al., 2015).

Interestingly, ADRB2 is also a target of two important transcriptional modulators involved in prostate cancer progression: ERG and EZH2 (Braadland et al., 2015). High expression of ERG and EZH2 in prostate cancer are associated with metastasis and castration-resistance (Abou-Ouf et al., 2016) (Xin, 2021). Both ERG and EZH2 exert a repressive action on ADRB2 transcription in vitro (J. Yu et al., 2007) (Braadland et al., 2015), suggesting a possible advantage of ADRB2 inhibition in prostate cancer development.

3.4.2 Discussion

The tumor suppressor DAB2IP is frequently downregulated in various human malignancies by multiple mechanisms that act at transcriptional and post-transcriptional levels. In contrast, DAB2IP is very rarely mutated, so it is a strong candidate for the development of anti-cancer drugs that increase its expression. In this Thesis, we screened a library of 1280 FDA-approved drugs and identified molecules able to modulate, both positively and negatively, the expression levels of endogenous DAB2IP. Drugs that induce DAB2IP downregulation are not interesting for their potential clinical application, but could reveal novel mechanisms of DAB2IP downregulation, that in turn may be targetable to promote DAB2IP stabilization in cancer.

The generation of CRISPR/Cas9 DAB2IP-tagged cell lines enabled to screen compounds that affect endogenous protein regulation and stability under native conditions. In fact, studying gene expression and protein functions based on ectopic protein overexpression may lead to inconveniences such as protein misfolding, false localization, and nonspecific protein-protein interactions, thus hampering the correct study of protein regulation (Gibson et al., 2013). Since many different studies described epigenetic regulations of DAB2IP in many types of tumors, such as promoter hypermethylation or microRNA-mediated regulation (Wang et al., 2016) (Yano et al., 2005), endogenous DAB2IP tagging allowed also to search for molecules that counteract cellular intrinsic mechanisms of DAB2IP downregulation, including those that involve its 5' and 3' untranslated regions. Moreover, the existence of multiple isoforms, possibly having different regulation and functions, renders it difficult to accurately study DAB2IP regulation using approaches that involve ectopic expression of the protein. Finally, the high accuracy and sensitivity of the bioluminescence detection of HiBiT-tagged DAB2IP enabled to detect even moderate variations in DAB2IP levels.

The choice of the insertion site was driven by the need to tag all possible isoforms, and, at the same time, to limit the impact on the structure and function of the protein. Given the complexity of multiple variants, but to avoid the potential disadvantages of an internal tag, such as protein misfolding or tag masking, we inserted the HiBiT peptide, followed by a stop codon, immediately upstream of the last splice donor site, in order to translate the same C-terminally tagged DAB2IP protein regardless of the C-terminal splicing. Thus, the HiBiT-derived luminescent signal theoretically matches with the total amount of expression of all possible DAB2IP isoforms.

Even though the screening was performed only once, the best hits were strongly confirmed by further experiments. In fact, four drugs were shown to up- or down- regulate endogenous DAB2IP protein in various cell lines. Focusing on the up-regulators, we identified three drugs – an antibiotic, thiostrepton, an anti-leukemic, ubenimex and an anti-asthmatic, salmeterol – able to enhance DAB2IP

expression. Our experiments indicate that all these drugs do not alter mRNAs expression, suggesting a post-transcriptional or post-translational mechanism of action. In this regard, DAB2IP has been reported to be downregulated by E3 ubiquitin-ligases such as Skp2 and Smurf1 (Tsai et al., 2014) (Xiaoning Li et al., 2016) and it could be subject to translational inhibition by microRNAs (Xu et al., 2015) (Bellazzo et al., 2018) (Xiaoli Li et al., 2019) (Ni et al., 2020). It is therefore possible that similar mechanisms are targeted by some of the identified compounds.

Preliminary experiments indicate that DAB2IP upregulator drugs are able to counteract some cancer-associated phenotypes, indicating a possible repositioning of these molecules for cancer treatment. In this regard, there are various preclinical evidences describing the effects of two of these drugs, thiostrepton and ubenimex, in inhibiting growth and invasion of many different tumor cells. Despite this, they are not yet approved by FDA for cancer treatment.

Here I will discuss the results separately for each drug:

Thiostrepton

Regarding the anti-cancer properties of thiostrepton, they have been mainly associated to the inhibition of expression of the transcription factor Forkhead box M1 (FoxM1) in cancer cells. FoxM1 regulates cell cycle genes essential for DNA replication and mitosis (L. Jiang et al., 2015) (Ju et al., 2015) (Qiao et al., 2012) (S.-X. Liu et al., 2022) (Radhakrishnan et al., 2006) (Kwok et al., 2008). Speculatively, it cannot be excluded that thiostrepton, by inhibiting FoxM1, counteracts the expression of proteins involved in DAB2IP downregulation, promoting its accumulation. Clearly, this hypothesis requires appropriate experiments, for instance to test the effects of transient knockdown of FoxM1, that will be planned in the near future.

Another action of thiostrepton is that it inhibits proteasome activities (Schoof et al., 2010) leading to the accumulation of non-degraded ubiquitinated proteins in cells (Sandu et al., 2014). The fact that thiostrepton increases DAB2IP protein levels without affecting mRNA levels may suggest that its action is proteasome-dependent. Specific experiments will be required to test this possibility.

Despite the robust DAB2IP-upregulatory effect of thiostrepton in different cell lines, we observed a paradoxical effect of this drug in DU145-HiBIT cells: luminescence assays indicate upregulation, but immunoblotting shows a dramatic reduction in protein levels. In this regard, we formulated two possible hypothesis: (i) maybe in DU145 DAB2IP is cleaved by cellular proteases in response to thiostrepton-induced toxicity and the C-terminal part of the protein, with the HiBiT peptide, remains available for complementation and luminescence activity; (ii) maybe the increase of DAB2IP triggered by thiostrepton in DU145 (and other cell lines) triggers cell death, and this renders

inaccurate – and therefore not meaningful – any measurement of the protein levels, either by luminescence or by immunoblotting.

To answer the first hypothesis we checked by western blot the presence of faster migrating bands in the lysate of DU145 treated with thiostrepton. However, our analysis did not detect shorter DAB2IP fragments (data not shown). Regarding the second hypothesis, we measured luminescence of DU145-HiBiT cells treated with escalating concentrations of thiostrepton. Strikingly, we observed that at drug concentrations responsible of half-maximal DAB2IP increase (EC50), the cell viability is strongly reduced (see Figure 26A). A plausible explanation would be that the toxicity effect masks detection of DAB2IP by immunoblotting. In this regard, we treated cells with a lower concentration (<EC50) of thiostrepton in order to reduce toxicity; in this case, we did not observe changes in DAB2IP levels with respect to DMSO controls (data not shown). Clearly western blot detection, differently to luminescence assay, is not sensitive enough to detect moderate protein variations. Anyhow, the fact that DAB2IP does not decrease after treatment with low thiostrepton concentration may suggest that the strong downregulation observed with higher doses is somehow related to a toxicity effect. It is also possible that the differential toxicity of thiostrepton observed in different cell lines may be a consequence of the tumor suppressive activity of increased DAB2IP levels. In fact, PC3 have lower basal levels of DAB2IP compared to the other cell lines; the increase in DABIP triggered by thiostrepton in these cells may be not enough to cause cell death. In contrast, in other cell lines the total amount of DAB2IP protein after drug treatment may be sufficient to trigger cell death. A model based on a threshold of DAB2IP levels is conceivable if we think of a stoichiometric interaction with a crucial cellular partner, for instance. Moreover, thiostrepton has a stronger effect on DAB2IP than the other drugs (almost 4-fold versus ~1,5-fold) (see Figure 22B), and this could explain its toxicity in DU145 as compared to the other compounds. In fact, the modest increase of protein expression induced by ubenimex and salmeterol may restore the physiological levels of DAB2IP without triggering its toxicity. Specific experiments will be required to clarify if the loss of viability is indeed related to DAB2IP upregulation; for instance, testing the effects of thiostrepton on DAB2IP-depleted DU145 cells.

Ubenimex

Ubenimex is a non-selective protease inhibitor with at least 12 different targets identified. Among the aminopeptidases targeted by ubenimex, aminopeptidase N (APN or CD13) plays a key role in tumor development and is thereby considered a promising target for development of anti-cancer drugs (Wickström et al., 2011). Evidences reported that ubenimex-sensitive tumor cell lines express APN on their surface, and the use of APN-specific antibodies as well as other peptidase inhibitors indicates

APN as the main mediator of the growth suppressive effect of ubenimex (Scornik & Botbol, 2001). Interestingly, the anti-proliferative effect of ubenimex has been reported to be dependent on the intracellular concentration of the drug, suggesting that either it is targeting a cytoplasmic pool of APN, or that additional intracellular targets of the drug exist, and are involved in cell proliferation (Barnieh et al., 2021). However, it still to be defined whether inhibition of APN by ubenimex modifies the intracellular concentrations of bioactive peptides, or interferes with the role of APN as a signal transduction molecule (Scornik & Botbol, 2001).

When we checked our cell lines for APN expression, we found abundant RNA in PC3, but low levels in all other lines. Highly variable levels of APN are reported in cancer cell lines also according to public gene expression data repositories (http://depmap.org). We did not measure APN protein levels, but our RT-PCR results seem to suggest the involvement of other molecules, in addition to APN, in ubenimex-induced DAB2IP accumulation. In any case, since the molecular axis involved in APN-mediated anti-cancer properties are well studied, it is important to understand in what measure APN inhibition may contribute to DAB2IP increase by ubenimex. To this aim, siRNA-mediated APN knockdown, or the selective inhibition of APN with monoclonal antibodies (mAbs), could be implemented to assess the contribution of APN in DAB2IP regulation.

Interestingly, ubenimex has been reported to exert anti-angiogenic properties (Chen et al., 2011) (Barnieh et al., 2021). Also the inhibition of APN has been shown to counteract angiogenesis; however it has not been fully clarified the role of APN in the anti-angiogenic properties of ubenimex (Barnieh et al., 2021). In endothelial cells, APN mRNA and protein are upregulated in response to hypoxia and other pro-angiogenic growth factors, and APN is detected by IHC in endothelial cells of human and mouse tumors (Pasqualini et al., 2000) (Curnis et al., 2002). We detected low expression levels of APN in HUVEC; this perhaps is not surprising, since we did not provide any angiogenic stimuli. Nonetheless, this observation further suggests that APN may not be the relevant target in ubenimex-induced DAB2IP-upregulation.

Notably, ubenimex counteracts proliferation and metastasis in bladder cancer by reducing AKT expression, and in glioma cells by limiting AKT activation (X. Wang et al., 2018) (Han et al., 2017). In this regard, it should be considered that DAB2IP decreases VEGFR- InsR- and Ras-induced activation of phosphoinositide-3-kinase (PI3K), inhibiting the PI3K-AKT axis (L. Liu et al., 2016) (Bellazzo et al., 2017). Additionally, through its PR and PER domains, DAB2IP respectively binds to PI3K and AKT, and preventing their interaction, directly counteracts the PI3K-induced phosphorylation and activation of AKT (Xie et al., 2009). Thus, part of the AKT inhibitory action of ubenimex could be mediated by DAB2IP. Interestingly, AKT is reported to regulate DAB2IP stability, suggesting a feedback regulatory loop between the two proteins. In detail, AKT

phosphorylates and activates the E3 ubiquitin ligase Smurf1, that induces DAB2IP ubiquitination and elimination (Xiaoning Li et al., 2016). Given these evidences, it is also possible that AKT inhibition by ubenimex might be responsible, at least in part, of the increased DAB2IP levels.
From a clinical point of view, it has been reported that combination of traditional chemotherapeutics with AKT inhibitors can yield better anti-tumor efficacy in mCRPC patients (Westaby et al., 2021) (Ku, Gleave, & Beltran, 2019); these evidences make ubenimex a promising drug for prostate cancer treatments. Understanding DAB2IP contribution in the anti-tumor properties of ubenimex might be very important to develop more specific anti-cancer therapies.

Salmeterol

Salmeterol is the only of the three drugs already approved by FDA for human use. Several studies indicated the involvement of its main target, the beta2-adrenoreceptor (ADRB2), in cancer; however, the effects of ADRB2 signaling in tumor development and progression are still not clear (Braadland et al., 2015). We detected very low levels of ADRB2 in HUVECs, despite a clear induction of DAB2IP after salmeterol treatment, and this suggests that additional cellular targets may be involved. In this regard, a study described an ADRB2-independent pro-apoptotic effect of salmeterol in leukemia cells, confirming that alternative mechanisms may exist behind its anti-cancer effect (Mamani-Matsuda et al., 2004).
To assess the contribution of ADRB2 to salmeterol-mediated DAB2IP upregulation, we may treat cells with other selective Beta2-receptor agonists (e.g. salbutamol), or block its action with ADRB2-specific antagonists (e.g. ICI-118551) (J. Yu et al., 2007) or siRNA-mediated knockdown.
Interestingly, in prostate cancer, the polycomb-group family member EZH2 represses both ADRB2 and DAB2IP expression (Chang & Hung, 2012) (Tamgue et al., 2013) (Y. Zhang et al., 2018), suggesting a shared mechanism of regulation of the two proteins; this may also suggest that PCa cells may benefit by the coordinated inactivation of DAB2IP and a receptor that could induce its upregulation.
In prostate cancer cells, the stimulation of ADRB2 by receptors agonists induces the expression and secretion of VEGF (Bavadekar et al., 2013). We found that salmeterol reduces the expression of pro-angiogenic markers in HUVECs, in line with increased DAB2IP levels. Even though the cell system is different, our data suggest that ADRB2 activation is probably not the main responsible of the observed anti-angiogenic effect of salmeterol in endothelial cells.

To summarize, we provide evidence that DAB2IP is a targetable molecule, and its increase – even small – is potentially able to counteract different pro-oncogenic features of prostate cancer cells.
Our results, although preliminary, set the basis to explore a possible repositioning of thiostrepton, ubenimex, and salmeterol for the treatment of solid cancers. Among the three drugs, salmeterol appears the most promising, given its minimal toxicity and the fact that it is already in clinical use.
Following on these preliminary studies, further analyses are required to confirm the anti-oncogenic properties of these compounds, and in particular to assess whether their effects are dependent on DAB2IP upregulation. In this Thesis, for cell behavior experiments we generally used the drugs at half-maximal effective concentration (EC50). However, since the compounds do not cause high toxicity – except for thiostrepton in some cell lines – we may use higher concentrations in order to have stronger readouts and assess the real contribution of DAB2IP to their anti-tumor effects.
Regarding the mechanisms of action, in addition to several specific experiments mentioned above, a comparative transcriptome analysis of cells treated with the three drugs could unveil potential mediators of drug-induced DAB2IP accumulation.
Notably, the identify drugs can increase DAB2IP levels in multiple cancer cell lines, thus supporting a possible broad effect. We intend to test their effects also on 3D cultures, such as spheroids or organoids of different cancers, in order to assess the impact of DAB2IP upregulation in a more complex heterogenous system, eventually in combination with traditional chemotherapeutics.

PART II

INTRODUCTION

In addition to chemicals and small molecules (i.e. FDA-approved drugs), another possible approach to increase the levels of a cellular protein is the use of non-coding RNAs (ncRNAs) that can control mRNA stability or translation. Essentially, two different RNA-based therapeutics can be considered: one concerns the inhibition of miRNAs that repress DAB2IP in cancer cells (Liao et al., 2015) (Xu et al., 2015) (H.-B. Lu, 2018) (Bellazzo et al., 2018) (Xiao et al., 2019) (Ni et al., 2020); the other concerns the specific enhancement of DAB2IP translation. We decided to explore the second approach, because it has the advantage of being largely independent of the cellular context, and may function both in tumor cells and in non-transformed cells of the TME.

4.1 SINEUPs: a novel tool for RNA therapeutics

SINEUPs are a new functional class of natural antisense long non-coding RNAs (lncRNAs) that increase the translation of partially overlapping mRNAs. Their activity is based on the combination of two domains: an embedded mouse inverted SINEB2 element that UP-regulates mRNA translation (effector domain) and an overlapping antisense region that provides specificity for the target sense transcript (binding domain) (**Figure 33**). In the recent years, different SINEUPs have been synthetically engineered in order to potentially target any mRNAs of interest, increasing translation and endogenous levels of a desired target protein (Zucchelli et al., 2015) (Espinoza et al., 2021).
The binding domain of natural SINEUPs are usually found to overlap the 5'UTR of the target mRNAs where, thanks to the effector domain, protein complexes responsible of protein translation are recruited on. To date the molecular mechanisms by which SINEUPs can enhance translation are not fully elucidated, and basic research is currently aimed to understand the relationship between structure of SINEUPs and their activity. This has led to an optimization of the design of artificial SINEUPs and the identification of the minimal structural features needed for their activity, improving their development as technological tools (Espinoza et al., 2021).

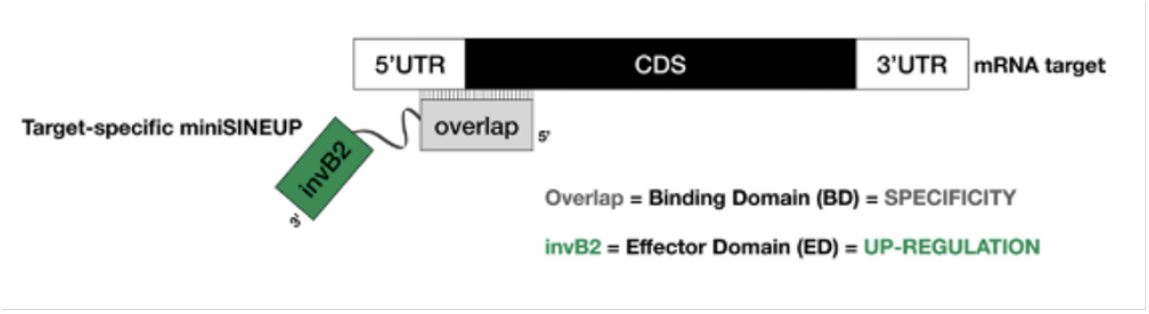

Figure 33. Schematic representation of SINEUPs functional domains. The binding domain (BD, gray) provides SINEUP specificity and it is in antisense orientation to the sense protein-coding mRNA. The inverted SINEB2 element (invB2) is the effector domain (ED, green) and confers enhancement of protein synthesis (Espinoza et al., 2021).

To date, there are many therapeutic needs to increase protein levels. For example genetic diseases caused by loss of one functional allele for a single gene, called haploinsufficiency; or more complex diseases, where the artificial increase of a compensatory pathway may restore the physiological activity of a mutated gene. Another example is cancer, where reduced levels of a tumor suppressor protein is often responsible for more aggressive features (Espinoza et al., 2021).

Moreover, afterwards the COVID-19 pandemic, a huge progress has been made in the field of RNA delivery, laying the foundation for development of increasingly efficient nucleic acids-based therapies. Two main strategies are currently used to deliver SINEUPs molecules. The first approach exploits the use of AAVs where a single SINEUP molecule can be chronically expressed in vivo. The second approach involves the delivery of SINEUPs as RNA molecules in liposomes; in this regard, the use of chemically synthesized SINEUPs represents an important advancement since RNA-based drugs do not cause stable modification to the genome, therefore reducing the risk of genotoxicity (Espinoza et al., 2021).

In the very recent years, SINEUPs technology has been successfully applied to revert pathological phenotypes in different biological models of human diseases. One is the Friedreich's ataxia (FRDA), an untreatable genetic disease due to decreased expression of frataxin (FXN), caused by the homozygous hyper-expansion of GAA triplet repeats. SINEUPs were successfully developed to positively regulate frataxin in the range of 2-fold in FRDA-derived fibroblasts and lymphoblasts, re-establishing physiological levels of the protein and normalizing mitochondrial activity - the main feature of the disease (Bon et al., 2019).

Another disease in which SINEUPs have been successfully applied is Parkinson. Parkinson's disease is a neurodegenerative disorder caused by loss of dopaminergic neurons in the substantia nigra, which underlies the motor symptoms that characterize the disease. A synthetic miniSINEUP was able to

increase endogenous Glial-Derived Neurotrophic Factor (GDNF) protein levels by approximately 2-fold in mice models, potentiating the function of the dopaminergic system. Notably, the moderate and selective increase of endogenous GDNF protein induced by SINEUPs abolished the common side effects that are observed after ectopic expression of GDNF in the same model (Espinoza et al., 2020).

It is not excluded that, in the next future, SINEUP constructs may be applied to increase the expression of downregulated tumor suppressors in human cancers, re-establishing their anti-oncogenic properties. DAB2IP falls perfectly in this category, and we therefore decided to explore the use of SINEUPs on DAB2IP, taking advantage of our model HiBiT edited cell lines, that allow accurate, quantitative, and sensitive detection of variations in endogenous DAB2IP protein levels.

RESULTS AND DISCUSSION

4.2 Explorative studies on the potential use of SINEUPs to modulate DAB2IP levels

In collaboration with Prof. Gustincich (IIT, Genova) we designed a small panel of SINEUP constructs for human DAB2IP. Unfortunately, the DAB2IP gene is complex, with 5 different TSSs identified by CAGE (**Figure 34A**), and multiple transcripts potentially encoding protein isoforms differing at their N-terminus. Considering only the three major transcripts listed in the NCBI database, DAB2IP can be potentially translated from 4 different start codons.

As a first approach, we designed six different SINEUPs. Two of them targeting the most upstream AUG of the variant 3 transcript (NM_001395010.1); this variant was chosen because it corresponds to a strong TSS according to CAGE data. Remaining SINEUPs were designed to target the first upstream AUG codon of the variant 2 transcript (NM_138709.2), and a second in-frame AUG located 78 nt (26 aminoacids) further downstream (**Figure 34B**). These AUG codons are the predicted translation start sites for transcripts originated from two different TSSs (**Figure 34A**); they are also included in all DAB2IP transcripts.

The constructs were synthesized in pCS2 expression vectors (Valentini et al., 2022), and were transfected in the PC3-HiBiT cell line, together with a small amount of plasmid encoding mCherry used to monitor transfection efficiency (**Figure 34C**). The luminescence/fluorescence ratio was measured 48 hours after transfection. In preliminary experiments, none of the six tested SINEUPs increased DAB2IP-HiBiT levels (**Figure 34D**).

This result may lead to three possible interpretations: (i) the efficiency of transient transfection is insufficient; (ii) the mechanism of SINEUP is not functional in PC3 cells; (iii) the selected AUG codons are not relevant in this cell line; (iv) none of the constructs is able to enhance DAB2IP translation.

As regarding the first hypothesis, additional tests and a careful optimization of the transfection procedure are needed to fully evaluate the feasibility of this approach. We had a 20%-25% transfection efficiency of the mCherry plasmid, but it is possible that this value is not really representative of the transfection efficiency of SINEUP plasmids. Especially considering that mCherry and SINEUP were transfected in much different amounts (200ng versus 2ug, respectively). To actually normalize for transfection efficiency of SINEUPs plasmids, we need to devise an alternative approach.

Regarding the second point, to test whether the SINEUP mechanism is active in PC3 cells a positive control is needed; for instance a miniSINEUP targeting GFP can be transfected together with a plasmid encoding eGFP, to check upregulation of an exogenous reporter.
As regarding the third and fourth points, the choice of best targetable AUG codons may be done after an accurate analysis of the transcripts that are actually expressed in the cell line of reference, using a specific technique to map the 5' end of the mRNAs (i.e. RACE), and perhaps a mass-spectrometry approach to define the actual N-terminus of the expressed DAB2IP proteins.

Figure 34

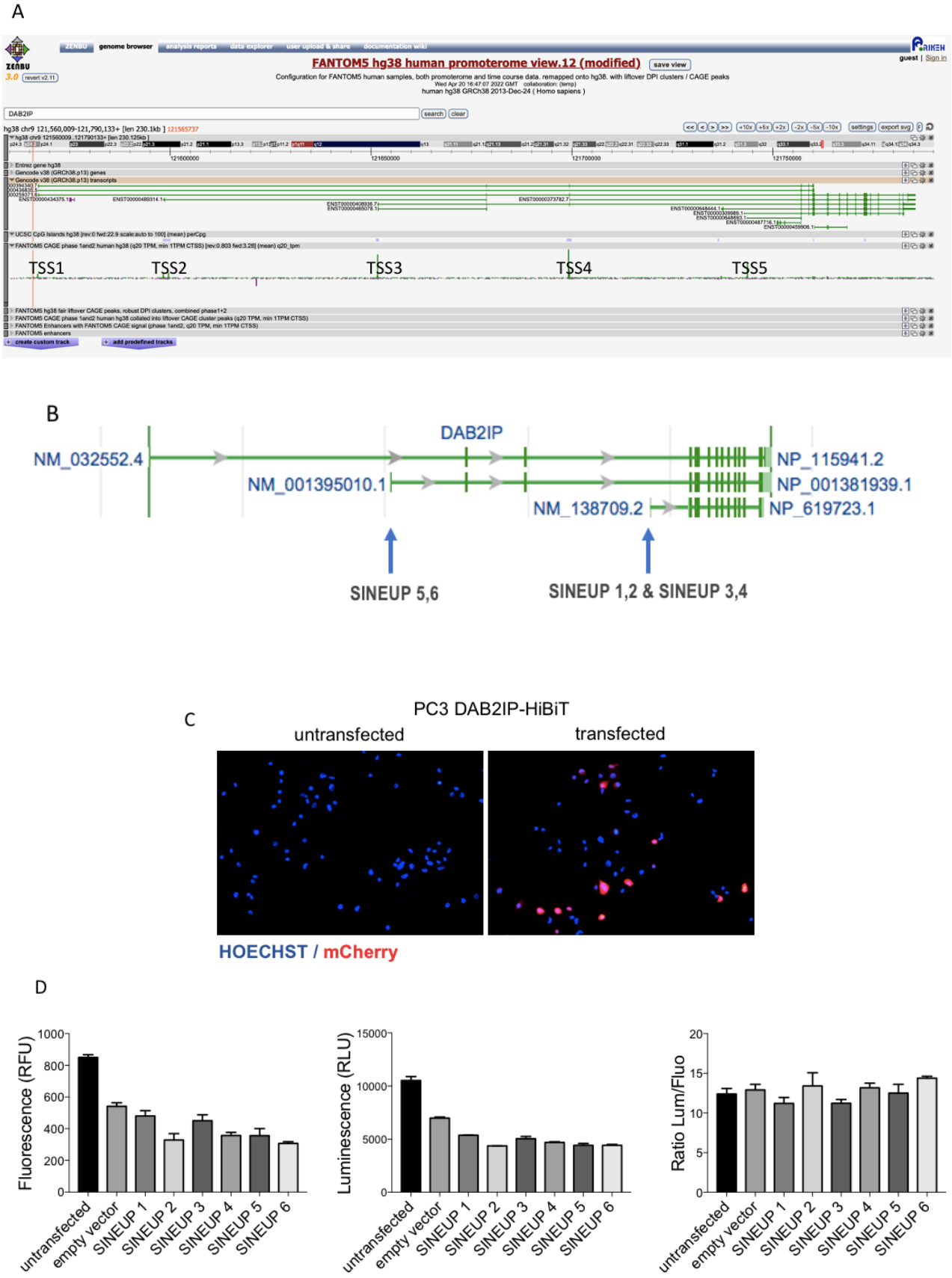

Figure 34 | Design and preliminary experiments with SINEUPs designed to target hDAB2IP. A) Zenbu genome browser view of the gene locus for human DAB2IP. Annotated UCSC transcripts are shown, with

exon (thick lines) and intron (thin lines) boundaries. Five putative TSSs are identified as green peaks proportional to the number of CAGE-tags detected in pooled human FANTOM5 libraries (Lizio et al., 2019). UCSC CpG islands are also shown. **B)** Representation of the main transcript variants of DAB2IP (data from NCBI, Homo sapiens Annotation Release 110, 2022), together with the predicted translation products. Arrows indicate the position of AUG codons targeted by SINEUP constructs. **C)** Representative immunofluorescence images of PC3-HiBiT cells transfected with a SINEUP plasmid together with a small amount of mCherry (red) expression vector to monitor transfection efficiency. Nuclei are stained with Hoechst. **D)** Histograms summarize values of fluorescence (i.e. viability), luminescence (i.e. DAB2IP-HiBiT) and lum/fluo ratio of PC3-HiBiT cells transfected for 48h with the indicated constructs. Values are the average of 3 wells. Data refer to a single experiment.

CONCLUSIONS AND FUTURE PERSPECTIVES

The results presented in this Thesis reveal thiostrepton, ubenimex and salmeterol as DAB2IP upregulators and suggest a possible repositioning of these drugs for treatment of solid cancer. Ubenimex and salmeterol modestly increased protein expression of about 1.5–3 fold, thus restoring physiological levels of DAB2IP without evidence of overexpression effects. These compounds seem to increase DAB2IP protein levels also in non-transformed endothelial cells. Since studies have shown that conditional DAB2IP depletion in vascular endothelial cells augments tumor growth and metastasis in mice (Ji et al., 2015), augmenting DAB2IP levels not only in tumor cells, but also in stromal cells, might be sufficient to limit, at least in part, cancer cells dissemination. DAB2IP up-regulator drugs might, therefore, show a potential therapeutic effect also acting on the tumor vasculature, thus possibly bypassing drug delivery-related issues.

Interestingly, DAB2IP is member of a family of Ras-GAPs that share sequence similarity and mechanisms of functional inhibition in cancer (Bellazzo & Collavin, 2020), and that may targeted by drugs aimed to increase their expression levels. Identifying strategies able to reactivate Ras-GAPs in cancer would have, in fact, an enormous potential to control the activation of oncogenic pathways in response to different extracellular signals.

From a methodologic perspective, our work also demonstrated the applicability of the HiBiT system for high-throughput screening of compounds that modulate the expression of an endogenous protein in a physiological manner, indicating it as an efficient tool for drug discovery. To date, indeed, there are many therapeutic needs to increase protein levels. One of them is represented by genetic diseases caused by the lack of one functional allele for a gene, called haploinsufficiency. Thus, it is not excluded that our approach might be applied to screen therapeutics molecules such as small molecules, but also nucleic acids (e.g. SINEUPs) or peptides, that increase (or decrease) the endogenous expression of any protein of interest.

ACKNOWLEDGMENTS

I am really grateful to Prof. Licio Collavin, for the opportunity to develop this project, and above all, for his numerous teachings. I learned a lot.

Important contribution to this work was given by Dr. Luca Braga (HTS facility at ICGEB) and his team for high-throughput screening and for validation experiments.
I thank Dr. Luca Braga for showing me the 'way'; his scientific knowledge has been fundamental.
I want also to thank Raffaella Klima and Serena Maiocchi for support and constructive discussions; in particular Serena, for her patience, tenacity and experimental help.

Essential contribution was given by Prof. Luca Fava and Sabrina Ghetti (University of Trento - CIBIO) for genome editing. Without her insights and her contagious passion, I think this project would not have been possible.

Finally, I would like to acknowledge all members, the old and the new, of the LC and STS groups, for fostering to improve myself every day. I thank also all the people of the II floor of building C11 who have supported and encouraged me over the last years.

BIBLIOGRAPHY

Abou-Ouf, H., Zhao, L., & Bismar, T. A. (2016). ERG expression in prostate cancer: biological relevance and clinical implication. *Journal of Cancer Research and Clinical Oncology*, *142*(8), 1781–1793. https://doi.org/10.1007/s00432-015-2096-x

Adams, B. S., & Nguyen, H. (2022). Salmeterol. Treasure Island (FL).

Albiñana, V., Recio-Poveda, L., González-Peramato, P., Martinez-Piñeiro, L., Botella, L. M., & Cuesta, A. M. (2022). Blockade of β2-Adrenergic Receptor Reduces Inflammation and Oxidative Stress in Clear Cell Renal Cell Carcinoma. *International Journal of Molecular Sciences*, *23*(3). https://doi.org/10.3390/ijms23031325

Anderson, D. A. S. A. M. L. M. (1989). Review Article Oncogenes a N D Onco-Suppressor Genes : Their Involvement in Cancer, *157*, 1–10.

Antoszczak, M., Markowska, A., Markowska, J., & Huczyński, A. (2020). Old wine in new bottles: Drug repurposing in oncology. *European Journal of Pharmacology*, *866*(July 2019). https://doi.org/10.1016/j.ejphar.2019.172784

Bailly, C. (2022). The bacterial thiopeptide thiostrepton. An update of its mode of action, pharmacological properties and applications. *European Journal of Pharmacology*, *914*(December 2021), 174661. https://doi.org/10.1016/j.ejphar.2021.174661

Banan, M. (2020). Recent advances in CRISPR/Cas9-mediated knock-ins in mammalian cells. *Journal of Biotechnology*, *308*(August 2019), 1–9. https://doi.org/10.1016/j.jbiotec.2019.11.010

Barik, S. (2008). An intronic microRNA silences genes that are functionally antagonistic to its host gene. *Nucleic Acids Research*, *36*(16), 5232–5241. https://doi.org/10.1093/nar/gkn513

Barnieh, F. M., Loadman, P. M., & Falconer, R. A. (2021). Is tumour-expressed aminopeptidase N (APN/CD13) structurally and functionally unique? *Biochimica et Biophysica Acta - Reviews on Cancermultiplemethionine*, *1876*(2), 188641. https://doi.org/10.1016/j.bbcan.2021.188641

Bavadekar, S., Budajaja, F., Patel, K., & Vansal, S. (2013). Epinephrine stimulates secretion of VEGF by human prostate cancer cells, LNCaP, through a beta2-adrenergic receptor-mediated pathway. *The FASEB Journal*, *27*(S1), 1105.11-1105.11. https://doi.org/https://doi.org/10.1096/fasebj.27.1_supplement.1105.11

Bedard, P. L., Hyman, D. M., Davids, M. S., & Siu, L. L. (2020). Small molecules, big impact: 20 years of targeted therapy in oncology. *The Lancet*, *395*(10229), 1078–1088. https://doi.org/10.1016/S0140-6736(20)30164-1

Bellazzo, A., & Collavin, L. (2020). Cutting the brakes on ras-cytoplasmic gaps as targets of inactivation in cancer. *Cancers*, *12*(10), 1–22. https://doi.org/10.3390/cancers12103066

Bellazzo, A., Di Minin, G., & Collavin, L. (2017a). Block one, unleash a hundred. Mechanisms of DAB2IP inactivation in cancer. *Cell Death and Differentiation*, *24*(1), 15–25. https://doi.org/10.1038/cdd.2016.134

Bellazzo, A., Di Minin, G., & Collavin, L. (2017b). Block one, unleash a hundred. Mechanisms of DAB2IP inactivation in cancer. *Cell Death and Differentiation*, *24*(1), 15–25. https://doi.org/10.1038/cdd.2016.134

Bellazzo, A., Di Minin, G., Valentino, E., Sicari, D., Torre, D., Marchionni, L., … Collavin, L. (2018). Cell-autonomous and cell non-autonomous downregulation of tumor suppressor DAB2IP by microRNA-149-3p promotes aggressiveness of cancer cells. *Cell Death and Differentiation*, *25*(7), 1224–1238. https://doi.org/10.1038/s41418-018-0088-5

Bon, C., Luffarelli, R., Russo, R., Fortuni, S., Pierattini, B., Santulli, C., … Gustincich, S. (2019). SINEUP non-coding RNAs rescue defective frataxin expression and activity in a cellular model of Friedreich's Ataxia. *Nucleic Acids Research*, *47*(20), 10728–10743. https://doi.org/10.1093/nar/gkz798

Braadland, P. R., Ramberg, H., Grytli, H. H., & Taskén, K. A. (2015). β-Adrenergic Receptor

Signaling in Prostate Cancer. *Frontiers in Oncology*, *4*(January), 1–11. https://doi.org/10.3389/fonc.2014.00375
Brosh, R., & Rotter, V. (2009). When mutants gain new powers: news from the mutant p53 field. *Nat Rev Cancer*, *9*(10), 701–713. Retrieved from http://dx.doi.org/10.1038/nrc2693
Buchner, M., Park, E., Geng, H., Klemm, L., Flach, J., Passegué, E., … Müschen, M. (2015). Identification of FOXM1 as a therapeutic target in B-cell lineage acute lymphoblastic leukaemia. *Nature Communications*, *6*. https://doi.org/10.1038/ncomms7471
Bukhari, H., & Müller, T. (2019). Endogenous Fluorescence Tagging by CRISPR. *Trends in Cell Biology*, *29*(11), 912–928. https://doi.org/https://doi.org/10.1016/j.tcb.2019.08.004
Bukowski, K., Kciuk, M., & Kontek, R. (2020). Mechanisms of multidrug resistance in cancer chemotherapy1. Bukowski K, Kciuk M, Kontek R. Mechanisms of multidrug resistance in cancer chemotherapy. Int J Mol Sci. 2020;21(9). doi:10.3390/ijms21093233. *International Journal of Molecular Sciences*, *21*(9).
Cao, H., Zhang, J., & Wang, W. (2020). DAB2IP Plays Important Clinical Significance and Correlates With Immune Infiltration in Renal Cell Carcinoma. *Technology in Cancer Research & Treatment*, *19*, 1533033820936682. https://doi.org/10.1177/1533033820936682
Chandrasekar, T., Yang, J. C., Gao, A. C., & Evans, C. P. (2015). Mechanisms of resistance in castration-resistant prostate cancer (CRPC). *Translational Andrology and Urology*, *4*(3), 365–380. https://doi.org/10.3978/j.issn.2223-4683.2015.05.02
Chang, C. J., & Hung, M. C. (2012). The role of EZH2 in tumour progression. *British Journal of Cancer*, *106*(2), 243–247. https://doi.org/10.1038/bjc.2011.551
Chen, H., Tu, S. W., & Hsieh, J. T. (2005). Down-regulation of human DAB2IP gene expression mediated by polycomb Ezh2 complex and histone deacetylase in prostate cancer. *Journal of Biological Chemistry*, *280*(23), 22437–22444. https://doi.org/10.1074/jbc.M501379200
Chen, L., Teng, Y., & Xu, W. (2011). Progress in the Development of Bestatin Analogues as Aminopeptidases Inhibitors. *Current Medicinal Chemistry*, *18*(7), 964–976. https://doi.org/10.2174/092986711794940879
Chen, Q., Wu, B., Ge, P., Zhang, P., & Chen, X. (2022). Ubenimex Combined with Pemetrexed Upregulates SOCS1 to Inhibit Lung Adenocarcinoma Progression via the JAK2-STAT3 Signaling Pathway. *Disease Markers*, *2022*. https://doi.org/10.1155/2022/5614939
Chen, S., Wang, L., Yao, B., Liu, Q., & Guoa, C. (2019). miR-1307-3p promotes tumor growth and metastasis of hepatocellular carcinoma by repressing DAB2 interacting protein. *Biomedicine and Pharmacotherapy*, *117*(May), 109055. https://doi.org/10.1016/j.biopha.2019.109055
Chen, W. C. W., Baily, J. E., Corselli, M., Diaz, M., Sun, B., Xiang, G., … Péault, B. (2016). The Mechanism of DAB2IP in Chemoresistance of Prostate Cancer Cells. *Clin Cancer Res*, *33*(2), 557–573. https://doi.org/10.1002/stem.1868.Human
Curnis, F., Arrigoni, G., Sacchi, A., Fischetti, L., Arap, W., Pasqualini, R., & Corti, A. (2002). Differential binding of drugs containing the NGR motif to CD13 isoforms in tumor vessels, epithelia, and myeloid cells. *Cancer Research*, *62*(3), 867–874.
Dagogo-Jack, I., & Shaw, A. T. (2018). Tumour heterogeneity and resistance to cancer therapies. *Nature Reviews Clinical Oncology*, *15*(2), 81–94. https://doi.org/10.1038/nrclinonc.2017.166
Dai, X., North, B. J., & Inuzuka, H. (2014). Negative regulation of DAB2IP by Akt and SCFFbw7 pathways. *Oncotarget*, *5*(10), 3307–3315. https://doi.org/10.18632/oncotarget.1939
Dale, B., Cheng, M., Park, K. S., Kaniskan, H. Ü., Xiong, Y., & Jin, J. (2021). Advancing targeted protein degradation for cancer therapy. *Nature Reviews Cancer*, *21*(10), 638–654. https://doi.org/10.1038/s41568-021-00365-x
Daniyal, M., Siddiqui, Z. A., Akram, M., & Asif, H. M. (2014). Ryanodine Receptor 2 (RYR2) (pSer2814) pAb Quality Control Certificate of Analysis Catalogue No .: A010-31 Unit Size : 50 µl Lot No : 0513-06. *Asian Pacific Journal of Cancer Prevention*, *15*(2002), 9575–9578.
Darwin, Charles. and Woolls, William. and Mort, H.S. and Usinger, R. L. (1859). On the Origin of Species by Means of Natural Selection, or Preservation of Favoured Races in the Struggle for

Life. *John Murray London*. https://doi.org/10.7748/ns.19.34.24.s28
Dewari, P. S., Southgate, B., McCarten, K., Monogarov, G., O'duibhir, E., Quinn, N., … Pollard, S. M. (2018). An efficient and scalable pipeline for epitope tagging in mammalian stem cells using Cas9 ribonucleoprotein. *ELife*, *7*, 1–29. https://doi.org/10.7554/eLife.35069
Di Minin, G., Bellazzo, A., DalFerro, M., Chiaruttini, G., Nuzzo, S., Bicciato, S., … Collavin, L. (2014). Mutant p53 Reprograms TNF Signaling in Cancer Cells through Interaction with the Tumor Suppressor DAB2IP. *Molecular Cell*, *56*(5), 617–629. https://doi.org/10.1016/j.molcel.2014.10.013
Ding, L., Wang, R., Shen, D., Cheng, S., Wang, H., Lu, Z., … Li, G. (2021). Role of noncoding RNA in drug resistance of prostate cancer. *Cell Death and Disease*, *12*(6). https://doi.org/10.1038/s41419-021-03854-x
Doudna, J. A., & Charpentier, E. (2014). The new frontier of genome engineering with CRISPR-Cas9. *Science*, *346*(6213). https://doi.org/10.1126/science.1258096
Duan, Y., Yin, X., Lai, X., Liu, C., Nie, W., Li, D., … Meng, F. (2020). Upregulation of DAB2IP Inhibits Ras Activity and Tumorigenesis in Human Pancreatic Cancer Cells. *Technology in Cancer Research and Treatment*, *19*, 1–11. https://doi.org/10.1177/1533033819895494
Dutta, P., & Li, W. X. (2013). Role of the JAK-STAT Signalling Pathway in Cancer. *ELS*, (October 2013). https://doi.org/10.1002/9780470015902.a0025214
Elia, I., Schmieder, R., Christen, S., & Fendt, S.-M. (2015). Organ-Specific Cancer Metabolism and Its Potential for Therapy Ilaria: Adipokines and the Endocrine Role of Adipose Tissues. *Handbook of Experimental Pharmacology*, (January), 251–263. https://doi.org/10.1007/164
Eoh, J., & Gu, L. (2019). Biomaterials as vectors for the delivery of CRISPR-Cas9. *Biomaterials Science*, *7*(4), 1240–1261. https://doi.org/10.1039/c8bm01310a
Espinoza, S., Bon, C., Valentini, P., Pierattini, B., Matey, A. T., Damiani, D., … Gustincich, S. (2021). SINEUPs: A novel toolbox for RNA therapeutics. *Essays in Biochemistry*, *65*(4), 775–789. https://doi.org/10.1042/EBC20200114
Espinoza, S., Scarpato, M., Damiani, D., Managò, F., Mereu, M., Contestabile, A., … Gustincich, S. (2020). SINEUP Non-coding RNA Targeting GDNF Rescues Motor Deficits and Neurodegeneration in a Mouse Model of Parkinson's Disease. *Molecular Therapy*, *28*(2), 642–652. https://doi.org/10.1016/j.ymthe.2019.08.005
Fan, X., Wang, Y., Fan, J., & Chen, R. (2019). Deletion of SMURF 1 represses ovarian cancer invasion and EMT by modulating the DAB2IP/AKT/Skp2 feedback loop. *Journal of Cellular Biochemistry*, *120*(6), 10643–10651. https://doi.org/10.1002/jcb.28354
Fang, P., Madden, J. A., Neums, L., Moulder, R. K., Forrest, M. L., & Chien, J. (2018). Olaparib-induced adaptive response Is disrupted by FOXM1 targeting that enhances sensitivity to PARP inhibition. *Molecular Cancer Research*, *16*(6), 961–973. https://doi.org/10.1158/1541-7786.MCR-17-0607
Feng, S., Huang, Q., Deng, J., Jia, W., Gong, J., Xie, D., … Liu, L. (2022). DAB2IP suppresses tumor malignancy by inhibiting GRP75-driven p53 ubiquitination in colon cancer. *Cancer Letters*, *532*, 215588. https://doi.org/10.1016/j.canlet.2022.215588
Fontijn, D., Duyndam, M. C. A., Van Berkel, M. P. A., Yuana, Y., Shapiro, L. H., Pinedo, H. M., … Boven, E. (2006). CD13/Aminopeptidase N overexpression by basic fibroblast growth factor mediates enhanced invasiveness of 1F6 human melanoma cells. *British Journal of Cancer*, *94*(11), 1627–1636. https://doi.org/10.1038/sj.bjc.6603157
Franken, N. A. P., Rodermond, H. M., Stap, J., Haveman, J., & van Bree, C. (2006). Clonogenic assay of cells in vitro. *Nature Protocols*, *1*(5), 2315–2319. https://doi.org/10.1038/nprot.2006.339
Fujioka, S., Kohno, N., & Hiwada, K. (1995). Ubenimex activates the E-cadherin-mediated adhesion of a breast cancer cell line YMB-S. *Japanese Journal of Cancer Research : Gann*, *86*(4), 368–373. https://doi.org/10.1111/j.1349-7006.1995.tb03066.x
Gaj, T., Staahl, B. T., Rodrigues, G. M. C., Limsirichai, P., Ekman, F. K., Doudna, J. A., &

Schaffer, D. V. (2017). Targeted gene knock-in by homology-directed genome editing using Cas9 ribonucleoprotein and AAV donor delivery. *Nucleic Acids Research*, *45*(11), 1–11. https://doi.org/10.1093/nar/gkx154

Gao, Y., Hisey, E., Bradshaw, T. W. A., Erata, E., Brown, W. E., Courtland, J. L., … Soderling, S. H. (2019). Plug-and-Play Protein Modification Using Homology-Independent Universal Genome Engineering. *Neuron*, *103*(4), 583-597.e8. https://doi.org/https://doi.org/10.1016/j.neuron.2019.05.047

Gartel, A. L. (2014). Suppression of the Oncogenic Transcription Factor FOXM1 by Proteasome Inhibitors. *Scientifica*, *2014*, 1–5. https://doi.org/10.1155/2014/596528

Ghetti, S., Burigotto, M., Mattivi, A., Magnani, G., Casini, A., Bianchi, A., … Fava, L. L. (2021). CRISPR/Cas9 ribonucleoprotein-mediated knockin generation in hTERT-RPE1 cells. *STAR Protocols*, *2*(2), 100407. https://doi.org/10.1016/j.xpro.2021.100407

Gibson, T. J., Seiler, M., & Veitia, R. A. (2013). The transience of transient overexpression. *Nature Methods*, *10*(8), 715–721. https://doi.org/10.1038/nmeth.2534

Gretarsdottir, S., Baas, A. F., Thorleifsson, G., Holm, H., den Heijer, M., de Vries, J.-P. P. M., … Stefansson, K. (2010). Genome-wide association study identifies a sequence variant within the DAB2IP gene conferring susceptibility to abdominal aortic aneurysm. *Nature Genetics*, *42*, 692. Retrieved from https://doi.org/10.1038/ng.622

Gu, Y., Wu, S., Chong, Y., Guan, B., Li, L., He, D., … Wu, K. (2022). DAB2IP regulates intratumoral testosterone synthesis and CRPC tumor growth by ETS1/AKR1C3 signaling. *Cellular Signalling*, *95*, 110336. https://doi.org/10.1016/j.cellsig.2022.110336

Guo, Q., Jing, F. J., Xu, W., Li, X., Li, X., Sun, J. L., … Jing, F. B. (2020). Ubenimex induces autophagy inhibition and EMT suppression to overcome cisplatin resistance in GC cells by perturbing the CD13/EMP3/PI3K/AKT/NF-κB axis. *Aging*, *12*(1), 80–105. https://doi.org/10.18632/aging.102598

Guo, Q., Sui, Z. G., Xu, W., Quan, X. H., Sun, J. L., Li, X., … Jing, F. B. (2017). Ubenimex suppresses Pim-3 kinase expression by targeting CD13 to reverse MDR in HCC cells. *Oncotarget*, *8*(42), 72652–72665. https://doi.org/10.18632/oncotarget.20194

Halasi, M., Schraufnagel, D. P., & Gartel, A. L. (2009). Wild-type p53 protects normal cells against apoptosis induced by thiostrepton. *Cell Cycle*, *8*(17), 2850–2851. https://doi.org/10.4161/cc.8.17.9414

Han, L., Zhang, Y., Liu, S., Zhao, Q., & Liang, X. (2017). Oncotarget-08-107730.Pdf, *8*(64), 107730–107743.

Harrison, M. M., Jenkins, B. V., O'Connor-Giles, K. M., & Wildonger, J. (2014). A CRISPR view of development. *Genes and Development*, *28*(17), 1859–1872. https://doi.org/10.1101/gad.248252.114

Hou, J., He, Z., Liu, T., Chen, D., Wang, B., Wen, Q., & Zheng, X. (2022). Evolution of Molecular Targeted Cancer Therapy: Mechanisms of Drug Resistance and Novel Opportunities Identified by CRISPR-Cas9 Screening. *Frontiers in Oncology*, *12*(March), 1–18. https://doi.org/10.3389/fonc.2022.755053

Huang, C., Zhang, X., Jiang, L., Zhang, L., Xiang, M., & Ren, H. (2019). FoxM1 Induced Paclitaxel Resistance via Activation of the FoxM1/PHB1/RAF-MEK-ERK Pathway and Enhancement of the ABCA2 Transporter. *Molecular Therapy - Oncolytics*, *14*(September), 196–212. https://doi.org/10.1016/j.omto.2019.05.005

Huang, J., Wang, B., Hui, K., Zeng, J., Fan, J., Wang, X., … Wu, K. (2016). miR-92b targets DAB2IP to promote EMT in bladder cancer migration and invasion. *Oncology Reports*, *36*(3), 1693–1701. https://doi.org/10.3892/or.2016.4940

Huang, Q., Qin, L., Dai, S., Zhang, H., & Pasula, S. (2013). NIH Public Access, *33*(4), 795–804. https://doi.org/10.1161/ATVBAHA.113.301220.AIP1

Inui, M., Miyado, M., Igarashi, M., Tamano, M., Kubo, A., Yamashita, S., … Takada, S. (2014). Rapid generation of mouse models with defined point mutations by the CRISPR/Cas9 system.

Scientific Reports, *4*, 1–8. https://doi.org/10.1038/srep05396
Jarvik, J. W., & Telmer, C. A. (1998). Epitope tagging. *Annual Review of Genetics*, *32*, 601–618. https://doi.org/10.1146/annurev.genet.32.1.601
Ji, L., Xu, F., Zhang, J., Song, T., Chen, W., Yin, X., … Chen, Z. (2022). ADRB2 expression predicts the clinical outcomes and is associated with immune cells infiltration in lung adenocarcinoma. *Scientific Reports*, *12*(1), 1–13. https://doi.org/10.1038/s41598-022-19991-y
Ji, W., Li, Y., He, Y., Yin, M., Zhou, H. J., Boggon, T. J., … Min, W. (2015). AIP1 expression in tumor niche suppresses tumor progression and metastasis. *Cancer Research*, *75*(17), 3492–3504. https://doi.org/10.1158/0008-5472.CAN-15-0088
Jiang, F., & Doudna, J. A. (2017). CRISPR – Cas9 Structures and Mechanisms, 505–531.
Jiang, L., Wu, X., Wang, P., Wen, T., Yu, C., Wei, L., & Chen, H. (2015). Targeting FoxM1 by thiostrepton inhibits growth and induces apoptosis of laryngeal squamous cell carcinoma. *Journal of Cancer Research and Clinical Oncology*, *141*(6), 971–981. https://doi.org/10.1007/s00432-014-1872-3
Jinek, M., Chylinski, K., Fonfara, I., Hauer, M., Doudna, J. A., & Charpentier, E. (2012). A programmable dual-RNA-guided DNA endonuclease in adaptive bacterial immunity. *Science*, *337*(6096), 816–821. https://doi.org/10.1126/science.1225829
Ju, S. Y., Huang, C. Y. F., Huang, W. C., & Su, Y. (2015). Identification of thiostrepton as a novel therapeutic agent that targets human colon cancer stem cells. *Cell Death and Disease*, *6*(155), 1–11. https://doi.org/10.1038/cddis.2015.155
Kepp, O., & Kroemer, G. (2020). Autophagy induction by thiostrepton for the improvement of anticancer therapy. *Autophagy*, *16*(6), 1166–1167. https://doi.org/10.1080/15548627.2020.1758417
Kim, S., Kim, D., Cho, S. W., Kim, J., & Kim, J. S. (2014). Highly efficient RNA-guided genome editing in human cells via delivery of purified Cas9 ribonucleoproteins. *Genome Research*, *24*(6), 1012–1019. https://doi.org/10.1101/gr.171322.113
Koch, Birgit, Nijmeijer1, Bianca, Kueblbeck, Moritz , Cai,Yin , Walther, Nike, and J. E. (2018). Generation and validation of homozygous fluorescent knock-in cells using CRISPR/Cas9 genome editing Birgit. *Nat Protoc.*, *176*(1), 139–148. https://doi.org/10.1016/j.physbeh.2017.03.040
Kong, Z., Xie, D., Boike, T., Raghavan, P., & Chen, D. J. (2010). Downregulation of Human DAB2IP Gene Expression in Prostate Cancer Cells Results in Resistance to Ionizing Radiation, 2829–2840. https://doi.org/10.1158/0008-5472.CAN-09-2919
Kongsema, M., Wongkhieo, S., Khongkow, M., Lam, E. W. F., Boonnoy, P., Vongsangnak, W., & Wong-Ekkabut, J. (2019). Molecular mechanism of Forkhead box M1 inhibition by thiostrepton in breast cancer cells. *Oncology Reports*, *42*(3), 953–962. https://doi.org/10.3892/or.2019.7225
Ku, S. Y., Gleave, M. E., & Beltran, H. (2019). Towards precision oncology in advanced prostate cancer. *Nature Reviews Urology*, *16*(11), 645–654. https://doi.org/10.1038/s41585-019-0237-8
Ku, S. Y., Rosario, S., Wang, Y., Mu, P., Seshadri, M., Goodrich, W., … Goodrich, D. W. (2018). Rb1 and Trp53 cooperate to suppress prostate cancer lineage plasticity, metastais, and antiandrogen resistance, *355*(6320), 78–83. https://doi.org/10.1126/science.aah4199.Rb1
Kuttikrishnan, S., Prabhu, K. S., Khan, A. Q., Alali, F. Q., Ahmad, A., & Uddin, S. (2021). Thiostrepton inhibits growth and induces apoptosis by targeting FoxM1/SKP2/MTH1 axis in B-precursor acute lymphoblastic leukemia cells. *Leukemia & Lymphoma*, *62*(13), 3170–3180. https://doi.org/10.1080/10428194.2021.1957873
Kwok, J. M. M., Myatt, S. S., Marson, C. M., Coombes, R. C., Constantinidou, D., & Lam, E. W. F. (2008). Thiostrepton selectively targets breast cancer cells through inhibition of forkhead box M1 expression. *Molecular Cancer Therapeutics*, *7*(7), 2022–2032. https://doi.org/10.1158/1535-7163.MCT-08-0188
Landschulz, W. H., Johnson, P. F., & Mcknight, S. L. (1988). A Hypothetical Structure Common to

a New Class of DNA Binding Proteins. *Advancement Of Science*, *240*(4860), 1759–1764.
Lee, G. H., Kim, S. H., Homayouni, R., & D'Arcangelo, G. (2012). Dab2ip Regulates Neuronal Migration and Neurite Outgrowth in the Developing Neocortex. *PLoS ONE*, *7*(10), 1–14. https://doi.org/10.1371/journal.pone.0046592
Lee, V. S., McRobb, L. S., Moutrie, V., Santos, E. D., & Siu, T. L. (2018). Effects of FOXM1 inhibition and ionizing radiation on melanoma cells. *Oncology Letters*, *16*(5), 6822–6830. https://doi.org/10.3892/ol.2018.9482
Li, H., Zhou, Y., Wang, M., Wang, H., Zhang, Y., Peng, R., … Liu, J. (2021). DOC-2/DAB2 interactive protein destabilizes c-Myc to impair the growth and self-renewal of colon tumor-repopulating cells. *Cancer Science*, *112*(11), 4593–4603. https://doi.org/10.1111/cas.15120
Li, S., Li, Q., Yu, W., & Xiao, Q. (2015). High glucose and/or high insulin affects HIF-1 signaling by regulating AIP1 in human umbilical vein endothelial cells. *Diabetes Research and Clinical Practice*, *109*(1), 48–56. https://doi.org/10.1016/j.diabres.2015.05.005
Li, Xiaoli, Zhang, X., Zhang, Q., & Lin, R. (2019). miR-182 contributes to cell proliferation, invasion and tumor growth in colorectal cancer by targeting DAB2IP. *The International Journal of Biochemistry & Cell Biology*, *111*, 27–36. https://doi.org/10.1016/j.biocel.2019.04.002
Li, Xiaoning, Dai, X., Wan, L., Inuzuka, H., Sun, L., & North, B. J. (2016). Smurf1 regulation of DAB2IP controls cell proliferation and migration. *Oncotarget*, *7*(18). https://doi.org/10.18632/oncotarget.8424
Li, Z., Li, L., Zhang, H., Zhou, H. J., Ji, W., & Min, W. (2020). Short AIP1 (ASK1-Interacting Protein-1) Isoform Localizes to the Mitochondria and Promotes Vascular Dysfunction. *Arteriosclerosis, Thrombosis, and Vascular Biology*, *40*(1), 112–127. https://doi.org/10.1161/ATVBAHA.119.312976
Liang, J., Wu, Y., Chen, B., Zhang, W., Tanaka, Y., & Sugiyama, H. (2013). The C-Kit Receptor-Mediated Signal Transduction and Tumor-Related Diseases, *9*. https://doi.org/10.7150/ijbs.6087
Liao, H., Xiao, Y., Hu, Y., Xiao, Y., Yin, Z., & Liu, L. (2015). microRNA-32 induces radioresistance by targeting DAB2IP and regulating autophagy in prostate cancer cells. *Oncology Letters*, *10*(4), 2055–2062. https://doi.org/10.3892/ol.2015.3551
Lin, J., Zheng, Y., Chen, K., Huang, Z., Wu, X., & Zhang, N. (2013). Inhibition of FOXM1 by thiostrepton sensitizes medulloblastoma to the effects of chemotherapy. *Oncol Rep*, *30*(4), 1739–1744. https://doi.org/10.3892/or.2013.2654
Liu, L., Xu, C., Hsieh, J.-T., Gong, J., & Xie, D. (2016). DAB2IP in cancer. *Oncotarget*, *7*(4). https://doi.org/10.18632/oncotarget.6501
Liu, S.-X., Zhou, Y., Zhao, L., Zhou, L.-S., Sun, J., Liu, G.-J., … Zhou, Y.-N. (2022). Thiostrepton confers protection against reactive oxygen species-related apoptosis by restraining FOXM1-triggerred development of gastric cancer. *Free Radical Biology and Medicine*. https://doi.org/10.1016/j.freeradbiomed.2022.09.018
Liu, X., Guo, Q., Jing, F., Zhou, C., Xiu, T., Shi, Y., & Jing, F. (2021). Ubenimex suppresses the ability of migration and invasion in gastric cancer cells by alleviating the activity of the cd13/nab1/mapk pathway. *Cancer Management and Research*, *13*, 4483–4495. https://doi.org/10.2147/CMAR.S300515
Liu, Z., Yu, Y., Huang, Z., Kong, Y., Hu, X., Xiao, W., … Fan, X. (2019). CircRNA-5692 inhibits the progression of hepatocellular carcinoma by sponging miR-328-5p to enhance DAB2IP expression. *Cell Death and Disease*, *10*(12). https://doi.org/10.1038/s41419-019-2089-9
Lizio, M., Abugessaisa, I., Noguchi, S., Kondo, A., Hasegawa, A., Hon, C. C., … Kawaji, H. (2019). Update of the FANTOM web resource: Expansion to provide additional transcriptome atlases. *Nucleic Acids Research*, *47*(D1), D752–D758. https://doi.org/10.1093/nar/gky1099
Lu, C., Amin, M. A., & Fox, D. A. (2020). CD13/Aminopeptidase N Is a Potential Therapeutic Target for Inflammatory Disorders. *The Journal of Immunology*, *204*(1), 3–11.

https://doi.org/10.4049/jimmunol.1900868
Lu, H.-B. (2018). MicroRNA-556-3p promotes the progression of esophageal cancer via targeting DAB2IP. *European Review for Medical and Pharmacological Sciences*, *22*(20), 6816–6823. https://doi.org/10.26355/eurrev_201810_16149
Luo, D., He, Y., Zhang, H., Yu, L., Chen, H., Xu, Z., … Min, W. (2008). AIP1 is critical in transducing IRE1-mediated endoplasmic reticulum stress response. *Journal of Biological Chemistry*, *283*(18), 11905–11912. https://doi.org/10.1074/jbc.M710557200
Maertens, O., & Cichowski, K. (2014). An expanding role for RAS GTPase activating proteins (RAS GAPs) in cancer. *Advances in Biological Regulation*, *55*, 1–14. https://doi.org/10.1016/j.jbior.2014.04.002
Mamani-Matsuda, M., Moynet, D., Molimard, M., Ferry-Dumazet, H., Marit, G., Reiffers, J., & Mossalayi, M. D. (2004). Long-acting β2-adrenergic formoterol and salmeterol induce the apoptosis of B-chronic lymphocytic Leukaemia cells. *British Journal of Haematology*, *124*(2), 141–150. https://doi.org/10.1046/j.1365-2141.2003.04746.x
Mansoori, B., Mohammadi, A., Davudian, S., Shirjang, S., & Baradaran, B. (2017). The different mechanisms of cancer drug resistance: A brief review. *Advanced Pharmaceutical Bulletin*, *7*(3), 339–348. https://doi.org/10.15171/apb.2017.041
Mantovani, F., Collavin, L., & Del Sal, G. (2019). Mutant p53 as a guardian of the cancer cell. *Cell Death and Differentiation*, *26*(2), 199–212. https://doi.org/10.1038/s41418-018-0246-9
Min, J., Zaslavsky, A., Fedele, G., McLaughlin, S. K., Reczek, E. E., De Raedt, T., … Cichowski, K. (2010). An oncogene-tumor suppressor cascade drives metastatic prostate cancer by coordinately activating Ras and nuclear factor-[kappa]B. *Nature Medicine*, *16*, 286+.
Min, J., Zaslavsky, A., Fedele, G., McLaughlin, S. K., Reczek, E. E., De Raedt, T., … Cichowski, K. (2010). An oncogene-tumor suppressor cascade drives metastatic prostate cancer by coordinately activating Ras and nuclear factor-kappaB. *Nature Medicine*, *16*(3), 286–294. https://doi.org/10.1038/nm.2100
Mu, P., Zhang, Z., Benelli, M., Karthaus, W. R., Hoover, E., Chen, C., … Sawyers, C. L. (2017). HHS Public Access, *355*(6320), 84–88. https://doi.org/10.1126/science.aah4307.SOX2
Musacchio, A., Gibson, T., Rice, P., Thompson, J., & Saraste, M. (1993). The PH domain: a common piece in the structural pathcwork of signalling proteins. *Trends in Biochemical Sciences*, *18*(9), 343–348. https://doi.org/10.1016/0968-0004(93)90071-T
Nalefski, E. A., & Falke, J. J. (1996). The C2 domain calcium-binding motif: Structural and functional diversity. *Protein Science*, *5*(12), 2375–2390. https://doi.org/10.1002/pro.5560051201
Ni, Q.-F., Zhang, Y., Yu, J.-W., Hua, R.-H., Wang, Q.-H., & Zhu, J.-W. (2020). miR-92b promotes gastric cancer growth by activating the DAB2IP-mediated PI3K/AKT signalling pathway. *Cell Proliferation*, *53*(1), e12630. https://doi.org/10.1111/cpr.12630
Oliveto, S., Mancino, M., Manfrini, N., & Biffo, S. (2017). Role of microRNAs in translation regulation and cancer. *World Journal of Biological Chemistry*, *8*(1), 45. https://doi.org/10.4331/wjbc.v8.i1.45
Pandit, B., & Gartel, A. L. (2010). New potential anti-cancer agents synergize with bortezomib and ABT-737 against prostate cancer. *Prostate*, *70*(8), 825–833. https://doi.org/10.1002/pros.21116
Pasqualini, R., Koivunen, E., Kain, R., Lahdenranta, J., Stryhn, A., Ashmun, R. A., … Arap, W. (2000). Aminopeptidase N Is a Receptor for Tumor-homing Peptides and a Target for Inhibiting Angiogenesis. *Cancer Res.*, *60*(3), 722–727.
Polakis, P. (2000). Wnt signaling and cancer. *Genes and Development*, *14*(15), 1837–1851. https://doi.org/10.1101/gad.14.15.1837
Pushpakom, S., Iorio, F., Eyers, P. A., Escott, K. J., Hopper, S., Wells, A., … Pirmohamed, M. (2018). Drug repurposing: Progress, challenges and recommendations. *Nature Reviews Drug Discovery*, *18*(1), 41–58. https://doi.org/10.1038/nrd.2018.168

Qiao, Shuhong, & Homayouni, R. (2015). Dab2IP regulates neuronal positioning, rap1 activity and integrin signaling in the developing cortex. *Developmental Neuroscience*, *37*(2), 131–141. https://doi.org/10.1159/000369092

Qiao, Shuhong, Kim, S. H., Heck, D., Goldowitz, D., LeDoux, M. S., & Homayouni, R. (2013). Dab2IP GTPase Activating Protein Regulates Dendrite Development and Synapse Number in Cerebellum. *PLoS ONE*, *8*(1), 1–12. https://doi.org/10.1371/journal.pone.0053635

Qiao, Shuxi, Lamore, S. D., Cabello, C. M., Lesson, J. L., Muñoz-Rodriguez, J. L., & Wondrak, G. T. (2012). Thiostrepton is an inducer of oxidative and proteotoxic stress that impairs viability of human melanoma cells but not primary melanocytes. *Biochemical Pharmacology*, *83*(9), 1229–1240. https://doi.org/10.1016/j.bcp.2012.01.027

Qureshi, A. A., Zuvanich, E. G., Khan, D. A., Mushtaq, S., Silswal, N., & Qureshi, N. (2018). Proteasome inhibitors modulate anticancer and anti-proliferative properties via NF-kB signaling, and ubiquitin-proteasome pathways in cancer cell lines of different organs. *Lipids in Health and Disease*, *17*(1), 1–26. https://doi.org/10.1186/s12944-018-0697-5

Radhakrishnan, S. K., Bhat, U. G., Hughes, D. E., Wang, I. C., Costa, R. H., & Gartel, A. L. (2006). Identification of a chemical inhibitor of the oncogenic transcription factor forkhead box M1. *Cancer Research*, *66*(19), 9731–9735. https://doi.org/10.1158/0008-5472.CAN-06-1576

Rajalingam, K., Schreck, R., Rapp, U. R., & Albert, Š. (2007). Ras oncogenes and their downstream targets. *Biochimica et Biophysica Acta - Molecular Cell Research*, *1773*(8), 1177–1195. https://doi.org/10.1016/j.bbamcr.2007.01.012

Ramberg, H., Eide, T., Krobert, K. A., Levy, F. O., Dizeyi, N., Bjartell, A. S., … Taskén, K. A. (2008). Hormonal regulation of β2-adrenergic receptor level in prostate cancer. *Prostate*, *68*(10), 1133–1142. https://doi.org/10.1002/pros.20778

Rawla, P. (2019). Épidémiologie du cancer de la prostate. Article de revue. *World J Oncol.*, *10(2):63-8*(1), 2–4. https://doi.org/10.1016/j.mednuc.2007.11.003

Robert, F., Barbeau, M., Éthier, S., Dostie, J., & Pelletier, J. (2015). Pharmacological inhibition of DNA-PK stimulates Cas9-mediated genome editing. *Genome Medicine*, *7*(1), 1–11. https://doi.org/10.1186/s13073-015-0215-6

Rothkamm, K., Krüger, I., Thompson, L. H., & Löbrich, M. (2003). Pathways of DNA Double-Strand Break Repair during the Mammalian Cell Cycle. *Molecular and Cellular Biology*, *23*(16), 5706–5715. https://doi.org/10.1128/mcb.23.16.5706-5715.2003

Saiki, I., Yoneda, J., Azuma, I., Fujii, H., Abe, F., Nakajima, M., & Tsuruo, T. (1993). Role of aminopeptidase N (CD13) in tumor-cell invasion and extracellular matrix degradation. *International Journal of Cancer*, *54*(1), 137–143. https://doi.org/10.1002/ijc.2910540122

Saito, Y., Koya, J., & Kataoka, K. (2021). Multiple mutations within individual oncogenes. *Cancer Science*, *112*(2), 483–489. https://doi.org/10.1111/cas.14699

Sander, J. D., & Joung, J. K. (2014). CRISPR-Cas systems for genome editing, regulation and targeting. *Nature Biotechnology*, *32*(4), 347–355. https://doi.org/10.1038/nbt.2842.CRISPR-Cas

Sandu, C., Ngounou Wetie, A. G., Darie, C. C., & Steller, H. (2014). Thiostrepton, a natural compound that triggers heat shock response and apoptosis in human cancer cells: A proteomics investigation. *Advances in Experimental Medicine and Biology*, *806*, 443–451. https://doi.org/10.1007/978-3-319-06068-2_21

Sayegh, N., Swami, U., & Agarwal, N. (2022). Recent Advances in the Management of Metastatic Prostate Cancer. *JCO Oncology Practice*, *18*(1), 45–55. https://doi.org/10.1200/op.21.00206

Schaber, M. D., Garsky, V. M., Boylan, D., Hill, W. S., Scolnick, E. M., Marshall, M. S., … Gibbs, J. B. (1989). Ras interaction with the GTPase-activating protein (GAP). *Proteins: Structure, Function, and Bioinformatics*, *6*(3), 306–315. https://doi.org/10.1002/prot.340060313

Schoof, S., Pradel, G., Aminake, M. N., Ellinger, B., Baumann, S., Potowski, M., … Arndt, H. D. (2010). Antiplasmodial thiostrepton derivatives: Proteasome inhibitors with a dual mode of action. *Angewandte Chemie - International Edition*, *49*(19), 3317–3321.

https://doi.org/10.1002/anie.200906988
Schwinn, M. K., Machleidt, T., Zimmerman, K., Eggers, C. T., Dixon, A. S., Hurst, R., … Wood, K. V. (2018). CRISPR-Mediated Tagging of Endogenous Proteins with a Luminescent Peptide. *ACS Chemical Biology*, *13*(2), 467–474. https://doi.org/10.1021/acschembio.7b00549
Scornik, O., & Botbol, V. (2001). Bestatin as an Experimental Tool in Mammals. *Current Drug Metabolism*, *2*(1), 67–85. https://doi.org/10.2174/1389200013338748
Smits, M., Van Rijn, S., Hulleman, E., Biesmans, D., Van Vuurden, D. G., Kool, M., … Wuřdinger, T. (2012). EZH2-regulated DAB2IP is a medulloblastoma tumor suppressor and a positive marker for survival. *Clinical Cancer Research*, *18*(15), 4048–4058. https://doi.org/10.1158/1078-0432.CCR-12-0399
Song, Z., Chen, C., He, J., Liu, B., Ji, W., Wu, L., & He, L. (2022). ASK1-Interacting Protein 1 Acts as a Novel Predictor of Type 2 Diabetes. *Frontiers in Endocrinology*, *13*, 896753. https://doi.org/10.3389/fendo.2022.896753
Subramani, J., Ghosh, M., Rahman, M. M., Caromile, L. A., Gerber, C., Rezaul, K., … Shapiro, L. H. (2013). Tyrosine phosphorylation of CD13 regulates inflammatory cell-cell adhesion and monocyte trafficking. *Journal of Immunology (Baltimore, Md. : 1950)*, *191*(7), 3905–3912. https://doi.org/10.4049/jimmunol.1301348
Sun, L., Yao, Y., Lu, T., Shang, Z., Zhan, S., Shi, W., … He, S. (2020). Erratum to "DAB2IP Downregulation Enhances the Proliferation and Metastasis of Human Gastric Cancer Cells by Derepressing the ERK1/2 Pathway". *Gastroenterology Research and Practice*. https://doi.org/10.1155/2020/7419534
Tamgue, O., Chai, C. Sen, Hao, L., Zambe, J. C. D., Huang, W. W., Zhang, B., … Wei, Y. M. (2013). Triptolide inhibits histone methyltransferase EZH2 and modulates the expression of its target genes in prostate cancer cells. *Asian Pacific Journal of Cancer Prevention*, *14*(10), 5663–5669. https://doi.org/10.7314/APJCP.2013.14.10.5663
Terpe, K. (2003). Overview of tag protein fusions: From molecular and biochemical fundamentals to commercial systems. *Applied Microbiology and Biotechnology*, *60*(5), 523–533. https://doi.org/10.1007/s00253-002-1158-6
Tong, Z., Fang, W., Xu, M., Xia, Y. Y., Wang, R., Li, Y., … Chen, X. (2022). DAB2IP predicts treatment response and prognosis of ESCC patients and modulates its radiosensitivity through enhancing IR-induced activation of the ASK1-JNK pathway. *Cancer Cell International*, *22*(1), 1–20. https://doi.org/10.1186/s12935-022-02535-9
Tsai, Y.-S., Lai, C.-L. L., Lai, C.-H., Chang, K.-H., Wu, K., Tseng, S.-F., … Hsieh, J.-T. (2014). The role of homeostatic regulation between tumor suppressor DAB2IP and oncogenic Skp2 in prostate cancer growth. *Oncotarget*, *5*(15). https://doi.org/10.18632/oncotarget.2228
Urh, M. (2012). HaloTag, a Platform Technology for Protein Analysis. *Current Chemical Genomics*, *6*(1), 72–78. https://doi.org/10.2174/1875397301206010072
Valentini, P., Pierattini, B., Zacco, E., Mangoni, D., Espinoza, S., Webster, N. A., … Gustincich, S. (2022). Towards SINEUP-based therapeutics: Design of an in vitro synthesized SINEUP RNA. *Molecular Therapy - Nucleic Acids*, *27*(March), 1092–1102. https://doi.org/10.1016/j.omtn.2022.01.021
Valentino, E., Bellazzo, A., Di, G., Sicari, D., Apollonio, M., & Scognamiglio, G. (2017). Mutant p53 potentiates the oncogenic effects of insulin by inhibiting the tumor suppressor DAB2IP. *Proc Natl Acad Sci USA*, 124. https://doi.org/10.1073/pnas.1700996114
Valentino, E., Bellazzo, A., Di Minin, G., Sicari, D., Apollonio, M., Scognamiglio, G., … Collavin, L. (2017). Mutant p53 potentiates the oncogenic effects of insulin by inhibiting the tumor suppressor DAB2IP. *Proceedings of the National Academy of Sciences*, *114*(29), 7623–7628. https://doi.org/10.1073/pnas.1700996114
Varadi, M., Anyango, S., Deshpande, M., Nair, S., Natassia, C., Yordanova, G., … Velankar, S. (2022). AlphaFold Protein Structure Database: Massively expanding the structural coverage of protein-sequence space with high-accuracy models. *Nucleic Acids Research*, *50*(D1), D439–

D444. https://doi.org/10.1093/nar/gkab1061
Varghese, V., Magnani, L., Harada-Shoji, N., Mauri, F., Szydlo, R. M., Yao, S., … Kenny, L. M. (2019). FOXM1 modulates 5-FU resistance in colorectal cancer through regulating TYMS expression. *Scientific Reports*, *9*(1), 1–16. https://doi.org/10.1038/s41598-018-38017-0
Vendramin, R., Litchfield, K., & Swanton, C. (2021). Cancer evolution: Darwin and beyond. *The EMBO Journal*, *40*(18), 1–20. https://doi.org/10.15252/embj.2021108389
Wan, J., Ling, X. an, Wang, J., Ding, G. gui, & Wang, X. (2020). Inhibitory effect of Ubenimex combined with fluorouracil on multiple drug resistance and P-glycoprotein expression level in non-small lung cancer. *Journal of Cellular and Molecular Medicine*, *24*(21), 12840–12847. https://doi.org/10.1111/jcmm.15875
Wang, G., Wang, X., Han, M., & Wang, X. (2021). Loss of dab2ip contributes to cell proliferation and cisplatin resistance in gastric cancer. *OncoTargets and Therapy*, *14*, 979–988. https://doi.org/10.2147/OTT.S289722
Wang, Jian-Yong, Jia, X., Xing, H., Li, Y., Fan, W., Li, N., & Xie, S. (2015). Inhibition of Forkhead box protein M1 by thiostrepton increases chemosensitivity to doxorubicin in T-cell acute lymphoblastic leukemia. *Mol Med Rep*, *12*(1), 1457–1464. https://doi.org/10.3892/mmr.2015.3469
Wang, Jianmei, Zhu, X., Hu, J., He, G., Li, X., Wu, P., … Ding, Y. (2015). The positive feedback between snail and DAB2IP regulates EMT, invasion and metastasis in colorectal cancer. *Oncotarget*, *6*(29), 27427–27439. https://doi.org/10.18632/oncotarget.4861
Wang, M., & Gartel, A. L. (2011). Micelle-encapsulated thiostrepton as an effective nanomedicine for inhibiting tumor growth and for suppressing FOXM1 in human xenografts. *Molecular Cancer Therapeutics*, *10*(12), 2287–2297. https://doi.org/10.1158/1535-7163.MCT-11-0536
Wang, M., Halasi, M., Kabirov, K., Banerjee, A., Landolfi, J., Lyubimov, A. V., & Gartel, A. L. (2012). Combination treatment with bortezomib and thiostrepton is effective against tumor formation in mouse models of DEN/PB-induced liver carcinogenesis. *Cell Cycle*, *11*(18), 3370–3372. https://doi.org/10.4161/cc.21290
Wang, X., Liu, Y., Liu, W., Zhang, Y., Guo, F., Zhang, L., … Wu, R. (2018). Ubenimex, an APN inhibitor, could serve as an anti-tumor drug in RT112 and 5637 cells by operating in an Akt-associated manner. *Molecular Medicine Reports*, *17*(3), 4531–4539. https://doi.org/10.3892/mmr.2018.8402
Wang, Y., Xie, W., Humeau, J., Chen, G., Liu, P., Pol, J., … Kroemer, G. (2020). Autophagy induction by thiostrepton improves the efficacy of immunogenic chemotherapy. *Journal for ImmunoTherapy of Cancer*, *8*(1), 1–11. https://doi.org/10.1136/jitc-2019-000462
Wang, Z.-R., Wei, J.-H., Zhou, J.-C., Haddad, A., Zhao, L.-Y., Kapur, P., … Luo, J.-H. (2016). Validation of DAB2IP methylation and its relative significance in predicting outcome in renal cell carcinoma. *Oncotarget*, *7*(21), 31508–31519. https://doi.org/10.18632/oncotarget.8971
Watari, A., Kodaka, M., Matsuhisa, K., Sakamoto, Y., Hisaie, K., Kawashita, N., … Kondoh, M. (2017). Identification of claudin-4 binder that attenuates tight junction barrier function by TR-FRET-based screening assay. *Scientific Reports*, *7*(1), 1–12. https://doi.org/10.1038/s41598-017-15108-y
Wei, X., Chen, L., Yang, A., Lv, Z., Xiong, M., & Shan, C. (2021). ADRB2 is a potential protective gene in breast cancer by regulating tumor immune microenvironment. *Translational Cancer Research*, *10*(12), 5280–5294. https://doi.org/10.21037/tcr-21-1257
Westaby, D., Viscuse, P. V., Ravilla, R., de la Maza, M. de los D. F., Hahn, A., Sharp, A., … Fleming, M. T. (2021). Beyond the Androgen Receptor: The Sequence, the Mutants, and New Avengers in the Treatment of Castrate-Resistant Metastatic Prostate Cancer. *American Society of Clinical Oncology Educational Book*, (41), e190–e202. https://doi.org/10.1200/edbk_321209
White, M. K., Kaminski, R., Young, W. Bin, Roehm, P. C., & Khalili, K. (2017). CRISPR Editing Technology in Biological and Biomedical Investigation. *Journal of Cellular Biochemistry*,

118(11), 3586–3594. https://doi.org/10.1002/jcb.26099
Wickström, M., Larsson, R., Nygren, P., & Gullbo, J. (2011). Aminopeptidase N (CD13) as a target for cancer chemotherapy. *Cancer Science*, *102*(3), 501–508. https://doi.org/10.1111/j.1349-7006.2010.01826.x
Williamson, M. P. (1994). The structure and function of proline-rich regions in proteins. *Biochemical Journal*, *297*(2), 249–260. https://doi.org/10.1042/bj2970249
Wongkhieo, S., Numdee, K., Lam, E. W. F., Choowongkomon, K., Kongsema, M., & Khongkow, M. (2021). Liposomal Thiostrepton Formulation and Its Effect on Breast Cancer Growth Inhibition. *Journal of Pharmaceutical Sciences*, *110*(6), 2508–2516. https://doi.org/10.1016/j.xphs.2021.01.018
Wu, K., Liu, J., Tseng, S. F., Gore, C., Ning, Z., Sharifi, N., … Hsieh, J. T. (2014). The role of DAB2IP in androgen receptor activation during prostate cancer progression. *Oncogene*, *33*(15), 1954–1963. https://doi.org/10.1038/onc.2013.143
Wu, Kaijie, Wang, B., Chen, Y., Zhou, J., Huang, J., Hui, K., … Fan, J. (2015). DAB2IP regulates the chemoresistance to pirarubicin and tumor recurrence of non-muscle invasive bladder cancer through STAT3/Twist1/P-glycoprotein signaling. *Cellular Signallingc*, *27*(12), 2515–2523. https://doi.org/10.1016/j.cellsig.2015.09.014
Wu, Kaijie, Xie, D., Zou, Y., Zhang, T., Pong, R. C., Xiao, G., … Hsieh, J. T. (2013). The mechanism of DAB2IP in chemoresistance of prostate cancer cells. *Clinical Cancer Research*, *19*(17), 4740–4749. https://doi.org/10.1158/1078-0432.CCR-13-0954
Wykosky, J., Fenton, T., Furnari, F., & Cavenee, W. K. (2011). Therapeutic targeting of epidermal growth factor receptor in human cancer: Successes and limitations. *Chinese Journal of Cancer*, *30*(1), 5–12. https://doi.org/10.5732/cjc.010.10542
Xiao, Y., Li, Z.-H., & Bi, Y.-H. (2019). MicroRNA-889 promotes cell proliferation in colorectal cancer by targeting DAB2IP. *European Review for Medical and Pharmacological Sciences*, *23*(8), 3326–3334. https://doi.org/10.26355/eurrev_201904_17695
Xie, D. ., Gore, C., Liu, J., Pong, R.-C., Mason, R., Hao, G., … Hsieh, J.-T. (2010). Role of DAB2IP in modulating epithelial-to-mesenchymal transition and prostate cancer metastasis. *Proceedings of the National Academy of Sciences*, *107*(6), 2485–2490. https://doi.org/10.1073/pnas.0908133107
Xie, D., Gore, C., Zhou, J., Pong, R.-C., Zhang, H., Yu, L., … Hsieh, J.-T. (2009). DAB2IP coordinates both PI3K-Akt and ASK1 pathways for cell survival and apoptosis. *Proceedings of the National Academy of Sciences*, *106*(47), 19878–19883. https://doi.org/10.1073/pnas.0908458106
Xie, T., Geng, J., Wang, Y., Wang, L., Huang, M., Chen, J., … Chu, X. (2016). FOXM1 evokes 5-fluorouracil resistance in colorectal cancer depending on ABCC10. *Oncotarget*, *8*(5), 8574–8589. https://doi.org/10.18632/oncotarget.14351
Xin, L. (2021). EZH2 accompanies prostate cancer progression. *Nature Cell Biology*, *23*(9), 934–936. https://doi.org/10.1038/s41556-021-00744-4
Xu, Y., He, J., Wang, Y., Zhu, X., Pan, Q., Xie, Q., & Sun, F. (2015). MiR-889 promotes proliferation of esophageal squamous cell carcinomas through DAB2IP. *FEBS Letters*, *589*(10), 1127–1135. https://doi.org/10.1016/j.febslet.2015.03.027
Yang, C., He, H., Zhang, T., Chen, Y., & Kong, Z. (2016). Decreased DAB2IP gene expression, which could be induced by fractionated irradiation, is associated with resistance to γ-rays and α-particles in prostate cancer cells. *Molecular Medicine Reports*, *14*(1), 567–573. https://doi.org/10.3892/mmr.2016.5281
Yang, N., Wang, C., Wang, J., Wang, Z., Huang, D., Yan, M., … Xu, B. L. (2019). Aurora kinase A stabilizes FOXM1 to enhance paclitaxel resistance in triple-negative breast cancer. *Journal of Cellular and Molecular Medicine*, *23*(9), 6442–6453. https://doi.org/10.1111/jcmm.14538
Yano, M., Toyooka, S., Tsukuda, K., Dote, H., Ouchida, M., Hanabata, T., … Shimizu, N. (2005). Aberrant promoter methylation of human DAB2 interactive protein (hDAB2IP) gene in lung

cancers. *International Journal of Cancer*, *113*(1), 59–66. https://doi.org/10.1002/ijc.20531
Yip, B. H. (2020). Recent advances in CRISPR/Cas9 delivery strategies. *Biomolecules*, *10*(6). https://doi.org/10.3390/biom10060839
Yu, H., Xu, Z., Guo, M., Wang, W., Zhang, W., Liang, S., … Lin, J. (2020). FOXM1 modulates docetaxel resistance in prostate cancer by regulating KIF20A. *Cancer Cell International*, *20*(1), 1–12. https://doi.org/10.1186/s12935-020-01631-y
Yu, J., Cao, Q., Mehra, R., Laxman, B., Yu, J., Tomlins, S. A., … Chinnaiyan, A. M. (2007). Integrative Genomics Analysis Reveals Silencing of β-Adrenergic Signaling by Polycomb in Prostate Cancer. *Cancer Cell*, *12*(5d), 419–431. https://doi.org/10.1016/j.ccr.2007.10.016
Yu, L., Lang, Y., Hsu, C.-C., Chen, W.-M., Chiang, J.-C., Hsieh, J.-T., … Saha, D. (2022). Mitotic phosphorylation of tumor suppressor DAB2IP maintains spindle assembly checkpoint and chromosomal stability through activating PLK1-Mps1 signal pathway and stabilizing mitotic checkpoint complex. *Oncogene*, *41*(4), 489–501. https://doi.org/10.1038/s41388-021-02106-8
Yu, L., Tumati, V., Tseng, S.-F., Hsu, F.-M., Kim, D. N., Hong, D., … Saha, D. (2015). DAB2IP Regulates Autophagy in Prostate Cancer in Response to Combined Treatment of Radiation and a DNA-PKcs Inhibitor. *Neoplasia*, *14*(12), 1203-IN36. https://doi.org/10.1593/neo.121310
Yun, E.-J., Kim, S., Hsieh, J.-T., & Baek, S. T. (2020). Wnt/β-catenin signaling pathway induces autophagy-mediated temozolomide-resistance in human glioblastoma. *Cell Death & Disease*, *11*(9), 771. https://doi.org/10.1038/s41419-020-02988-8
Yun, E.-J., Lin, C.-J., Dang, A., Hernandez, E., Guo, J., Chen, W.-M., … Hsieh, J.-T. (2019). Downregulation of Human DAB2IP Gene Expression in Renal Cell Carcinoma Results in Resistance to Ionizing Radiation. *Clinical Cancer Research : An Official Journal of the American Association for Cancer Research*, *25*(14), 4542–4551. https://doi.org/10.1158/1078-0432.CCR-18-3004
Yun, E. J., Baek, S. T., Xie, D., Tseng, S. F., Dobin, T., Hernandez, E., … Hsieh, J. T. (2015). DAB2IP regulates cancer stem cell phenotypes through modulating stem cell factor receptor and ZEB1. *Oncogene*, *34*(21), 2741–2752. https://doi.org/10.1038/onc.2014.215
Zalli, A., Bosch, J. A., Goodyear, O., Riddell, N., McGettrick, H. M., Moss, P., & Wallace, G. R. (2015). Targeting ß2 adrenergic receptors regulate human T cell function directly and indirectly. *Brain, Behavior, and Immunity*, *45*, 211–218. https://doi.org/10.1016/j.bbi.2014.12.001
Zhang, B., Liu, L. L., Mao, X., & Zhang, D. H. (2014). Effects of metformin on FOXM1 expression andon the biological behavior of acute leukemia cell lines. *Molecular Medicine Reports*, *10*(6), 3193–3198. https://doi.org/10.3892/mmr.2014.2629
Zhang, H., He, Y., Dai, S., Xu, Z., Luo, Y., Wan, T., … Min, W. (2008). AIP1 functions as an endogenous inhibitor of VEGFR2-mediated signaling and inflammatory angiogenesis in mice. *Journal of Clinical Investigation*, *118*(12), 3904–3916. https://doi.org/10.1172/JCI36168
Zhang, H., Zhang, R., Luo, Y., D'Alessio, A., Pober, J. S., & Min, W. (2004). AIP1/DAB2IP, a novel member of the Ras-GAP family, transduces TRAF2-induced ASK1-JNK activation. *Journal of Biological Chemistry*, *279*(43), 44955–44965. https://doi.org/10.1074/jbc.M407617200
Zhang, J., Chen, C., Li, L., Zhou, H. J., Li, F., & Zhang, H. (2018). Endothelial AIP1 Regulates Vascular Remodeling by Suppressing NADPH, *9*(April), 1–14. https://doi.org/10.3389/fphys.2018.00396
Zhang, Meng, Xu, C., Wang, H.-Z., Peng, Y.-N., Li, H.-O., Zhou, Y.-J., … Liu, J. (2019). Soft fibrin matrix downregulates DAB2IP to promote Nanog-dependent growth of colon tumor-repopulating cells. *Cell Death & Disease*, *10*(3), 151. https://doi.org/10.1038/s41419-019-1309-7
Zhang, Mengna, Peng, Y., Yang, Z., Zhang, H., Xu, C., Liu, L., … Liu, J. (2022). DAB2IP down-regulates HSP90AA1 to inhibit the malignant biological behaviors of colorectal cancer. *BMC Cancer*, *22*(1), 561. https://doi.org/10.1186/s12885-022-09596-z

Zhang, R., He, X., Liu, W., Lu, M., Hsieh, J., & Min, W. (2003). AIP1 mediates TNF- α – induced ASK1 activation by facilitating dissociation of ASK1 from its inhibitor 14-3-3, *111*(12), 1933–1943. https://doi.org/10.1172/JCI200317790.Introduction

Zhang, W., Gong, M., Zhang, W., Mo, J., Zhang, S., Zhu, Z., … Wang, Z. (2022). Thiostrepton induces ferroptosis in pancreatic cancer cells through STAT3/GPX4 signalling. *Cell Death and Disease*, *13*(7), 1–12. https://doi.org/10.1038/s41419-022-05082-3

Zhang, Y., Zheng, D., Zhou, T., Song, H., Hulsurkar, M., Su, N., … Li, W. (2018). Androgen deprivation promotes neuroendocrine differentiation and angiogenesis through CREB-EZH2-TSP1 pathway in prostate cancers. *Nature Communications*, *9*(1). https://doi.org/10.1038/s41467-018-06177-2

Zheng, H. C. (2017). The molecular mechanisms of chemoresistance in cancers. *Oncotarget*, *8*(35), 59950–59964. https://doi.org/10.18632/oncotarget.19048

Zhong, L., Li, Y., Xiong, L., Wang, W., Wu, M., Yuan, T., … Yang, S. (2021). Small molecules in targeted cancer therapy: advances, challenges, and future perspectives. *Signal Transduction and Targeted Therapy*, *6*(1). https://doi.org/10.1038/s41392-021-00572-w

Zhou, J., Ning, Z., Wang, B., Yun, E. J., Zhang, T., Pong, R. C., … Wu, K. (2015a). DAB2IP loss confers the resistance of prostate cancer to androgen deprivation therapy through activating STAT3 and inhibiting apoptosis. *Cell Death and Disease*, *6*(10). https://doi.org/10.1038/cddis.2015.289

Zhou, J., Ning, Z., Wang, B., Yun, E. J., Zhang, T., Pong, R. C., … Wu, K. (2015b). DAB2IP loss confers the resistance of prostate cancer to androgen deprivation therapy through activating STAT3 and inhibiting apoptosis. *Cell Death and Disease*, *6*(10). https://doi.org/10.1038/cddis.2015.289

Zhu, X., Li, S., Xu, B., & Luo, H. (2021). Cancer evolution: A means by which tumors evade treatment. *Biomedicine and Pharmacotherapy*, *133*(August 2020), 111016. https://doi.org/10.1016/j.biopha.2020.111016

Zhu, Y., Liu, X., Wang, Y., Pan, Y., Han, X., Peng, B., … Gao, S. (2022). DMDRMR promotes angiogenesis via antagonizing DAB2IP in clear cell renal cell carcinoma. *Cell Death & Disease*, *13*(5), 456. https://doi.org/10.1038/s41419-022-04898-3

Zong, X., Wang, W., Ozes, A., Fang, F., Sandusky, G. E., & Nephew, K. P. (2020). EZH2-Mediated Downregulation of the Tumor Suppressor DAB2IP Maintains Ovarian Cancer Stem Cells. *Cancer Research*, *80*(20), 4371–4385. https://doi.org/10.1158/0008-5472.CAN-20-0458

Zucchelli, S., Cotella, D., Takahashi, H., Carrieri, C., Cimatti, L., Fasolo, F., … Gustincich, S. (2015). SINEUPs: A new class of natural and synthetic antisense long non-coding RNAs that activate translation. *RNA Biology*, *12*(8), 771–779. https://doi.org/10.1080/15476286.2015.1060395